AN ABSTRACT OF A DISSERTATION

ANALYSIS OF COMBUSTION INSTABILITY
IN LIQUID FUEL ROCKET MOTORS

Kin-Wing Wong

Doctor of Philosophy in Engineering Mechanics

The primary objective of this study is the develop-
ment of a new analytical technique to be used in the solution
of nonlinear velocity-sensitive combustion instability
problems. Such a method should be relatively easy to apply
and should require relatively little computation time. In
an attempt to achieve this aim, the orthogonal collocation
method is investigated first. However, it is found that
the results are heavily dependent on the location of the
collocation points and characteristics of the equations.
Therefore, the method is rejected as unreliable. Next, the
Galerkin method, which has proved to be very successful in
analysis of the pressure sensitive combustion instability,
is considered. This method is found to work very well. It
is found that the pressure wave forms exhibit a strong
second harmonic distortion and a variety of behaviors are
possible depending on the nature of the combustion process
and the parametric values involved. Finally, a one-
dimensional model provides further insight into the problem
by allowing a comparison of Galerkin solutions with more
exact finite-difference computations.

ANALYSIS OF COMBUSTION INSTABILITY

IN LIQUID FUEL ROCKET MOTORS

———————

A Dissertation

Presented to

the Faculty of the Graduate School

Tennessee Technological University

by

Kin-Wing Wong

———————

In Partial Fulfillment

of the Requirements for the Degree

DOCTOR OF PHILOSOPHY

Engineering Mechanics

———————

August 1979

CERTIFICATE OF APPROVAL OF DISSERTATION

ANALYSIS OF COMBUSTION INSTABILITY

IN LIQUID FUEL ROCKET MOTORS

by

Kin-Wing Wong

Graduate Advisory Committee:

_____ 8/1/79
Chairman   date

_____ 8/1/79
Member   date

_____ 8/1/79
Member   date

_____ 8/1/79
Member   date

Approved for the Faculty:

_____
Dean, Graduate School

_____
Date

ii

ACKNOWLEDGMENTS

TABLE OF CONTENTS

LIST OF TABLES

LIST OF FIGURES

Chapter 1

INTRODUCTION

The steady operation of a liquid-propellant rocket engine is often disturbed by the occurrence of large pressure oscillations in the combustion chamber. These oscillations, which can lead to damage to or failure of the motor, are caused by amplification of initially small acoustic disturbances due to the energy released by unsteady burning of the propellant. This is usually referred to as combustion instability. It is generally accepted that unsteady burning can be correlated with the gas pressure (pressure sensitivity) and the magnitude of velocity of the fuel drops relative to the gas (velocity sensitivity). This dissertation is concerned with mathematical modeling of velocity-sensitive combustion instability in liquid-propellant rocket motors.

A survey of literature dealing with mathematical modeling of pressure-sensitive combustion instability can be found in the dissertation of Powell (1). One of the first papers to examine nonlinear effects is that of Maslen and Moore (2) who considered only the fluid mechanical effects in a circular cylinder. The paper by Priem and Guentert (3) is one of the first to include the effect of velocity sensitivity. They discussed combustion instability

1

in a thin annulus.

Since direct numerical solution of the governing equations is very time consuming and difficult to extract information from, many investigators such as Powell and Zinn (4), Lores and Zinn (5), and Peddieson, Ventrice, and Purdy (6) have employed methods of weighted residuals such as Galerkin and collocation methods.

Previous applications of the method of weighted residuals to combustion-instability problems have dealt with pressure-sensitive combustion. In this work this method will be extended to handle situations in which velocity sensitivity is important. Both the collocation and Galerkin methods will be considered. Stability boundaries and pressure wave forms will be computed numerically for transverse motion in a cylindrical combustion chamber. In addition a finite-difference method will be used to solve the one-dimensional problem of transverse motion in a thin annular chamber. These results will be compared with those obtained by a method of weighted residuals solution of the same problem in order to assess the accuracy of the approximate solution.

In this study, attempts to solve the velocity-sensitive combustion instability problem by various numerical methods are considered. The governing equations that describe the flow conditions inside liquid-propellant rocket motors will be derived in Chapter Two. An analytical solution is obtained in Chapter Three for nonlinear acoustic motion in a cylindrical chamber. The collocation method is

applied to combustion instability in a cylindrical chamber

in Chapter Four. In Chapter Five, the Galerkin method is

applied to the same problem. In Chapter Six, attention is

given to the analysis of combustion instability in a thin

annulus. This allows the comparison of the Galerkin method

and a finite-difference solution in a one-dimensioned

context. Finally, a summary of this research is contained

in Chapter Seven.

Chapter 2

COMBUSTOR EQUATIONS

It is the objective of the discussion presented in
this chapter to analyze the combustor conservation equations
and reduce them to a tractable system. The simplification
will be done in such a manner that will allow the resulting
equations to retain both the mathematical and physical
essence of the original problem.

Under the assumptions that the usual balance
principles of mechanics can be applied separately to each
phase, the following equations are derived by applying the
laws of conservation of mass, momentum, and energy to an
arbitrary stationary control volume.

Conservation of mass of the fluid requires that the
time rate of change of mass in a volume v equals the rate
at which mass enters v plus the rate at which mass is
generated inside v and can be expressed as follows (for a
fixed volume):

$$\partial_t * \int_v \overset{*}{\rho} dv = - \int_s \overset{*}{\rho}\overset{*}{\vec{u}} \cdot \vec{n} ds + \int_v \overset{*}{w} dv$$

where $\vec{n}$ is an outward unit vector normal to s, $\overset{*}{\rho}$ is the
density of fluid, $\overset{*}{u}$ is the velocity of fluid, $\overset{*}{w}$ is the rate
at which mass is generated per unit volume, and $\overset{*}{t}$ is the time.

4

Using the divergence theorm and the arbitrariness of
the stationary control volume, yields

$$\partial_t {*}\overset{*}{\rho} + \overset{*}{\vec{\nabla}} \cdot (\overset{*}{\rho}\overset{*}{\vec{u}}) = \overset{*}{w}. \tag{2.1}$$

Similarly, the balance law of mass for fuel phase is

$$\partial_t {*}\overset{*}{\rho}_L + \overset{*}{\vec{\nabla}} \cdot (\overset{*}{\rho}_L \overset{*}{\vec{u}}_L) = - \overset{*}{w} \tag{2.2}$$

where $\overset{*}{\rho}_L$ is the density of fuel and $\overset{*}{\vec{u}}_L$ is the velocity of
fuel.

The balance law of linear momentum states that the
rate of change of linear momentum in the volume v equals
the rate of entry of linear momentum across the surface s
plus the sum of all external forces acting on the volume v
and can be expressed as

$$\partial_t {*}\int_v \overset{*}{\rho}\overset{*}{\vec{u}}\,dv = - \int_s \overset{*}{\rho}\overset{*}{\vec{u}}(\overset{*}{\vec{u}}\cdot\vec{n})\,ds + \int_v \overset{*}{\vec{F}}\,dv + \int_v \overset{*}{w}\overset{*}{\vec{u}}_L\,dv - \int_s \overset{*}{P}\vec{n}\,ds$$

where $\overset{*}{\vec{F}}$ is the force per unit volume applied to the gas by
the fuel and $\overset{*}{P}$ is the pressure of the gas.

Using the same argument, the equation becomes

$$\partial_t {*}(\overset{*}{\rho}\overset{*}{\vec{u}}) + \overset{*}{\vec{\nabla}} \cdot (\overset{*}{\rho}\overset{*}{\vec{u}}\overset{*}{\vec{u}}) = \overset{*}{\vec{F}} + \overset{*}{w}\overset{*}{\vec{u}}_L - \overset{*}{\vec{\nabla}}\overset{*}{P}. \tag{2.3}$$

Similarly, the balance of momentum for the fuel phase is

$$\partial_{t^*}\,(\overset{*}{\rho}_L \overset{*}{\vec{u}}_L) + \overset{*}{\vec{\nabla}}\cdot(\overset{*}{\rho}_L \overset{*}{\vec{u}}_L \overset{*}{\vec{u}}_L) = -\overset{*}{\vec{F}} - \overset{*}{w}\overset{*}{\vec{u}}_L. \tag{2.4}$$

Substituting (2.1) in (2.3) yields

$$\overset{*}{\rho}(\partial_{t^*}\overset{*}{\vec{u}} + \overset{*}{\vec{u}}\cdot\overset{*}{\vec{\nabla}}\overset{*}{\vec{u}}) = \overset{*}{\vec{F}} + \overset{*}{w}(\overset{*}{\vec{u}}_L - \overset{*}{\vec{u}}) - \overset{*}{\vec{\nabla}}P. \tag{2.5}$$

Similarly for the fuel phase

$$\overset{*}{\rho}_L(\partial_{t^*}\overset{*}{\vec{u}}_L + \overset{*}{\vec{u}}_L\cdot\overset{*}{\vec{\nabla}}\overset{*}{\vec{u}}_L) = -\overset{*}{\vec{F}}. \tag{2.6}$$

The law of conservation of energy states that the rate of change of energy in a volume v equals the rate at which energy enters the volume v plus the rate at which energy is generated internally plus the rate at which work is done by external forces and gives

$$\partial_{t^*}\!\int_v \overset{*}{\rho}(\overset{*}{e} + \tfrac{1}{2}\overset{*}{u}^2)dv = -\int_s \overset{*}{\rho}(\overset{*}{e} + \tfrac{1}{2}\overset{*}{u}^2)(\overset{*}{\vec{u}}\cdot\vec{n})ds - \int_s (P\vec{n})\cdot\overset{*}{\vec{u}}ds$$

$$+ \int_v \overset{*}{\vec{F}}\cdot\overset{*}{\vec{u}}_L dv + \int_v \overset{*}{w}(\overset{*}{e}_L + \tfrac{1}{2}\overset{*}{u}_L^2)dv + \int_v Qdv$$

where $\overset{*}{e} + \tfrac{1}{2}\overset{*}{u}^2$ is the energy of gas per unit volume, $\overset{*}{e}_L + \tfrac{1}{2}\overset{*}{u}_L^2$ is the energy of fuel per unit volume, and $\overset{*}{Q}$ is the heat transfer rate from the fuel to the gas.

Following the same argument, the equation becomes

$$\partial_{t^*}(\overset{*}{\rho}(\overset{*}{e} + \tfrac{1}{2}\overset{*}{u}{}^2)) + \overset{*}{\vec{\nabla}}\cdot(\overset{*}{\rho}(\overset{*}{e} + \tfrac{1}{2}\overset{*}{u}{}^2)\overset{*}{\vec{u}}) = -\overset{*}{\vec{\nabla}}\cdot(\overset{**}{P\vec{u}})$$

$$+ \overset{*}{\vec{F}}\cdot\overset{*}{\vec{u}}_L + \overset{*}{w}(\overset{*}{e}_L + \tfrac{1}{2}\overset{*}{u}{}^2_L) + \overset{*}{Q}. \qquad (2.6)$$

Similarly, the balance of energy for the fuel phase becomes

$$\partial_{t^*}(\overset{*}{\rho}_L(\overset{*}{e}_L + \tfrac{1}{2}\overset{*}{u}{}^2_L)) + \overset{*}{\vec{\nabla}}\cdot(\overset{*}{\rho}_L(\overset{*}{e}_L + \tfrac{1}{2}\overset{*}{u}{}^2_L)\overset{*}{\vec{u}}_L)$$

$$= - \overset{*}{\vec{F}}\cdot\overset{*}{\vec{u}}_L - \overset{*}{w}(\overset{*}{e}_L + \tfrac{1}{2}\overset{*}{u}{}^2_L) - \overset{*}{Q}. \qquad (2.7)$$

Substituting (2.1), (2.2) into (2.6), (2.7) respectively yields

$$\overset{*}{\rho}(\partial_{t^*}(\overset{*}{e} + \tfrac{1}{2}\overset{*}{u}{}^2) + \overset{*}{\vec{u}}\cdot\overset{*}{\vec{\nabla}}(\overset{*}{e} + \tfrac{1}{2}\overset{*}{u}{}^2)) = - \overset{*}{\vec{\nabla}}\cdot(\overset{**}{P\vec{u}})$$

$$+ \overset{*}{\vec{F}}\cdot\overset{*}{\vec{u}}_L + \overset{*}{w}((\overset{*}{e}_L + \tfrac{1}{2}\overset{*}{u}{}^2_L) - (\overset{*}{e} + \tfrac{1}{2}\overset{*}{u}{}^2)) + \overset{*}{Q} \qquad (2.8)$$

$$\overset{*}{\rho}_L(\partial_{t^*}(\overset{*}{e}_L + \tfrac{1}{2}\overset{*}{u}{}^2_L) + \overset{*}{\vec{u}}_L\cdot\overset{*}{\vec{\nabla}}(\overset{*}{e}_L$$

$$+ \tfrac{1}{2}\overset{*}{u}{}^2_L)) = - \overset{*}{\vec{F}}\cdot\overset{*}{\vec{u}}_L - \overset{*}{Q}. \qquad (2.9)$$

It is more convenient to work with the thermal energy equation for each phase. For gas phase this is done by

dotting $\overset{*}{\vec{u}}$ into (2.3) to obtain the mechanical energy equation and subtracting this from (2.8) and using (2.1) to get

$$\overset{*}{\rho}D\overset{*}{e}/Dt^* = \overset{*}{P}D^*/Dt^*(\log\overset{*}{\rho}) + \overset{*}{\vec{F}}\cdot(\overset{*}{\vec{u}}_L - \overset{*}{\vec{u}}) + \overset{*}{Q} + \overset{*}{w}((\overset{*}{e}_L - \overset{*}{e})$$

$$+ (\overset{*}{u}{}^2_L - \overset{*}{u}{}^2)/2 + \overset{*}{\vec{u}}\cdot(\overset{*}{\vec{u}} - \overset{*}{\vec{u}}_L) - \overset{*}{P}/\overset{*}{\rho}) . \qquad (2.10)$$

In a similar way, it can be shown that

$$\rho_L D_L \overset{*}{e}_L/Dt^* = -\overset{*}{Q} \qquad (2.11)$$

where $D^*/Dt^* = \partial_{t^*} + \overset{*}{\vec{u}}\cdot\vec{\nabla}$, $D_L{}^*/Dt^* = \partial_{t^*} + \overset{*}{\vec{u}}_L\cdot\vec{\nabla}$ are the comoving derivatives for each phase.

For simplicity, gas phase viscosity and heat conduction were neglected in the previous analysis. Since these produce dissipation, equations derived in this way should give a conservative estimate of the stability of the system.

It appears (see, for instance, Powell (1)) that the primary effect of the burning fuel is that of interphase mass transfer. Thus, the balance laws for mass, momentum, and thermal energy for each phase will be further simplified by neglecting all interphase transfer terms other than those appearing in the mass-balance equations.

This leads to the system of equations:

$$D^*\rho/Dt^* + \rho\vec{\nabla}^*\cdot\vec{u}^* = \overset{*}{w}$$

$$D^*\rho_L/Dt^* + \rho_L\vec{\nabla}^*\cdot\vec{u}_L^* = -\overset{*}{w}$$

$$\rho\overset{*}{D}\vec{u}^*/Dt^* = -\vec{\nabla}^*\overset{*}{P}$$

$$\rho_L D_L\vec{u}_L^*/Dt^* = 0$$

$$\rho C_v \overset{*}{D}\overset{*}{T}/Dt^* = \overset{*}{P}(D^*/Dt^*)(\log\overset{*}{\rho})$$

$$\rho_L C_{vL} D\overset{*}{T}_L/Dt^* = 0 \qquad (2.12)$$

where the constitutive equations $\overset{*}{e} = C_v\overset{*}{T}$ and $\overset{*}{e}_L = C_{vL}\overset{*}{T}_L$ have been used (with $\overset{*}{T}$ denoting temperature and C_v specific heat). The equation of state for an ideal gas is

$$\overset{*}{P} = \overset{*}{\rho}R\overset{*}{T} \qquad (2.13)$$

where R is the gas constant.

The governing equations will now be nondimensionalized with respect to a steady reference state, which will be denoted by the subscript "r". All lengths will be referred to some characteristic length L_r, such as the chamber radius. The characteristic velocity is the speed of sound at the

reference state, and the characteristic time is the wave
travel time L_r/C_r. The dimensionless quantities are
defined below:

$$\overset{*}{\vec{v}} = \vec{v}/L_r \qquad\qquad \overset{*}{t} = L_r t/C_r$$

$$\overset{*}{\vec{u}} = C_r\vec{u} \qquad\qquad \overset{*}{\vec{u}}_L = C_r\vec{u}_L$$

$$\overset{*}{\rho} = \rho_r\rho \qquad\qquad \overset{*}{\rho}_L = \rho_r\rho_L$$

$$\overset{*}{P} = P_r P \qquad\qquad \overset{*}{w} = \rho_r C_r w/L_r$$

$$\overset{*}{T} = C_r^2 T/(\gamma R) \qquad\qquad \overset{*}{T}_L = C_r^2 T_L/(\gamma R)$$

$$C_r^2 = \gamma P_r/\rho_r \qquad\qquad P_r = \rho_r C_r^2/\gamma .$$

The dimensionless conservation equations become

Continuity

$$D\rho/Dt + \rho\vec{\nabla}\cdot\vec{u} = w$$

$$D\rho_L/Dt + \rho_L\vec{\nabla}\cdot\vec{u}_L = -w \qquad\qquad (2.14)$$

Momentum

$$D\vec{u}/Dt = -\vec{\nabla}P/\gamma$$

$$D\vec{u}_L/Dt = 0 \qquad (2.15)$$

Energy

$$DT/Dt = (\gamma - 1)P(D/Dt)(\log\rho)$$

$$DT_L/Dt = 0 \qquad (2.16)$$

Equation of state

$$P = \rho T . \qquad (2.17)$$

By solving (2.16a) one obtains

$$T = \rho^{\gamma-1} . \qquad (2.18)$$

Equation (2.17) then becomes

$$P = \rho^{\gamma} . \qquad (2.19)$$

Substituting (2.19) to (2.15a) produces

$$D\vec{u}/Dt = -\vec{\nabla}(\rho^{\gamma-1})/(\gamma- 1) . \qquad (2.20)$$

Taking the curl on both sides of equation (2.20) gives

$$\vec{\nabla} \times D\vec{u}/Dt = 0 . \qquad (2.21)$$

It can be shown using vector identity that (2.21) leads to the following equation which describes the generation of the vorticity $\vec{\Omega} = \vec{\nabla} \times \vec{u}$ in the flow.

$$D\vec{\Omega}/Dt = \vec{\Omega}\cdot(\vec{\nabla}\,\vec{u}) - \vec{\Omega}(\vec{\nabla}\cdot\vec{u}) . \qquad (2.22)$$

This equation describes the variation of vorticity for a given fluid particle. Suppose that at t = 0, this particle has zero vorticity and at the point where it is located the velocity gradients are bounded. Then by (2.22) the rate of change of vorticity of the particle vanishes. It follows from this that the vorticity will be zero at the next instant. By induction, it is seen that as long as the velocity gradients are bounded at each point occupied by the particle, its vorticity will remain zero for all time. If all fluid particles in the system have zero vorticity at t = 0, the vorticity will vanish at all points in the flow field and for all $t \geq 0$, therefore, as long as the velocity gradients are bounded through the flow field (as they would not be, for example, at a shock wave). Assuming this condition to be satisfied implies irrotational flow ($\vec{\Omega} = 0$) and allows the definition of a velocity potential ϕ defined such that

$$\vec{u} = \vec{\nabla}\phi \ .$$
(2.23)

Substituting (2.23) to (2.20) gives

$$\partial_t \phi + \tfrac{1}{2}\vec{\nabla}\phi \cdot \vec{\nabla}\phi + \rho^{\gamma-1}/(\gamma-1) = F(t) \ .$$

Since the velocity is the space derivative of ϕ, it is permissible to add to ϕ any arbitrary function of time. This is equivalent to a statement that F(t) is arbitrary. For future convenience F(t) was selected to be $1/(\gamma-1)$. This choice yields

$$\rho^{\gamma-1} = 1 - (\gamma-1)(\partial_t\phi + \tfrac{1}{2}\vec{\nabla}\phi\cdot\vec{\nabla}\phi) \ . \qquad (2.24)$$

Substituting (2.24) into (2.14a), (2.18) and (2.19) gives

$$\partial_{tt}\phi - \nabla^2\phi(1 - (\gamma-1)(\partial_t\phi + \tfrac{1}{2}\vec{\nabla}\phi\cdot\vec{\nabla}\phi)) + \vec{\nabla}\phi\cdot\vec{\nabla}(2\partial_t\phi$$

$$+ \tfrac{1}{2}\vec{\nabla}\phi\cdot\vec{\nabla}\phi) + (1 - (\gamma-1)(\partial_t\phi + \tfrac{1}{2}\vec{\nabla}\phi\cdot\vec{\nabla}\phi))^{(\gamma-2)/(\gamma-1)}{}_{w} = 0$$

$$T = 1 - (\gamma-1)(\partial_t\phi + \tfrac{1}{2}\vec{\nabla}\phi\cdot\vec{\nabla}\phi)$$

$$P = (1 - (\gamma-1)(\partial_t\phi + \tfrac{1}{2}\vec{\nabla}\phi\cdot\vec{\nabla}\phi))^{\gamma/(\gamma-1)}. \qquad (2.25)$$

This system of equations contains nonlinear gas dynamics terms of all orders.

Due to their highly nonlinear and mathematically complicated nature, the system of equations obtained above cannot be solved exactly. In order to obtain simpler, but approximate, equations which can be more easily analyzed, all nonlinear terms of order higher than two are neglected. This has the effect of retaining the most important nonlinear effect, while greatly simplifying the form of the equations. The system of equations then becomes

$$\rho = 1 - (\partial_t\phi + \tfrac{1}{2}\vec{\nabla}\phi\cdot\vec{\nabla}\phi) + \tfrac{1}{2}(2-\gamma)(\partial_t\phi)^2$$

$$T = 1 - (\gamma-1)(\partial_t\phi + \tfrac{1}{2}\vec{\nabla}\phi\cdot\vec{\nabla}\phi)$$

$$P = 1 - \gamma(\partial_t \phi + \tfrac{1}{2}\vec{\nabla}\phi \cdot \vec{\nabla}\phi) + \tfrac{1}{2}\gamma(\partial_t \phi)^2$$

$$\partial_{tt}\phi - \nabla^2\phi \, (1 - (\gamma-1)\partial_t\phi) + 2\vec{\nabla}\phi \cdot \vec{\nabla}(\partial_t\phi)$$

$$+ (1 - (\gamma-2)\partial_t\phi)w = 0 \; . \qquad (2.26)$$

For a cylindrical combustor, it is desired to investigate the stability of the steady-state solution of (2.26d). To do this the steady-state solution must be obtained. It is assumed that the steady-state burning rate depends on z only ($w = \underline{w}(z)$) and that the flow is axial ($\phi = \underline{\phi}(z)$). Thus (2.26) simplifies to

$$d\underline{u}/dz = \underline{w} \qquad (\underline{u} = d\underline{\phi}/dz)$$

$$\underline{T} = 1 - \tfrac{1}{2}(\gamma-1)\underline{u}^2$$

$$\underline{P} = 1 - \tfrac{1}{2}\gamma\underline{u}^2$$

$$\underline{\rho} = 1 - \tfrac{1}{2}\underline{u}^2 \; . \qquad (2.27)$$

It can be seen from (2.27) that the deviations of the steady-state solution from a uniform state are $O(\underline{u}^2)$. To allow a discussion of orders of magnitude of various terms define the ordering parmeter ε such that

$$\varepsilon = \max \, (\underline{u}). \qquad (2.28)$$

This implies that

$$\underline{u} = O(\varepsilon), \quad \underline{w} = O(\varepsilon), \quad \underline{\phi} = O(\varepsilon). \tag{2.29}$$

The stability analysis will now be carried out by assuming that

$$\phi = \underline{\phi}(z) + \varepsilon\phi'(x,y,z,t)$$

$$w = \underline{w}(z) + \varepsilon^2 w'(x,y,z,t) \tag{2.30}$$

where $\phi' = O(1)$, $w' = O(1)$. $\tag{2.31}$

It is being assumed that the unsteady perturbation of the velocity potential from the steady state is of the same order of magnitude as the deviation of the steady state from a uniform state and that the unsteady burning rate perturbation is of the same order as the unsteady nonlinear gas-dynamic terms. The first assumption is necessary to be consistent with the quadratic approximation inherent in (2.26) while the second eliminates nonlinear terms involving products of w' and ϕ'. These assumptions are made for simplicity and are not meant to imply that other orders of magnitude for the various terms are impossible or even unlikely. The objective of this work is to pick one case which is mathematically tractable and subject it to extensive analysis. While it is felt that most of the features of the stability problem will be reflected by this case, it is recognized that many other possibilities remain to be explored.

Substituting (2.30) and

$$\rho = \underline{\rho} + \epsilon\rho', \quad P = \underline{P} + \epsilon P', \quad T = \underline{T} + \epsilon T' \qquad (2.32)$$

$\{\rho' = O(1),\ P' = O(1),\ T' = O(1)\}$ into (2.26), retaining all terms of $O(\epsilon^3)$ or lower, and dividing all resulting equations by ϵ leads to

$$\partial_{tt}\phi' - \nabla^2\phi' + 2\underline{u}\,\partial_{zt}\phi' + \underline{w}\,\partial_t\phi'$$

$$+ \epsilon\{(\gamma-1)\nabla^2\phi'\,\partial_t\phi' + 2\vec{\nabla}\phi'\cdot\vec{\nabla}(\partial_t\phi') + w'\} = 0$$

$$\rho' = -\{\partial_t\phi' + \underline{u}\,\partial_z\phi' + \tfrac{1}{2}\epsilon(\vec{\nabla}\phi'\cdot\vec{\nabla}\phi' - (2-\gamma)(\partial_t\phi')^2)\}$$

$$P' = -\gamma\{\partial_t\phi' + \underline{u}\,\partial_z\phi' + \tfrac{1}{2}\epsilon(\vec{\nabla}\phi'\cdot\vec{\nabla}\phi' - (\partial_t\phi')^2)\}$$

$$T' = -(\gamma-1)(\partial_t\phi' + \underline{u}\,\partial_z\phi' + \tfrac{1}{2}\epsilon\nabla\phi'\cdot\nabla\phi'). \qquad (2.33)$$

The equations derived from this perturbation analysis are expected to be valid as long as the amplitudes of the perturbation quantities are finite and smaller than unity.

For simplicity the primes appearing in the above equations will be dropped and it will be understood that unprimed quantities are associated with perturbation from the steady state.

Chapter 3

ANALYTICAL SOLUTION OF WAVE EQUATION

In this chapter a second-order solution for the velocity potential associated with transverse acoustic wave motion of an ideal gas in a circular cylinder is obtained. The solution is found in the form of a Fourier-Bessel series. This provides a standard to compare the proposed methods which will be discussed in the following chapters.

The governing equation is obtained from (2.33a) by assumption that the burning rate function is absent. Then the equation reduces to the second-order form of the one discussed by Maslen and Moore (2) for pure gas motion in a cylinder.

$$\partial_{tt}\phi - \nabla^2\phi + \epsilon(2\vec{\nabla}\phi\cdot\vec{\nabla}\partial_t\phi + (\gamma-1)\nabla^2\phi\,\partial_t\phi) = 0 \qquad (3.1)$$

For a cylinder of radius L_r, a set of cylindrical polar coordinates (r,θ,z) with the z axis being coincident with the cylinder's axis of symmetry is used. In seeking a second-order transverse wave solution, one assumes

$$\phi = \phi_1(r,\theta,t) + \epsilon\phi_2(r,\theta,t) + \ldots . \qquad (3.2)$$

Substituting (3.2) into (3.1) and (2.33) leads to

$$\partial_{tt}\phi_1 - \nabla^2\phi_1 = 0$$

$$\partial_{tt}\phi_2 - \nabla^2\phi_2 = -(\partial_t(u_1^2) + (\gamma-1)\nabla^2\phi_1 \partial_t\phi_1) \qquad (3.3)$$

$$P = 1 + \epsilon P_1 + \epsilon^2 P_2 \qquad (3.4)$$

where $P_1 = -\gamma\partial_t\phi_1$, $P_2 = -\gamma(\partial_t\phi_2 + \tfrac{1}{2}(u_1^2 - (\partial_t\phi_1)^2))$ $\quad (3.5)$

$$\nabla^2\phi_i = \partial_{rr}\phi_i + \partial_r\phi_i/r + \partial_{\theta\theta}\phi_i/r^2, \quad i = 1, 2$$

$$u_1^2 = (\partial_r\phi_1)^2 + (\partial_\theta\phi_1/r)^2. \qquad (3.6)$$

Three different cases are discussed below. For the initial conditions

$$\phi(r,\theta,0) = J_1(S_{11}r)\cos\theta, \quad \partial_t\phi(r,\theta,0) = 0 \qquad (3.7)$$

the solution of (3.3a) is

$$\phi_1 = J_1(S_{11}r)\cos\theta\cos(S_{11}t).$$

Substituting this equation to (3.3b) produces

$$\partial_{tt}\phi_2 - \nabla^2\phi_2 = (b_{00} + \sum_{\substack{m=0 \\ m\neq 1}}^{2}\sum_{n=1}^{\infty} J_m(S_{mn}r)\cos(m\theta))\sin(2S_{11}t) \qquad (3.8)$$

where J_n is used to denote an n'th order Bessel function of the first kind, S_{mn} is used to denote the m'th root of the equation $J_n' = 0$, and a prime indicates differentiation

with respect to the argument of the Bessel function. The coefficients b_{mn} are integrals of Bessel functions which must be computed numerically. The details of this calcuation are discussed in appendix A.

Solving (3.8) one obtains

$$\phi_2 = (b_{00}/(4S_{11}^2))(2S_{11}t - \sin(2S_{11}t))$$

$$+ \sum_{\substack{m=0 \\ m \neq 1}}^{2} \sum_{n=1}^{\infty} (b_{mn}/(S_{mn}^2 - 4S_{11}^2))J_m(S_{mn}r)\cos(m\theta)(\sin(2S_{11}t)$$

$$- (2S_{11}/S_{mn})\sin(S_{mn}t)). \tag{3.9}$$

The other two solutions to be discussed subsequently are found in the same way. For the initial conditions

$$\phi(r,\theta,0) = 0, \quad \partial_t\phi(r,\theta,0) = S_{11}J_1(S_{11}r)\cos\theta \tag{3.10}$$

it is found that

$$\phi_1 = J_1(S_{11}r)\cos\theta\sin(S_{11}t) \tag{3.11}$$

and that ϕ_2 is given by the negative of (3.9). For the initial conditions

$$\phi(r,\theta,0) = J_1(S_{11}r)\cos\theta,$$

$$\partial_t\phi(r,\theta,0) = S_{11}J_1(S_{11}r)\sin\theta \tag{3.12}$$

the solution is

$$\phi_1 = J_1(S_{11}r)\cos(S_{11}t - \theta)$$

$$\text{and } \phi_2 = \sum_{n=1}^{\infty} \{2b_{2n}/(S_{2n}^2 - 4S_{11}^2)\}J_2(S_{2n}r)(\sin(2\theta)\{\cos(2S_{11}t)$$

$$- \cos(S_{2n}t)\} + \cos(2\theta)\{\sin(2S_{11}t) - (2S_{11}/S_{2n})\sin(S_{2n}t)\}).$$

It can be seen that for these initial conditions ϕ_1 represents a spinning wave but $\phi_1 + \epsilon\phi_2$ does not. Some typical results for the pressure functions P_1 and P_2 were computed using the solutions for initial conditions (3.7) (labeled standing wave) and initial conditions (3.12) (labeled traveling wave) for $r = 1$, $\theta = 0$, and $\gamma = 1.2$. These data are presented graphically in Figure 1. For these computations the series expansions were terminated at $n = 5$. There is virtually no difference between the results for $n = 4$ and $n = 5$, and even the results for $n = 1$ provide a reasonably accurate solution.

The results discussed above were used to check the numerical calculations to be discussed in the next two chapters. These results generalize those of Maslen and Moore (2) to initial conditions which do not lead to periodic solutions.

Chapter 4

COLLOCATION

In previous investigations of velocity-sensitive combustion instability {see, for instance, (6) and the references therein} the most widely used burning-rate equation is that associated with the vaporization limited combustion model discussed by Priem and Guentert (3). In the notation of the present thesis the second-order version of this equation can be expressed as

$$w = (\underline{w}/\epsilon^2)((1 - \tfrac{1}{2}\epsilon\,\partial_t\phi)((1 - u_z/u_L)^2 + (u_t'/u_L)^2)^{\frac{1}{2}} - 1) \quad (4.1)$$

where u_z is the component of perturbed gas velocity in the axial direction and u_t is the perturbed component normal to the axis of symmetry, and u_L is the magnitude of the droplet velocity vector which assumed to be axial. Substituting (4.1) into (2.33a) yields

$$\partial_{tt}\phi + \underline{w}\,\partial_t\phi + 2\underline{u}\,\partial_{zt}\phi - \nabla^2\phi(1 - \epsilon(\gamma-1)\partial_t\phi)$$

$$+ 2\epsilon\vec{\nabla}\phi\cdot\vec{\nabla}\partial_t\phi + (\underline{w}/\epsilon)((1 - \tfrac{1}{2}\epsilon\,\partial_t\phi)((1 - \partial_z\phi/u_L)^2$$

$$+ (\vec{\nabla}\phi\cdot\vec{\nabla}\phi - (\partial_z\phi)^2)/u_L^2)^{\frac{1}{2}} - 1) = 0. \quad (4.2)$$

21

No exact solutions are to be expected to (4.2). Fully numerical solutions, on the other hand, are expected to be quite time consuming for multidimensional problems. For these reasons it was decided to attempt approximate partially analytical solutions using the method of weighted residuals {see for instance, (6)}. For problems of pressure sensitive combustion instability Powell (1) successfully employed the Galerkin method. This method is limited in applicability, however, to equations containing nonlinearities involving only polynomial functions of the dependent variable and its derivatives. It is clear that (4.2) is not of this form. The orthogonal collocation method was, therefore, chosen because of its simplicity and adaptability to equations containing nonlinearities of any algebraic form. The application of this method to the problem of transverse wave motion in a cylindrical chamber will be discussed below.

Consider the transverse wave motion in a cylindrical combustor. It is convenient to describe this problem in terms of cylindrical polar coordinates (r, θ, z). Then

$$\phi = \phi(r, \theta, t).$$ (4.3)

It will also be assumed that $\underline{w}$ and u_L are constants. Then (3.2) becomes

$$\partial_{tt}\phi + \underline{w}\partial_t\phi - (\partial_{rr}\phi + \partial_r\phi/r + \partial_{\theta\theta}\phi/r^2)(1 - \epsilon(\gamma-1)\partial_t\phi)$$

$$+ 2\epsilon(\partial_r\phi\,\partial_{rt}\phi + \partial_\theta\phi\,\partial_{\theta t}\phi/r^2) + (\underline{w}/\epsilon)((1 - \tfrac{1}{2}\epsilon\,\partial_t\phi)((1$$

$$+ ((\partial_r\phi)^2 + (\partial_\theta\phi/r)^2)/u_L^2)^{\frac{1}{2}} - 1) = 0 . \qquad (4.4)$$

Now, assume an approximate solution of the form

$$\phi = \sum_{m=0}^{P}\sum_{n=1}^{Q} J_m(S_{mn}r)\cos(m\theta)f_{mn}(t). \qquad (4.5)$$

Equation (4.5) is a superposition of the normal modes associated with the corresponding linear acoustic problem. A solution of this form allows one to investigate the influence of nonlinearities on the behavior of modal amplitudes which would exhibit simple harmonic motion in the linear case. Only standing modes can be described by (4.5). To represent spinning modes another series involving sin(mθ) must be added. This is omitted for simplicity in this discussion. It is convenient to rewrite (4.5) as

$$\phi = \sum_{j=1}^{N} J_{m_j}(S_{m_j n_j}r)\cos(m_j\theta)f_j(t) \qquad (4.6)$$

where N = (P + 1)Q .

The equation is now evaluated at N points (the collocation points) to yield

$$\phi_i = \sum_{j=1}^{N} C_{ij}f_j \qquad i = 1,2,\ldots N \qquad (4.7)$$

where
$$C_{ij} = J_{m_j}(S_{m_j n_j} r_i)\cos(m_j \theta_i). \tag{4.8}$$

Next, (4.7) is inverted to obtain

$$f_i = \sum_{j=1}^{N} C_{ij}^{-1} \phi_j. \tag{4.9}$$

Then the various derivatives of (4.6) can be expressed in terms of value of ϕ_i as

$$(\partial_r \phi)_i = \sum_{j=1}^{N} C_{ij}^{r} \phi_j, \quad (\partial_{rr}\phi)_i = \sum_{j=1}^{N} C_{ij}^{rr} \phi_j$$

$$(\partial_\theta \phi)_i = \sum_{j=1}^{N} C_{ij}^{\theta} \phi_j, \quad (\partial_{\theta\theta}\phi)_i = \sum_{j=1}^{N} C_{ij}^{\theta\theta} \phi_j \quad i=1,\ldots N \tag{4.10}$$

where
$$C_{ij}^{r} = (\partial_{r_i} C_{ik}) C_{kj}^{-1}, \quad C_{ij}^{rr} = (\partial_{r_i r_i} C_{ik}) C_{kj}^{-1}$$

$$C_{ij}^{\theta} = (\partial_\theta C_{ik}) C_{kj}^{-1}, \quad C_{ij}^{\theta\theta} = (\partial_{\theta_i \theta_i} C_{ik}) C_{kj}^{-1}. \tag{4.11}$$

Substituting into (4.4), a set of N ordinary second-order differential equations having the following form is generated.

$$\ddot{\phi}_i + \underline{w}\dot{\phi}_i - \sum_{j=1}^{N} C_{ij}^{\nabla} \phi_j (1-\epsilon(\gamma-1)\dot{\phi}_j) + 2\epsilon \sum_{j=1}^{N} \sum_{k=1}^{N} C_{ijk} \phi_j \dot{\phi}_k$$

$$+ (\underline{w}/\epsilon)((1-\tfrac{1}{2}\epsilon\dot{\phi}_i)(1 + \sum_{j=1}^{N} \sum_{k=1}^{N} C_{ijk} \phi_j \phi_k / u_L^2)^{\frac{1}{4}} - 1) = 0 \tag{4.12}$$

where
$$C_{ij}^{\nabla} = C_{ij}^{rr} + C_{ij}^{r}/r_i + C_{ij}^{\theta\theta}/r_i^2$$

$$C_{ijk} = C_{ij}^r C_{ik}^r + C_{ij}^\theta C_{ik}^\theta / r_i^2 . \tag{4.13}$$

Solutions were obtained by a fourth-order Runge-Kutta method to the set of equations (4.12). It was found that the results were very sensitive to the number and locations of collocation points, especially to the radial distribution of points. It was found that even in cases when $\underline{w}$ was equated to zero (no combustion) it was possible to find many choices of collocation points which lead to the computed modal amplitudes increasing without bound.

In order to illustrate the difficulties involved in a simple case, consider a one-dimensional problem of longitudinal wave motion with $\gamma = 1$, $\underline{u} = 0$ and $\underline{w} = 0$. In this case (4.2) reduces to

$$\partial_{tt}\phi - \partial_{zz}\phi + 2\epsilon(\partial_z\phi\partial_{zt}\phi) = 0 . \tag{4.14}$$

First consider the boundary condition

$$\partial_z\phi(0,t) = 0, \qquad \phi(\pi,t) = 0 . \tag{4.15}$$

A one-term solution satisfying (4.15) is

$$\phi = f(t)\cos(\tfrac{1}{2}z). \tag{4.16}$$

Applying the collocation method with a collocation point z_0 produces an equation for $\phi_0 = \phi(z_0,t)$ of the form

$$\ddot{\phi}_0 + \tfrac{1}{4}\dot{\phi}_0 + \tfrac{1}{4}(\tan^2(z_0/2)\phi_0\dot{\phi}_0) = 0. \tag{4.17}$$

The Galerkin method (to be discussed in detail in the next chapter) when applied to the same problem yields an equation for f of the form

$$\ddot{f} + \tfrac{1}{4}\dot{f} + 4\ f\dot{f}/(3\pi) = 0. \tag{4.18}$$

As another example consider the boundary conditions

$$\partial_z\phi(0,t) = 0, \qquad \partial_z\phi(\pi,t) = 0. \tag{4.19}$$

A solution satisfying (4.19) is

$$\phi = f(t)\cos(z) \tag{4.20}$$

for which the collocation method leads to

$$\ddot{\phi}_0 + \phi_0 - 2\varepsilon\tan^2 z_0 \phi_0\dot{\phi}_0 = 0 \tag{4.21}$$

and the Galerkin method leads to

$$\ddot{f} + f = 0. \tag{4.22}$$

From the above two cases, one can observe that the last term in each of the equations obtained by collocation can take on any value between 0 and ∞ depending on the location z_0 of the collocation point. No such difficulty is encountered when using the Galerkin method. Even if more points were used, the same behavior was obtained. Therefore

there appears to be no way to rationally decide which sets
of collocation points can produce the correct result. For
this reason, after the expenditure of much effort, the
collocation method was abandoned and the Galerkin method
was adopted. This will be discussed in the next chapter.

Chapter 5

THE GALERKIN METHOD

The Galerkin method is a special application of the method of weighted residuals (usually referred to as MWR). It has been extensively used in the solution of various stability and aeroelasticity problems (see for instance Powell (1)) and proved itself as a useful tool for the solution of both linear and nonlinear problems. Although it is an approximate mathematical technique, it has nevertheless produced results which were in excellent agreement with available exact solutions. These approximate solutions are usually simpler in form than the exact solutions obtained by numerical integration, and their quantitative evaluation requires considerably less computation time. However, this method is known to be reliable and applied conveniently only to equations involving nonlinearities of a polynomial type. Therefore, if this method is used in conjunction with the varporization-limited burning rate function of (4.1) the problem becomes intractable. Thus, the following simpler purely phenomenological burning-rate function was employed for the case of instantaneous combustion response.

$$w = \underline{w}nu^2 \qquad (5.1)$$

where n is a constant which will subsequently be referred to
as the interaction coefficient. It can be determined either
by comparison of predictions of the theory directly with
experiment or by comparison with burning rate laws meant to
apply to special types of combustion processes. As an
example of the latter method consider the vaporization-
limited burning rate law (4.1). As it stands (4.1) exhibits
both pressure and velocity sensitivity. A purely velocity
sensitive law can be obtained by assuming $\varepsilon \ll 1$ to get

$$w_v = (\underline{w}/\varepsilon^2)((1 + (u/u_L)^2)^{\frac{1}{4}} - 1) \tag{5.2}$$

where the v is used to denote the vaporization model. If one
equates the slopes of (5.1) and (5.2) at $u^2 = 0$ and plots
both functions, the graph would look as follows.
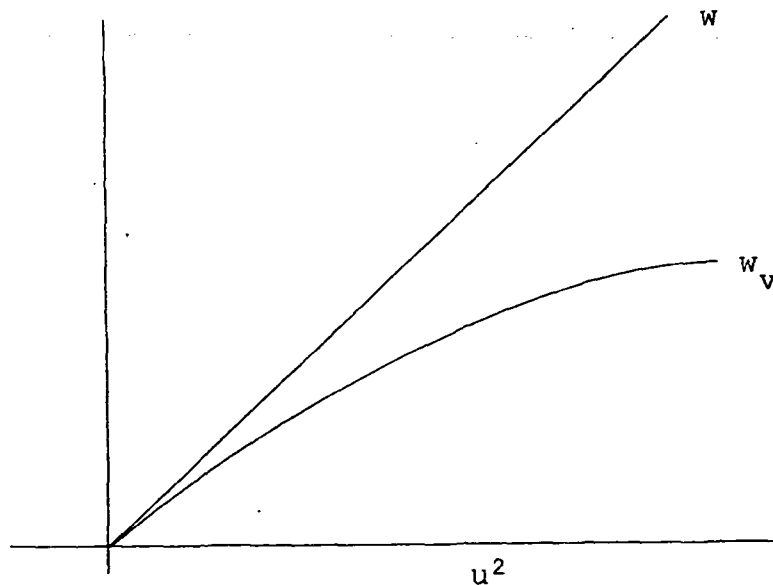
It can be seen that (5.1) would overestimate the burning rate. Thus the upper bound for n can be computed. From (5.1) and (5.2)

$$d_{u^2}w = \underline{w}n, \quad d_{u^2}w_v = (\underline{w}/(4\epsilon^2 u_L^2))/(1+(u/u_L)^2)^{3/4}.$$

Thus $\quad d_{u^2}w(0) = \underline{w}n, \quad d_{u^2}w_v(0) = \underline{w}/(4\epsilon^2 u_L^2).$

Equating these results, one gets

$$n_{m\bar{a}x} = 1/(4\epsilon^2 u_L^2). \qquad (5.3)$$

The phenomonological law (5.1) can be related to other special burning-rate laws in a similar manner.

If it is desired to consider history-dependent combustion processes, this can be done through the general formula

$$w = n\int_0^t G(t-\xi)d_\xi(u^2)d\xi \qquad (5.4)$$

where G is memory function and ξ is a dummy variable. If $G(t) = H(t)$ (H being the unit step function) all increments of change in u^2 occurring in the past are counted equally and (5.1) is recovered. If $G(t) = H(t) - H(t-\tau)$ all increments of change in u^2 are counted equally up to τ units of time in the past while those previous to that time are not counted at all. Substituting this expression into (5.4)

and integrating one obtains

$$w = \underline{w}n(u^2 - u_\tau^2) \tag{5.5}$$

where $u_\tau = u(t-\tau)$ and τ is called the time delay. Equation (5.5) will be used to account for the history of the burning process in a rough way. More sophisticated treatments of this phenomenon could be obtained by employing a more realistic function for G(t). Substituting (5.5) and (5.1) into (2.33a) one obtains

$$\partial_{tt}\phi - \nabla^2\phi + 2\underline{u}\partial_{zt}\phi + \underline{w}\partial_t\phi + \epsilon((\gamma-1)\nabla^2\phi\partial_t\phi + 2\vec{\nabla}\phi\cdot\vec{\nabla}\partial_t\phi$$

$$+ \underline{w}n(\vec{\nabla}\phi\cdot\vec{\nabla}\phi - j\vec{\nabla}\phi_\tau\cdot\vec{\nabla}\phi_\tau)) = 0 \tag{5.6}$$

where $j = 0$ for instantaneous combustion and $j = 1$ for history-dependent combustion.

The most general solution of (5.6) (subject to hard-wall boundary conditions for the unsteady variables) can be written in the form of the following Fourier-Bessel series.

$$\phi = f_{00}(t) + \sum_{n=1}^{\infty} f_{0n}(t)J_0(S_{0n}r)$$

$$+ \sum_{m=1}^{\infty}\sum_{n=1}^{\infty} (f_{mn}(t)\cos(m\theta)+g_{mn}(t)\sin(m\theta))J_m(S_{mn}r) \tag{5.7}$$

Substituting (5.7) into (5.6) and applying the usual Galerkin orthogonalization procedure leads to an infinite

set of coupled ordinary differential equations governing the functions f_{mn} and g_{mn}. No solution can be obtained unless the series (5.7) is truncated so as to produce a finite set of equations. If the terms neglected are actually small, an accurate solution will result.

In this thesis attention will be focused on initial disturbances having the form of the first tangential mode. The simplest finite series contained in (5.7) capable of modeling the effect of quadradic nonlinearities in (5.6) is

$$\phi = f_0(t)J_0(S_{01}r) + f_1(t)J_1(S_{11}r)\cos\theta + f_2(t)J_2(S_{21}r)\cos2\theta$$

$$+ g_1(t)J_1(S_{11}r)\sin\theta + g_2(t)J_2(S_{21}r)\sin2\theta. \qquad (5.8)$$

The Galerkin method then produces the following ordinary differential equations governing these five variables.

$$\ddot{f}_0 + \underline{w}\dot{f}_0 + S_{01}^2 f_0 + \epsilon(C_1 f_0\dot{f}_0 + C_2(f_1\dot{f}_1 + g_1\dot{g}_1)$$

$$+ C_3(f_2\dot{f}_2 + g_2\dot{g}_2) + \underline{w}n(C_{11}f_0^2 + C_{12}(f_1^2 + g_1^2) + C_{13}(f_2^2 + g_2^2)$$

$$-j(C_{11}f_{0\tau} + C_{12}(f_{1\tau}^2 + g_{1\tau}^2) + C_{13}(f_{2\tau}^2 + g_{2\tau}^2)))) = 0$$

$$\ddot{f}_1 + \underline{w}\dot{f}_1 + S_{11}^2 f_1 + \epsilon(C_4 f_0\dot{f}_1 + C_5 f_1\dot{f}_0 + C_6(g_1\dot{g}_2 + f_1\dot{f}_2)$$

$$+ C_7(g_2\dot{g}_1 + f_2\dot{f}_1) + \underline{w}n(C_{14}f_0 f_1 + C_{15}(f_1 f_2 + g_1 g_2)$$

$$- j(C_{14}f_{0\tau}f_{1\tau} + C_{15}(f_{1\tau}f_{2\tau} + g_{1\tau}g_{2\tau})))) = 0$$

$$\ddot{f}_2 + \underline{w}\dot{f}_2 + S_{21}^2 f_2 + \epsilon(C_8 f_0 \dot{f}_2 + C_9 f_2 \dot{f}_0 + C_{10}(g_1 \dot{g}_1 - f_1 \dot{f}_1)$$

$$+\underline{wn}(C_{16}(f_1^2 - g_1^2) + C_{17}f_0 f_2 - j(C_{16}(f_{1\tau}^2 - g_{1\tau}^2) + C_{17}f_{0\tau}f_{2\tau})))) = 0$$

$$\ddot{g}_1 + \underline{w}\dot{g}_1 + S_{11}^2 g_1 + \epsilon(C_4 f_0 \dot{g}_1 + C_5 g_1 \dot{f}_0 + C_6(f_1 \dot{g}_2 - g_1 \dot{f}_2)$$

$$+ C_7(g_2 \dot{f}_1 - f_2 \dot{g}_1) + \underline{wn}(C_{14}f_0 g_1 + C_{15}(f_1 g_2 - g_1 f_2)$$

$$- j(C_{14}f_{0\tau}g_{1\tau} + C_{15}(f_{1\tau}g_{2\tau} - g_{1\tau}f_{2\tau})))) = 0$$

$$\ddot{g}_2 + \underline{w}\dot{g}_2 + S_{21}^2 g_2 + \epsilon(C_8 f_0 \dot{g}_2 + C_9 g_2 \dot{f}_0 - C_{10}(g_1 \dot{f}_1$$

$$+ f_1 \dot{g}_1) + \underline{wn}(C_{17}f_0 g_2 + 2C_{16}f_1 g_1$$

$$- j(C_{17}f_{0\tau}g_{2\tau} + 2C_{16}f_{1\tau}g_{1\tau})))) = 0 \qquad (5.9)$$

The coefficients C_i (i=1,2,...17) are integrals of Bessel functions which must be computed numerically. The details of this calculation are discussed in appendix A.

The stability boundaries in the (n,ϵ) plane were determined first. For a given value of $\underline{w}$, a value of ϵ was selected and solutions were obtained for various values of n. In each case, if the modal amplitudes exhibited growth with time, the value of n was decreased for the next run while if decay of modal amplitudes was observed, the

value of n was increased accordingly. A systematic iteration process was devised so that the computer could carry out these calculations without analyst intervention. In this way,one point on the stability boundary was established. Then a new value of ϵ was chosen and the iteration process was repeated to determine another point on the stability boundary. This procedure (which consumed a considerable amount of computer time) was continued until enough points had been found to establish the shape of the stability boundary. It should be pointed out that the amplitude of the 1T mode always initially decreases due to the fact that purely velocity-sensitive combustion instability is always linearly stable. Thus it is necessary to continue the calculation for a considerable period of time to determine whether a given set of conditions corresponds to nonlinear stability or instability.

Figures 2 and 3 show some typical stability boundaries for instantaneous combustion using the initial conditions

$$f_1(0) = 1, \quad f_0(0) = f_2(0) = g_1(0) = g_2(0) = 0$$

$$\dot{f}_0(0) = \dot{f}_1(0) = \dot{f}_2(0) = \dot{g}_1(0) = \dot{g}_2(0) = 0 \qquad (5.10)$$

and $\quad f_1(0) = 1, \quad f_0(0) = f_2(0) = g_1(0) = g_2(0) = 0$

$$\dot{g}_1(0) = 1, \quad \dot{f}_0(0) = \dot{f}_1(0) = \dot{f}_2(0) = \dot{g}_2(0) = 0, \quad (5.11)$$

respectively. The region below and to the left of the stability boundary is associated with stable conditions, while the region above and to the right is associated with unstable conditions.

In the case of linear acoustics, the first set of initial conditions would lead to a standing wave and the second set of initial conditions corresponds to a traveling wave. In both cases,it can be seen that the stability boundaries have roughly the forms of rectangular hyperbolas. As expected, increasing the steady-state burning rate reduces the value of n required to produce instability. This effect is somewhat more pronounced for the traveling waves than for the standing waves. There does not appear to be a distinct pattern to the results. Thus for $\underline{w}$ = 0.2 standing waves are more stable than traveling waves while for $\underline{w}$ = 0.1 traveling waves are more stable than standing waves.

Figures 4 and 5 show stability boundaries associated with initial conditions (5.10) and (5.11), respectively, for history-dependent combustion. It is apparent that the influence of the time delay parameter on the results for standing waves is much greater than on the results for traveling waves. Again, no clear pattern emerges from the results. Comparing Figures 2 and 4, and 3 and 5 shows that instantaneous combustion can be either more or less stable than history dependent combustion depending on the value of the time-delay parameter. Comparing Figures 4 and 5, it can be seen that standing waves can be either more or less

stable than standing waves for history dependent combustion.
Figures 4 and 5 also illustrate the fact that increasing the
amount of time delay can either increase or decrease the
stability of the system. Thus, for both standing and
traveling waves, $\tau = \pi$ corresponds to a more stable situation
than either $\tau = 0.5\pi$ or $\tau = 1.5\pi$. The lack of patterns
exhibited by these results emphasizes the need for numerical
methods of the type developed during the present research.
It appears that the only way to find out what will happen in
a given situation is to solve the equations for that
particular case. This matter will be discussed further
subsequently.

The pressure perturbation can be calculated from the
velocity potential perturbation by substituting equation
(5.8) into (2.33c), expanding the result in a Fourier-Bessel
series and retaining only the terms corresponding to the 1T,
2T and 1R modes to obtain

$$P = - \gamma((d_{01}\dot{f}_0 + \varepsilon(d_{02}f_0^2 + d_{03}(f_1^2 + g_1^2) + d_{04}(f_2^2 + g_2^2)$$

$$+ d_{05}\dot{f}_0^2 + d_{06}(\dot{f}_1^2 + \dot{g}_1^2) + d_{07}(\dot{f}_2^2 + \dot{g}_2^2)))J_0(S_{01}r)$$

$$+ ((d_{11}\dot{f}_1 + \varepsilon(d_{12}f_0f_1 + d_{13}(f_1f_2 + g_1g_2) + d_{14}\dot{f}_0\dot{f}_1$$

$$+ d_{15}(\dot{f}_1\dot{f}_2 + \dot{g}_1\dot{g}_2)))\cos\theta$$

$$+ (d_{11}\dot{g}_1 + \epsilon(d_{12}f_0\dot{g}_1 + d_{13}(\dot{f}_1 g_1 - g_1 \dot{f}_2) + d_{14}f_0\dot{g}_1$$

$$+ d_{15}(\dot{f}_1 \dot{g}_2 - \dot{f}_2 \dot{g}_1)))\sin\theta)J_1(S_{11}r)$$

$$+ ((d_{21}\dot{f}_2 + \epsilon(d_{22}f_0\dot{f}_2 + d_{23}(f_1^2 - g_1^2) + d_{24}\dot{f}_0\dot{f}_2$$

$$+ d_{25}(\dot{f}_1^2 - \dot{g}_1^2)))\cos2\theta$$

$$+ (d_{21}\dot{g}_1 + \epsilon(d_{22}f_0\dot{g}_2 + 2d_{23}\dot{f}_1 g_1 + d_{24}\dot{f}_0\dot{g}_2$$

$$+ 2d_{25}\dot{f}_1 \dot{g}_1))\sin2\theta)J_2(S_{21}r)). \hspace{2cm} (5.12)$$

The coefficients d_{0s}, d_{1s}, d_{2s} are calculated in the same fashion as those discussed previously and the values are listed in table 8 of the appendix.

Some typical results for wall pressure waveforms are presented in figures 6 through 37.

Figures 6 through 9 correspond to instantaneous combustion with $\epsilon = .05$, $\underline{w} = .1$, $n = 175$, and initial conditions (5.10). This leads to a stable standing wave oscillation and the pressure can be observed to decrease gradually. However, by changing the interaction index to $n = 220$ (Figures 10-13) the pressure is seen to grow gradually. This is an unstable situation. In both cases the response is dominated by the 1T mode but distorted to some extent by the presence of the 2T and 1R components.

Figures 14 through 17 correspond to history-dependent

combustion with n = 345, while the other parameters are the same as before. This is a stable situation and the amplitude of the pressure slowly decays with time.

Figures 18 through 21 are obtained by changing the interaction index to n = 352. This is an unstable situation as indicated by the growth of the pressure amplitude with time. In both of these cases the presence of the 2T and 1R components is much more noticable than it was in the first two situations.

Figures 22 through 25 correspond to instantaneous combustion with n = 180, ε = .05, $\underline{w}$ = .1, and initial condition (5.11). This produces a traveling wave. The pressure is observed to be decreasing with time (a stable situation) while changing the interaction index n to 210 (Figures 26 through 29) causes the pressure to increase (an unstable situation). Figures 30 through 37 show the significance of the time delay function. Figures 30 through 33 are obtained by setting τ = π and n = 197. This is a stable case. The pressure is observed to decrease. Setting n = 199 (Figures 34 through 37), on the other hand, produces an unstable situation when the pressure increases very rapidly. In both of these situations the response appears to be dominated by 2T contribution to the pressure.

From these figures one can conclude that the pressure waveforms exhibit a strong second harmonic distortion and this distortion arises from the effect of the quadratic nonlinear terms. A variety of behaviors are possible

depending on the nature of the combustion process and the parametric values involved.

Chapter 6

ONE-DIMENSIONAL MODEL

In this chapter an annular combustion chamber with a
gap width much smaller than the inner radius is considered.
This geometry will henceforth be referred to as that of a
narrow annulus. While this geometry is not of much practical
interest,it is quite useful for the purposes of analysis.
This is because only one space coordinate is needed to
describe the problem. This makes a direct finite-difference
numerical solution of the original partial differential
equation feasible and also simplifies the algebra required
to carry out the Galerkin modal analysis. In what follows
three questions will be investigated. First,the effect of
changing the numerical values of certain coefficients
appearing in the governing equations for the modal amplitudes
will be discussed. Second,the Galerkin solution will be
checked using a finite difference numerical solution of the
complete equation. Third, numerical solutions of the
complete wave equation using the vaporization-limited
burning-rate law will be compared to similar solutions
associated with the phenomenological burning-rate law
employed in the previous chapter.

The appropriate wave equation for transverse wave
motion in a narrow annulus can be obtained from (5.6) by

setting $r = 1$ and $\partial_r = 0$. To further simplify the results the parametic values $\gamma = 1$ (isothermal process) and $j = 0$ (instantenous burning response) will be employed. For this situation (5.6) simplifies to

$$\partial_{tt}\phi + \underline{w}\partial_t\phi - \partial_{\theta\theta}\phi + 2\epsilon\partial_\theta\phi\partial_{\theta t}\phi + \underline{w}n\epsilon(\partial_\theta\phi)^2 = 0. \quad (6.1)$$

To carry out the modal analysis, it is assumed that the potential function can be expressed as

$$\phi = f_1(t)\cos\theta + f_2(t)\cos2\theta + g_1(t)\sin\theta + g_2(t)\sin2\theta. \quad (6.2)$$

Then applying the usual Galerkin orthogonalization procedure leads to

$$\ddot{f}_1 + \Omega_1^2 f_1 + \underline{w}\dot{f}_1 + \epsilon A_1(f_1\dot{f}_2 + f_2\dot{f}_1 + g_1\dot{g}_2 + g_2\dot{g}_1)$$

$$+ \epsilon\underline{w}nA_2(f_1f_2 + g_1g_2) = 0$$

$$\ddot{f}_2 + \Omega_2^2 f_2 + \underline{w}\dot{f}_2 + \epsilon A_3(g_1\dot{g}_1 - f_1\dot{f}_1) + \epsilon\underline{w}nA_4(g_1^2 - f_1^2) = 0$$

$$\ddot{g}_1 + \Omega_1^2 g_1 + \underline{w}\dot{g}_1 + \epsilon A_1(g_2\dot{f}_1 + f_1\dot{g}_2 - g_1\dot{f}_2 - f_2\dot{g}_1)$$

$$+ \epsilon\underline{w}nA_2(f_1g_2 - g_1f_2) = 0$$

$$\ddot{g}_2 + \Omega_2^2 g_2 + \underline{w}\dot{g}_2 - \epsilon A_3(g_1\dot{f}_1 + f_1\dot{g}_1) - 2\epsilon\underline{w}nA_4f_1g_1 = 0 \quad (6.3)$$

where $\Omega_1 = 1$, $\Omega_2 = 2$, $A_1 = 2$, $A_2 = 2$, $A_3 = 1$ and $A_4 = .5$. The symbols Ω_1, Ω_2, A_1, A_2, A_3 and A_4 have been inserted to illustrate the effect of changing their numerical values.

McDonald (7) in his analysis of combustion-instability in an annulus found that for a given value of ε the value of n required to produce instability was approximately twice as high for standing waves as for traveling waves. The results discussed in the previous chapter for a full cylinder indicated no such relationship. Equations (6.3) were employed in an attempt to determine the factors which have a significant effect on the stability boundary. Several calculations were made and a representative sample of the data thus obtained is presented in Tables 1 and 2. It was determined by McDonald that the terms representing gas-dynamic nonlinearities, had a small qualitative effect on stability calculations. Thus the coefficients A_1 and A_3 were held fixed during these calculations.

The entries in the first two lines of each table were computed using the correct equation for an annulus. It can be seen that the standing wave is twice as stable as the traveling wave, in agreement with the results of McDonald. The third and fourth lines in each table were computed by changing A_4 from .5 to .77 (This makes the ratio A_4/A_3 the same as the ratio of the corresponding terms in the governing equations for the full cylinder.). It can be seen that this lowers the stability limit in all cases but does not alter the fact that an initial disturbance in the

Table 1

Stability Limits for Standing Wave
in Annular Combustor

n	Ω_2	A_4	ε
91	2	.5	.05
46	2	.5	.1
74	2	.77	.05
37	2	.77	.1
735	1.66	.5	.05
379	1.66	.5	.1
595	1.66	.77	.05
307	1.66	.77	.1

Table 2

Stability Limits for Traveling Wave
in Annular Combustor

n	Ω_2	A_4	ε
44	2	.5	.05
22	2	.5	.1
36	2	.77	.05
18	2	.77	.1
66	1.66	.5	.05
31	1.66	.5	.1
54	1.66	.77	.05
26	1.66	.77	.1

form of a standing wave is twice as stable as one in the form of a traveling wave.

The fifth and sixth lines in Tables 1 and 2 are found by restoring A_4 to its original value .5 and changing Ω_2 from 2.00 to 1.66 (This makes the ratio Ω_2/Ω_1 equal to the ratio S_{21}/S_{11} associated with the full cylinder.). For this situation it can be seen that the standing wave is approximately ten times as stable as the traveling wave. Furthermore, the effect of the value of Ω_2 on the location of stability boundary is much greater for a standing-wave motion than for a traveling-wave motion. The last two lines are associated with implementing both of the changes discussed above simultaneously. These results confirm that the change in A_4 lowers the stability limit in all cases but does not affect the relative stability of standing-wave and traveling-wave disturbances.

The data presented above indicate that standing waves will be twice as stable as traveling waves only under very special circumstances ($\Omega_2/\Omega_1 \approx 2$). There is no reason to expect this to be a characteristic of other systems exhibiting combustion instability as, in fact, it is not for a full cylinder.

In this section, a finite different procedure is employed to generate a set of second order differential equations. The central difference formulas

$$\partial_\theta \phi_i = (\phi_{i+1} - \phi_{i-1})/(2\Delta\theta)$$

$$\partial_{\theta\theta}\phi_i = (\phi_{i+1} - 2\phi_i + \phi_{i-1})/(\Delta\theta)^2 \qquad (6.4)$$

are used to produce the following set of governing equations

$$\ddot{\phi}_i = -\underline{w}\dot{\phi}_i + (\phi_{i+1} - 2\phi_i + \phi_{i-1})(1 - \epsilon(\gamma-1)\dot{\phi}_i)/(\Delta\theta)^2$$

$$- \epsilon(\phi_{i+1} - \phi_{i-1})(\dot{\phi}_{i+1} - \dot{\phi}_{i-1})/(2\Delta\theta)^2$$

$$- \epsilon w_i \qquad\qquad 2 < i < N - 1 \qquad (6.5)$$

where N is the number of points employed. A forward difference formula

$$\partial_\theta\phi_1 = (-3\phi_1 + 4\phi_2 - \phi_3)/(2\Delta\theta) \qquad (6.6)$$

and backward difference formula

$$\partial_\theta\phi_N = (\phi_{N-2} - 4\phi_{N-1} + 3\phi_N)/(2\Delta\theta) \qquad (6.7)$$

are used for the boundary conditions

$$\partial_\theta\phi(0) = 0, \qquad\qquad \partial_\theta\phi(\pi) = 0. \qquad (6.8)$$

Hence, along the boundaries, (6.5) becomes

$$\ddot{\phi}_2 = -\underline{w}\dot{\phi}_2 + 2(\phi_3 - \phi_2)(1 - \epsilon(\gamma-1)\dot{\phi}_2)/(3\Delta\theta^2)$$

$$- 8\varepsilon(\phi_3 - \phi_2)(\dot{\phi}_3 - \dot{\phi}_2)/(9\Delta\theta^2) - \varepsilon w_2$$

and
$$\ddot{\phi}_{N-1} = -\underline{w}\dot{\phi}_{N-1} + 2(\phi_{N-2} - \phi_{N-1})(1-\varepsilon(\gamma-1)\dot{\phi}_{N-1})/(3\Delta\theta^2)$$

$$- 8\varepsilon(\phi_{N-1} - \phi_{N-2})(\dot{\phi}_{N-1} - \dot{\phi}_{N-2})/(9\Delta\theta^2) - \varepsilon w_{N-1}. \quad (6.9)$$

For the phenomenological model, the burning rate function becomes

$$w_i = n\underline{w}(\phi_{i+1} - \phi_{i-1})^2/(4\Delta\theta^2) \quad 2 < i < N-1. \quad (6.10)$$

Combining (6.8) and (6.10) one obtains

$$w_2 = 4n\underline{w}(\phi_3 - \phi_2)^2/(9\Delta\theta^2)$$

$$w_{N-1} = 4n\underline{w}(\phi_{N-1} - \phi_{N-2})^2/(9\Delta\theta^2) \quad (6.11)$$

respectively.

For the vaporization model, the burning rate function becomes

$$w_i = \underline{w}((1 - \varepsilon\dot{\phi}_i/2)(1 + (\phi_{i+1}$$

$$- \phi_{i-1})^2/(2\Delta\theta u_L)^2)^{\frac{1}{4}} - 1)/\varepsilon^2 \quad 2 < i < N-1 \quad (6.12)$$

and, along the boundary, yields

$$w_2 = \underline{w}((1 - \tfrac{1}{2}\epsilon\dot{\phi}_2)(1 + (2(\phi_3 - \phi_2)/(3\Delta\theta u_L))^2)^{\frac{1}{4}} - 1)/\epsilon^2$$

$$w_{N-1} = \underline{w}((1-\tfrac{1}{2}\epsilon\dot{\phi}_{N-1})(1+(2(\phi_{N-1}-\phi_{N-2})/(3\Delta\theta u_L))^2)^{\frac{1}{4}}-1)/\epsilon^2, \quad (6.13)$$

accordingly.

Using either the phenomonological or the vaporization-limited combustion model,(6.5) and (6.9) can be solved by the Runge-Kutta method to obtain ϕ_i, i = 2,3,..., N-1. Then the modal amplitudes can be obtained by using the Fourier-cosine transform

$$f_i(t) = 2\int_0^\pi \phi\cos i\theta d\theta/\pi. \quad (6.14)$$

These integrals must be computed numerically since ϕ is known only at the grid points.

Some typical results for standing waves are presented in Table 3. They are intended to illustrate the accuracy of the two-term Galerkin solution and to compare the results associated with the phenomenological and vaporization-limited combustion laws. The column labeled PG indicates the results with a two-term Galerkin solution using the phenomenological model, the column labeled PF contains the results of a finite-difference solution of these equations, and the column labeled VF presents results of a finite difference solution using the vaporization-limited model.

Table 3

Stability Limits For Phenomenological and
Vaporization-Limited Combustion Model

	PG	PF	VF
ε	n	n	u_L
.1	46	28	1.3
.05	91	56	2.1
.01	452	286	5.2

It can be seen that the order of magnitude of the
interaction index n required for instability for both the
finite difference and Galerkin methods are roughly the same
but the stability boundaries predicted by the Galerkin method
are approximately twice as high as those predicted by the
Finite-difference method. It is to be expected that the
Galerkin method will lead to higher stability limits than
the use of an exact solution procedure. This can be explained
as follows. The instability mechanism is basically a feed-
back process. Consider the form of (6.3) associated with
standing waves in an annulus. This is

$$\ddot{f}_1 + \underline{w}\dot{f}_1 + f_1 + 2\varepsilon(f_1\dot{f}_2 + f_2\dot{f}_1) + 2\varepsilon\underline{w}nf_1f_2 = 0$$

$$\ddot{f}_2 + \underline{w}\dot{f}_2 + 4f_2 - \varepsilon f_1\dot{f}_1 - \tfrac{1}{2}\varepsilon\underline{w}nf_1^2 = 0. \qquad (6.14)$$

For clarity the gas-dynamic nonlinearities will be neglected to give

$$\ddot{f}_1 + \underline{w}\dot{f}_1 + f_1 + 2\epsilon\underline{w}nf_1f_2 = 0$$

$$\ddot{f}_2 + \underline{w}\dot{f}_2 + 4f_2 - \tfrac{1}{2}\epsilon\underline{w}nf_1^2 = 0. \qquad (6.15)$$

A one-term Galerkin solution would lead to the equation

$$\ddot{f}_1 + \underline{w}\dot{f}_1 + f_1 = 0.$$

This would indicate unconditional stability. Instability can arise only when the presence of the last term in (6.15b) causes f_2 to grow and this then causes f_1 to grow because of the last term in (6.15a). The growth of f_2 also produces the growth of higher modes which in turn causes additional growth of f_1. The contributions of these higher modes are neglected in a two-term Galerkin analysis and thus the energy input due to unsteady burning is underestimated. For this reason the Galerkin analysis will overestimate the stability of the system. This overestimation will decrease as the number of terms retained is increased. An example of this can be seen by comparing the one- and two-term analyses. A one-term solution predicts that the system is always stable. A two-term solution predicts the correct qualitative behavior but overestimates the system's stability by

roughly a factor of two. It is to be expected that further increases in accuracy can be obtained by keeping more terms in the assumed solution but that this will not seriously affect the quatitative prediction.

In Chapter 5, it was found that equating dw/du_L^2 the phenomenological and vaporization-limited combustion laws at $u^2 = 0$ lead to the formula

$$n = 1/(4\epsilon^2 u_L^2).$$

(6.16)

Assuming that the actual data can be fitted to a formula of the form

$$n = C/(4\epsilon^2 u_L^2)$$

(6.17)

the data give in Table 3 provide an opportunity to estimate C. The results are shown below.

ϵ	.1	.05	.01
C	1.89	2.47	3.09

It appears that a value of C = 2.5 would give acceptable accuracy over this range of ϵ.

For a given value of u_L the n computed from (6.16) will overestimate the burning rate. Thus it might be thought that C should be less than unity. The stability criterion was, however, based on the magnitude of the modal amplitudes. Inspection of Tables 4 and 5 shows that the

vaporization-limited combustion model involves the higher
modes to a greater extent than does the phenomenological
combustion model. Thus, a given value of u_L can be associated
with lower individual modal amplitudes in the former case
than in the latter. These two effects interact and calcula-
tion shows that C is greater than unity in this range of ϵ.

TABLE 4

MODAL AMPLITUDE FOR PHENOMENLOGICAL MODEL
IN ANNULAR COMBUSTOR

T	MODE 1	MODE 2	MODE 3	MODE 4	MODE 5	MODE 6	MODE 7	MODE 8
0.00	1.000	0.000	-0.000	0.000	-0.000	0.000	-0.000	0.000
1.25	0.337	0.029	0.002	0.000	0.000	-0.000	-0.000	-0.000
2.50	-0.687	-0.018	-0.000	0.000	0.000	-0.000	0.000	0.000
3.75	-0.700	0.064	-0.008	0.001	-0.000	0.000	0.000	-0.000
5.00	0.209	-0.043	0.009	-0.001	-0.000	0.000	-0.000	0.000
6.25	0.751	0.040	-0.006	-0.003	-0.001	0.000	0.000	0.000
7.50	0.237	0.025	0.000	-0.002	-0.001	-0.000	-0.000	-0.000
8.75	-0.535	-0.060	0.015	0.004	-0.002	-0.000	0.000	0.000
10.00	-0.523	0.105	-0.028	0.009	-0.003	0.001	-0.000	0.000
11.25	0.187	-0.088	0.024	-0.000	-0.003	0.002	-0.000	-0.000
12.50	0.585	0.062	-0.009	-0.011	-0.005	-0.001	0.001	0.001
13.75	0.153	0.011	-0.010	-0.010	-0.006	-0.003	-0.002	-0.001
15.00	-0.440	-0.065	0.032	0.007	-0.007	-0.001	0.002	0.000
16.25	-0.390	0.112	-0.043	0.020	-0.010	0.005	-0.002	0.001
17.50	0.183	-0.105	0.030	0.005	-0.010	0.004	0.001	-0.002
18.75	0.463	0.078	-0.004	-0.017	-0.013	-0.004	0.001	0.002
20.00	0.085	-0.009	-0.023	-0.020	-0.014	-0.008	-0.004	-0.002
21.25	-0.374	-0.050	0.045	0.004	-0.015	0.001	0.006	-0.000
22.50	-0.287	0.101	-0.048	0.028	-0.018	0.011	-0.007	0.003
23.75	0.184	-0.107	0.025	0.015	-0.018	0.005	0.004	-0.005
25.00	0.371	0.089	0.009	-0.016	-0.019	-0.010	0.001	0.005
26.25	0.030	-0.031	-0.037	-0.030	-0.020	-0.012	-0.006	-0.002
27.50	-0.327	-0.027	0.052	-0.005	-0.021	0.005	0.010	-0.002
28.75	-0.206	0.081	-0.044	0.030	-0.023	0.017	-0.011	0.006
30.00	0.191	-0.102	0.013	0.028	-0.023	0.003	0.008	-0.006
31.25	0.302	0.098	0.026	-0.009	-0.023	-0.017	-0.003	0.004
32.50	-0.019	-0.054	-0.051	-0.038	-0.024	-0.012	-0.004	0.001
33.75	-0.297	0.000	0.056	-0.019	-0.024	0.012	0.010	-0.005
35.00	-0.141	0.058	-0.034	0.027	-0.024	0.020	-0.013	0.008
36.25	0.207	-0.095	-0.005	0.040	-0.023	-0.003	0.012	-0.005
37.50	0.252	0.108	0.046	0.004	-0.023	-0.022	-0.008	0.001
38.75	-0.067	-0.079	-0.064	-0.042	-0.022	-0.007	0.002	0.005
40.00	-0.284	0.031	0.056	-0.036	-0.020	0.019	0.005	-0.008
41.25	-0.085	0.033	-0.019	0.018	-0.019	0.016	-0.010	0.007
42.50	0.236	-0.087	-0.029	0.052	-0.017	-0.013	0.013	-0.001
43.75	0.218	0.120	0.070	0.023	-0.014	-0.022	-0.014	-0.006
45.00	-0.122	-0.109	-0.076	-0.039	-0.011	0.006	0.012	0.010
46.25	-0.292	0.070	0.049	-0.055	-0.007	0.025	-0.007	-0.008
47.50	-0.029	-0.001	0.005	-0.001	-0.003	0.002	0.000	-0.000
48.75	0.290	-0.073	-0.063	0.058	0.003	-0.026	0.007	0.009
50.00	0.192	0.135	0.098	0.053	0.011	-0.008	-0.014	-0.013
51.25	-0.207	-0.152	-0.081	-0.020	0.016	0.026	0.019	0.006
52.50	-0.328	0.134	0.022	-0.073	0.026	0.015	-0.022	0.006
53.75	0.055	-0.060	0.055	-0.044	0.034	-0.028	0.022	-0.015
55.00	0.404	-0.033	-0.119	0.037	0.046	-0.022	-0.020	0.012
56.25	0.151	0.140	0.125	0.094	0.061	0.038	0.019	0.008
57.50	-0.403	-0.219	-0.045	0.054	0.065	0.025	-0.013	-0.022
58.75	-0.412	0.276	-0.092	-0.036	0.071	-0.051	0.013	0.012
60.00	0.324	-0.246	0.183	-0.117	0.060	-0.017	-0.011	0.022

TABLE 5

MODAL AMPLITUDE FOR VAPORIZATION MODEL
IN ANNULAR COMBUSTOR

T	MODE 1	MODE 2	MODE 3	MODE 4	MODE 5	MODE 6	MODE 7	MODE 8
0.00	1.000	0.000	-0.000	0.000	-0.000	0.000	-0.000	0.000
1.25	0.384	-0.193	0.039	-0.007	0.002	-0.001	0.000	-0.000
2.50	-0.455	0.095	-0.033	0.009	-0.002	0.000	0.000	-0.000
3.75	-0.514	-0.111	0.042	0.018	-0.007	-0.003	0.002	0.000
5.00	0.060	-0.035	-0.036	-0.029	-0.020	-0.012	-0.007	-0.003
6.25	0.443	0.106	-0.022	-0.041	-0.021	-0.002	0.006	0.006
7.50	0.293	-0.225	0.077	0.020	-0.043	0.019	0.007	-0.013
8.75	-0.324	0.160	-0.104	0.071	-0.049	0.034	-0.024	0.017
10.00	-0.717	-0.029	0.192	-0.037	-0.072	0.042	0.020	-0.032
11.25	-0.224	-0.455	-0.330	-0.172	-0.040	0.041	0.065	0.047
12.50	1.281	0.558	0.300	0.131	0.040	-0.003	-0.021	-0.030
13.75	2.176	-0.505	-0.474	0.087	0.172	0.024	-0.078	-0.053
15.00	0.264	-0.967	0.644	-0.327	0.068	0.076	-0.105	0.057
16.25	-2.907	0.857	-0.311	0.100	-0.053	0.005	0.019	-0.031
17.50	-3.416	-1.125	0.382	0.037	-0.193	0.052	0.072	-0.074
18.75	0.448	-0.794	-0.551	-0.324	-0.057	0.085	0.110	0.056
20.00	3.619	0.546	0.200	0.077	0.001	-0.024	-0.039	-0.044
21.25	2.747	-1.259	-0.224	0.106	0.166	-0.024	-0.087	-0.025
22.50	-1.442	-0.328	0.340	-0.271	0.145	-0.042	-0.032	0.063
23.75	-3.229	0.136	-0.113	-0.068	0.068	-0.080	0.058	-0.038
25.00	-1.329	-1.066	0.005	0.181	-0.028	-0.102	0.012	0.059
26.25	1.794	0.024	-0.009	-0.085	-0.086	-0.083	-0.067	-0.049
27.50	2.388	-0.063	-0.093	-0.167	-0.089	-0.030	0.022	0.041
28.75	0.463	-0.881	0.235	0.090	-0.114	-0.006	0.069	-0.027
30.00	-1.807	0.272	-0.195	0.095	-0.067	0.043	-0.031	0.021
31.25	-2.088	-0.294	0.261	-0.143	-0.024	0.075	-0.052	-0.003
32.50	-0.063	-0.796	-0.404	-0.100	0.077	0.093	0.025	-0.040
33.75	2.115	0.417	0.250	0.120	0.079	0.049	0.033	0.021
35.00	2.172	-0.647	-0.302	-0.018	0.128	0.062	-0.032	-0.059
36.25	-0.447	-0.603	0.422	-0.241	0.058	0.049	-0.079	0.050
37.50	-2.586	0.434	-0.193	0.046	-0.004	-0.025	0.035	-0.039
38.75	-2.044	-1.000	0.179	-0.126	-0.127	-0.044	0.074	0.000
40.00	1.142	-0.253	-0.260	-0.241	-0.154	-0.072	-0.004	0.038
41.25	2.848	0.253	0.055	-0.083	-0.089	-0.081	-0.054	-0.027
42.50	1.497	-1.140	0.032	0.196	0.007	-0.109	0.006	0.063
43.75	-1.721	0.082	0.011	-0.091	0.095	-0.093	0.077	-0.057
45.00	-2.759	-0.014	0.116	-0.188	0.105	-0.038	-0.020	0.044
46.25	-0.807	-1.084	-0.251	0.126	0.118	-0.033	-0.081	-0.012
47.50	2.050	0.301	0.193	0.083	0.050	0.024	0.010	-0.001
48.75	2.514	-0.289	-0.260	-0.186	-0.011	0.062	0.068	0.023
50.00	0.206	-0.932	0.405	-0.043	-0.117	0.082	0.014	-0.063
51.25	-2.255	0.397	-0.263	0.134	-0.096	0.066	-0.051	0.040
52.50	-2.287	-0.575	0.312	-0.076	-0.106	0.084	-0.002	-0.053
53.75	0.331	-0.709	-0.439	-0.200	-0.000	0.083	0.074	0.017
55.00	2.477	0.407	0.229	0.082	0.038	0.004	-0.011	-0.021
56.25	2.025	-0.858	-0.236	0.073	0.141	-0.002	-0.072	-0.031
57.50	-0.915	-0.377	0.322	-0.252	0.129	-0.030	-0.036	0.060
58.75	-2.669	0.303	-0.109	-0.033	0.057	-0.068	0.057	-0.042
60.00	-1.588	-1.060	0.038	0.179	-0.051	-0.099	0.028	0.055

Chapter 7

CONCLUSIONS

The primary objective of this study was the
development of a new analytical technique to be used in the
solution of nonlinear velocity-sensitive combustion
instability problems. Such a method should be relatively
easy to apply and should require relatively little
computation time.

In an attempt to achieve this aim, the orthogonal
collocation method was investigated first. However, it was
found that the results were heavily dependent on the location
of the collocation points and characteristics of the
equations. Therefore, the method was rejected as unreliable.

Next, the Galerkin method, which has proved to be
very successful in analysis of the pressure sensitive
combustion instability, was considered. This method proved
to work very well. It was found that the pressure waveforms
exhibit a strong second harmonic distortion and a variety
of behaviors are possible depending on the nature of the
combustion process and the parametric values involved.

Finally, a one-dimensional model provided further
insight into the problem by allowing a comparison of
Galerkin solutions with more exact finite-difference
computations.

Some major conclusions of this research are as follows. (1) The form of (2.33a) is somewhat insensitive to the specific assumptions used to derive it. This is demonstrated by the fact that Powell (1) developed an equation of a very similar form using a different set of assumptions. (2) The orthogonal collocation method is unsuited to solution of problems of the type under discussion here. (3) The Galerkin method is well suited to the solution of such problems. (4) Stability boundaries and pressure wave forms appear to be highly dependent on the parameters of the problem (interaction index, time delay, steady-state burning rate, etc.). Furthermore,there appears to be no clear pattern to the computed results. (5) The phenomenological burning-rate law employed in the majority of the work discussed predicts results which are qualitatively similar to those associated with the vaporization-limited burning-rate law used by previous investigators. The phenomenological law, furthermore, can be used in conjunction with the Galerkin method while the vaporization-limited law cannot. (6) The computer programs developed in the course of this work can be employed to determine stability boundaries and pressure waveforms without the expenditure of excessive computer time. This is important because the lack of clear trends discussed above make an individual analysis of each situation desirable.

REFERENCES

1. Powell, E. A., "Nonlinear Combustion Instability in Liquid Propellant Rocket Engines," Ph. D. Dissertation, Georgia Institute of Technology, 1970.

2. Maslen, S. H., and Moore, F. K., "On strong Transverse Waves without Shocks in a Circular Cylinder," Journal of Aeronautical Sciences, Vol. 23 (1956), pp. 533-593.

3. Priem, R. J., and Guentert, D. C., "Combustion Instability Limits Determined by a Nonlinear Theory and a One-Dimensional Model," TN-1409, NASA Lewis Research Center (1962).

4. Powell, E. A., and Zinn, B. T., "A Single Mode Approximation in The Solution of Nonlinear Combustion Instability Problems," Combustion Science and Technology, Vol. 3 (1971), pp. 121-132.

5. Lores, M. E., and Zinn, B. T., "Nonlinear Longitudinal Combustion Instability in Rocket Motors," Combustion Science and Technology, Vol. 7 (1973), pp. 245-256.

6. Peddieson, J., Jr., Ventrice, M. B., and Purdy, K. R., "Effects of Nonlinear Combustion on the Stability of a Liquid Propellant System," Proceedings of 14th JANNAF Combustion Meeting (CPIA Publication 292), pp. 525-538 (1977).

7. McDonald, G. H., "Stability Analysis of A Liquid Fuel Annular Combustion Chamber," M. S. Thesis, TENN. TECH. UNIV., August 1979.
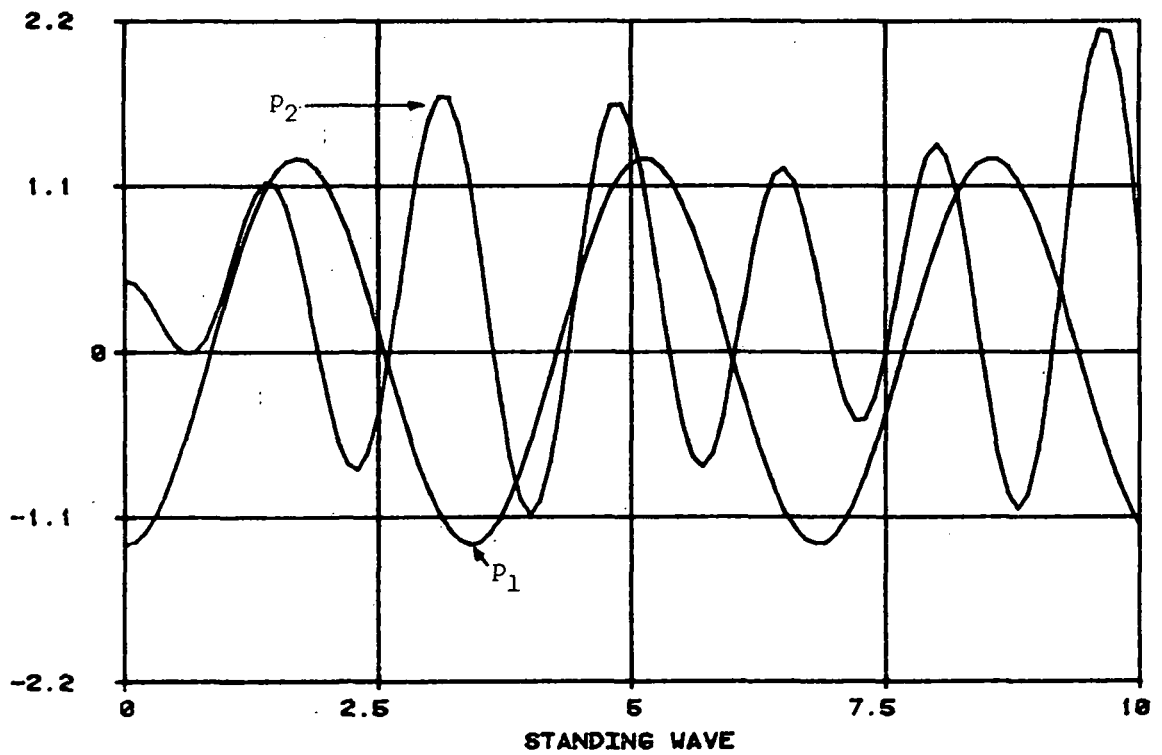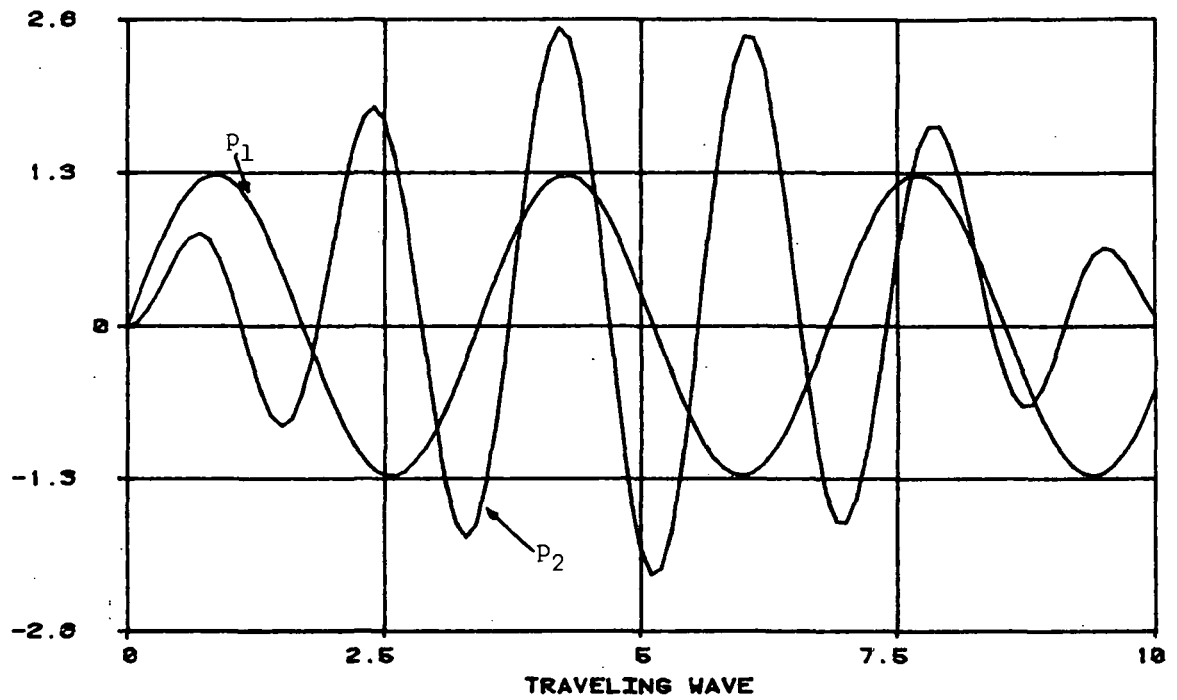
Figure 1. Pressure functions for standing and traveling waves
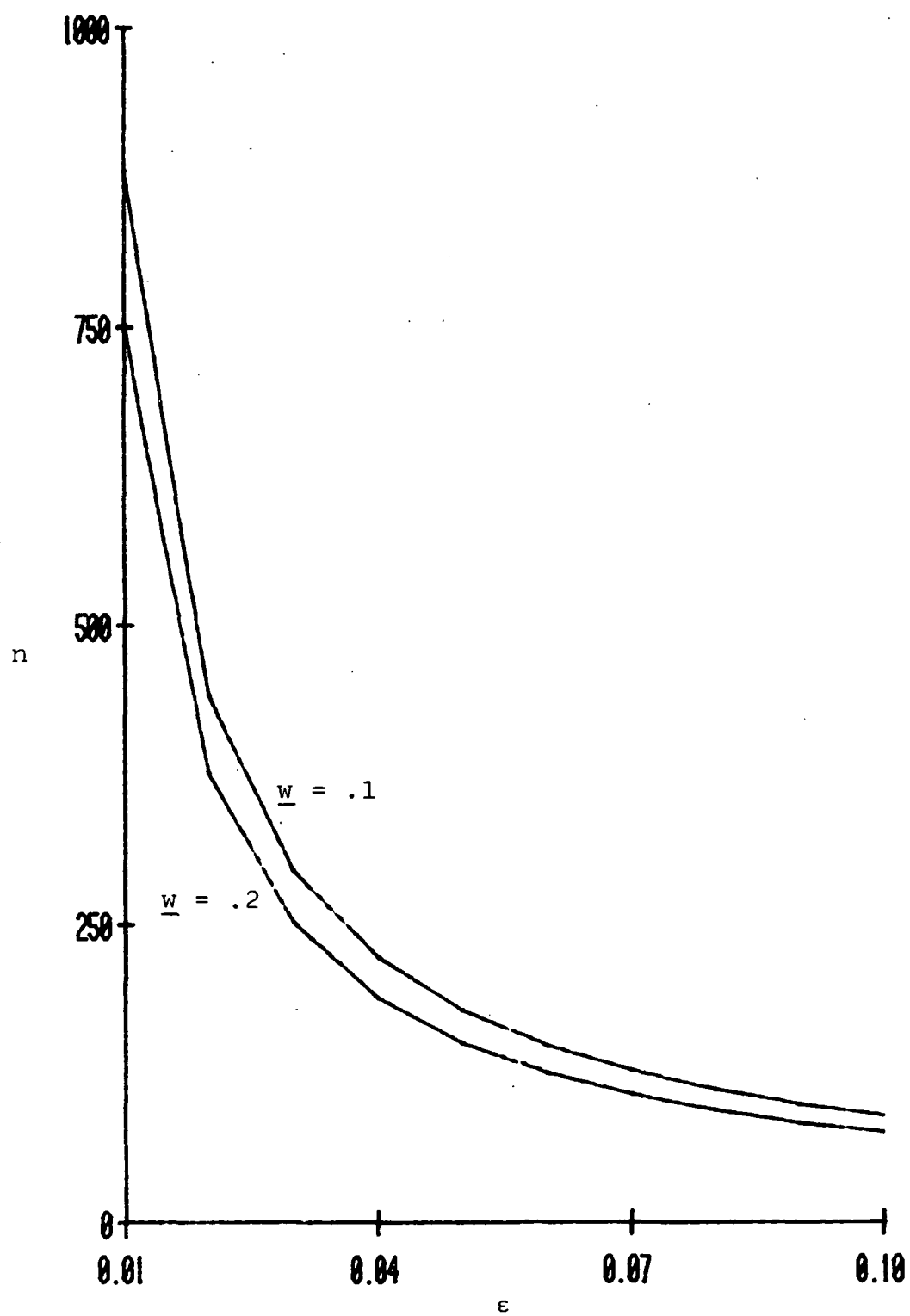
Figure 2. Stability Boundary for Standing Waves
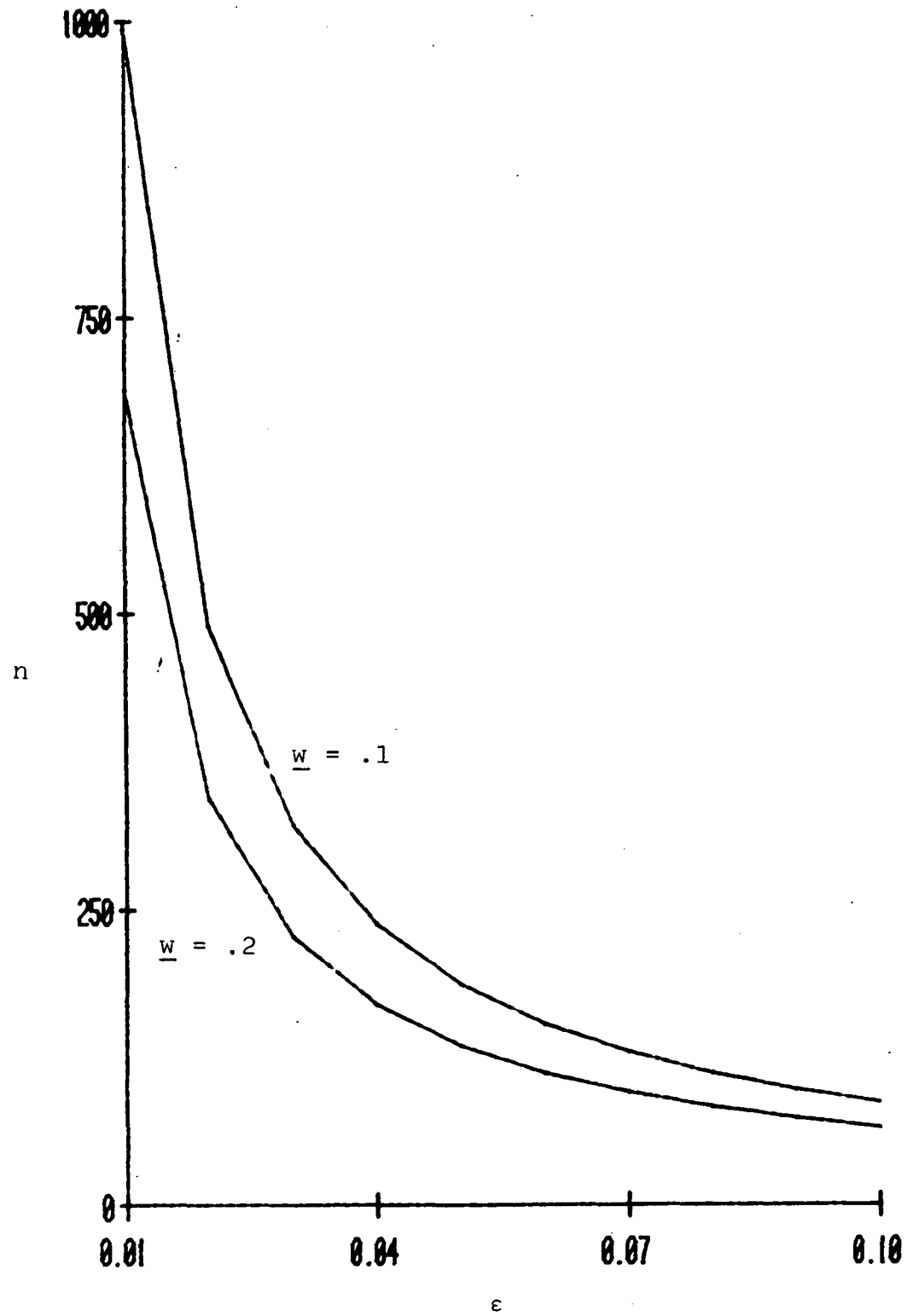
Figure 3. Stability Boundary for Traveling Waves
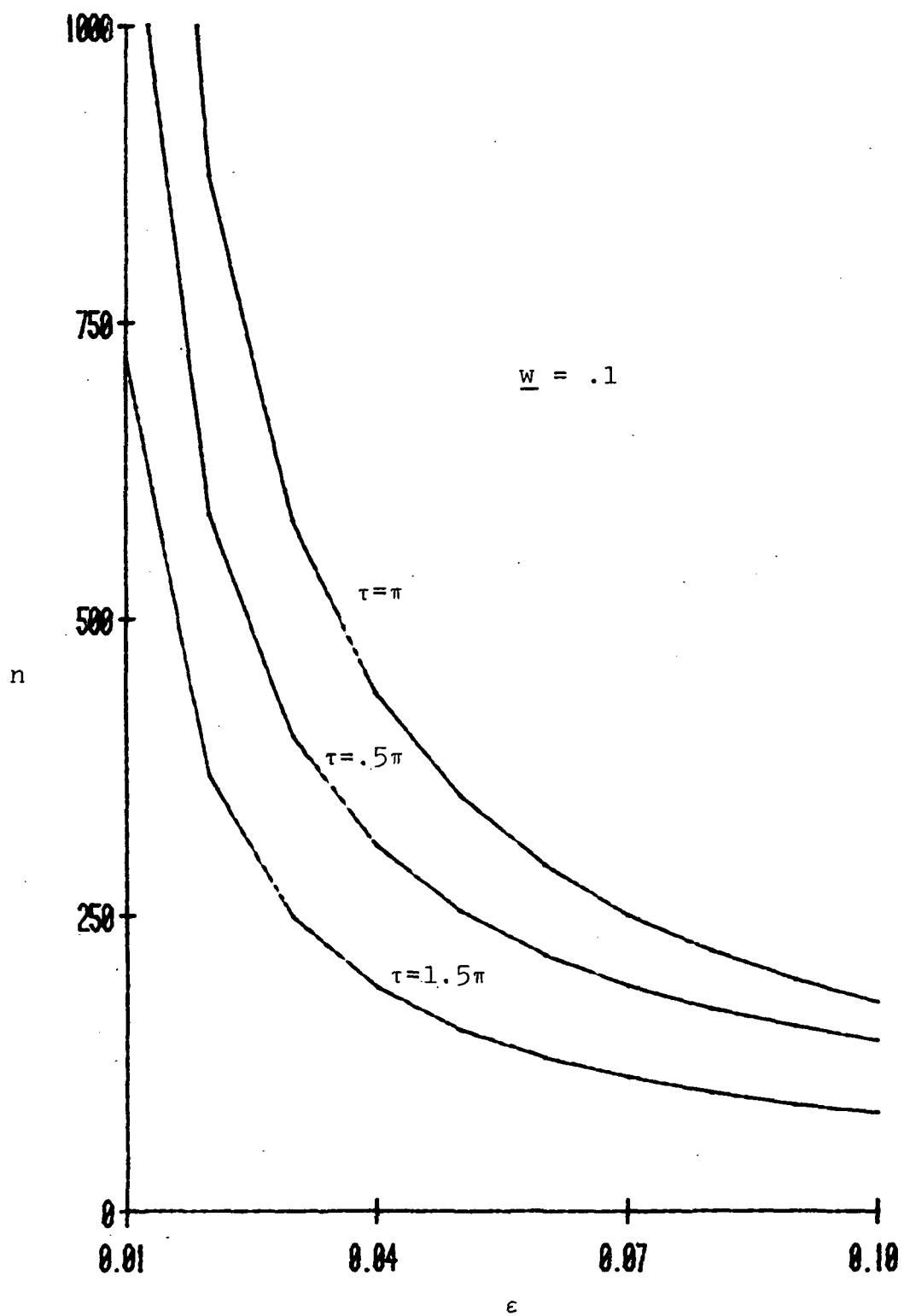
Figure 4. Stability Boundary for Standing Waves
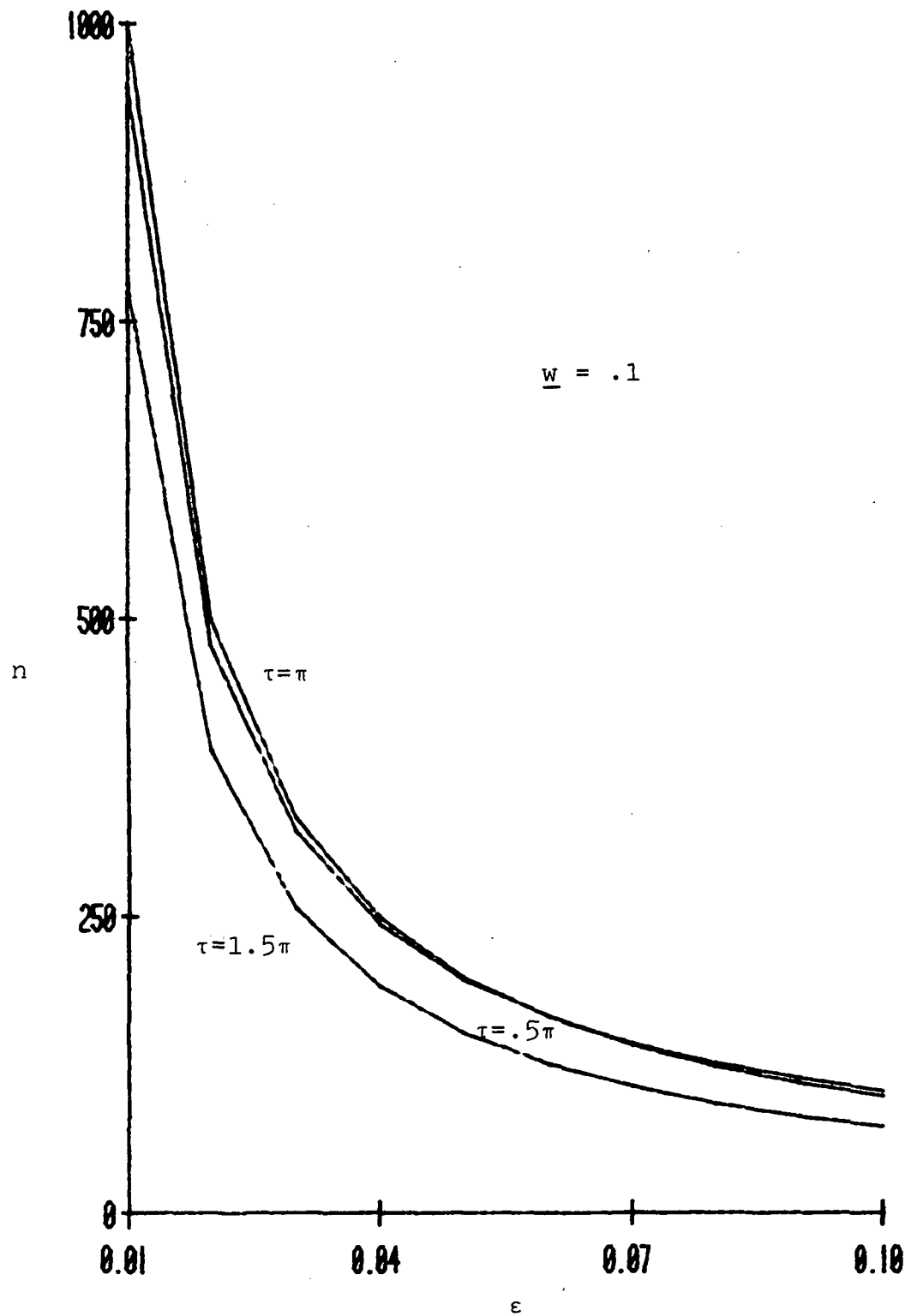
Figure 5. Stability Boundary for Traveling Waves
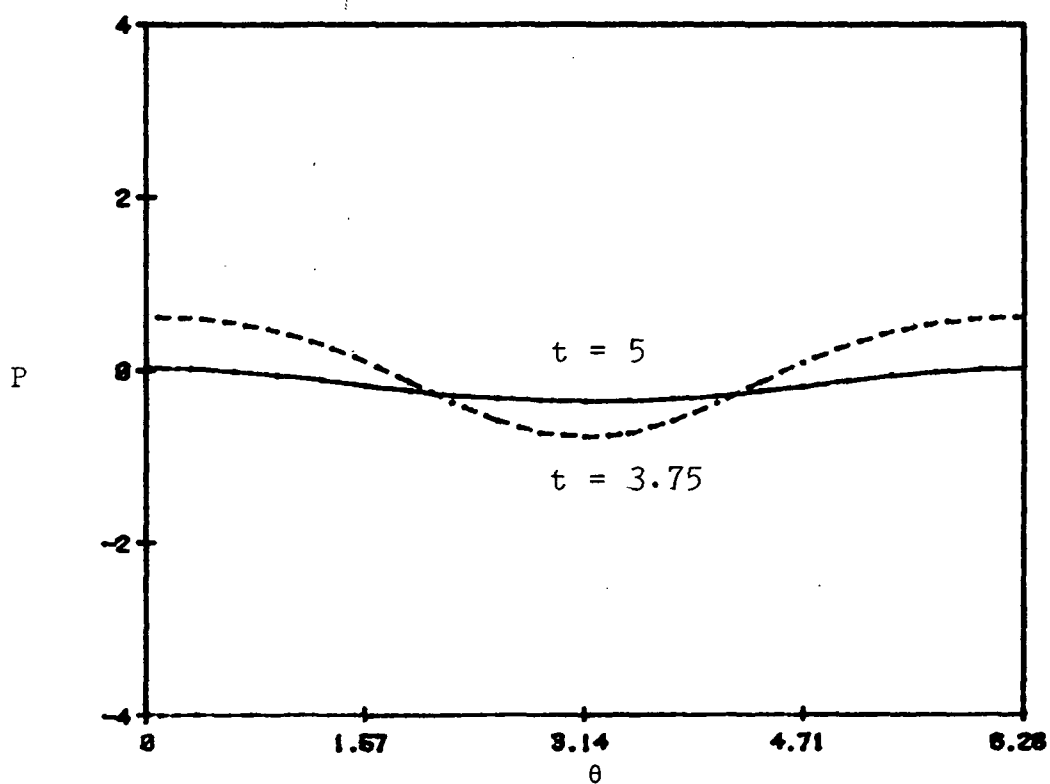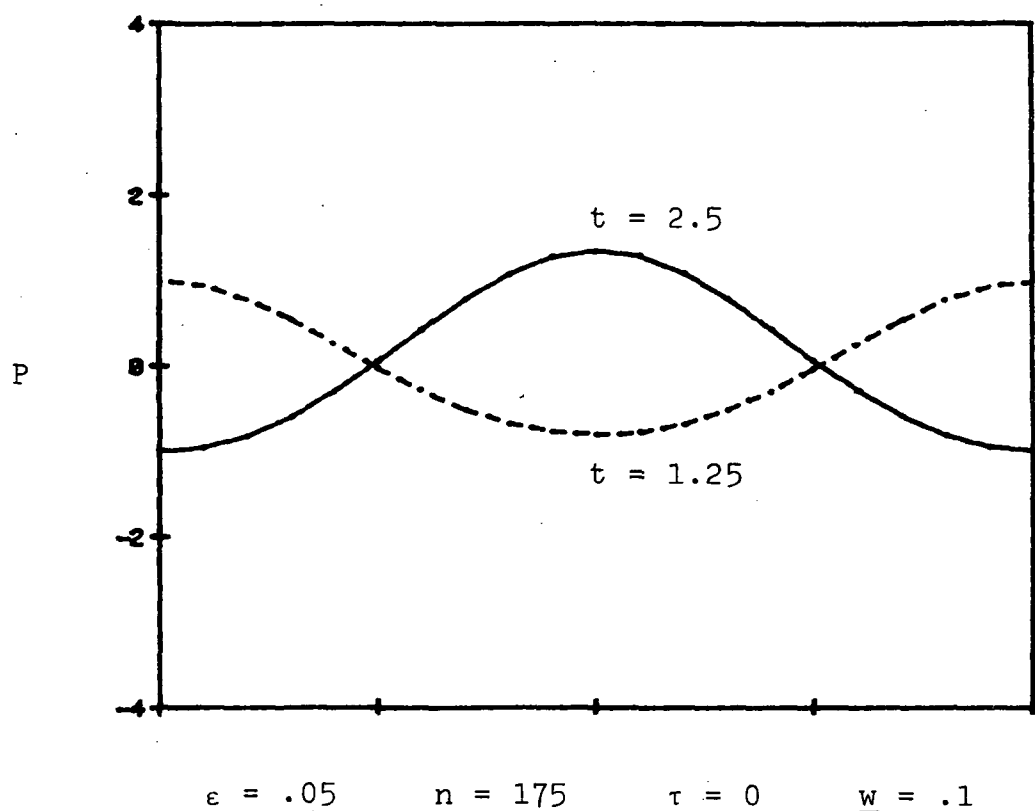
Figure 6. The Wall Pressure Waveforms for Standing Waves
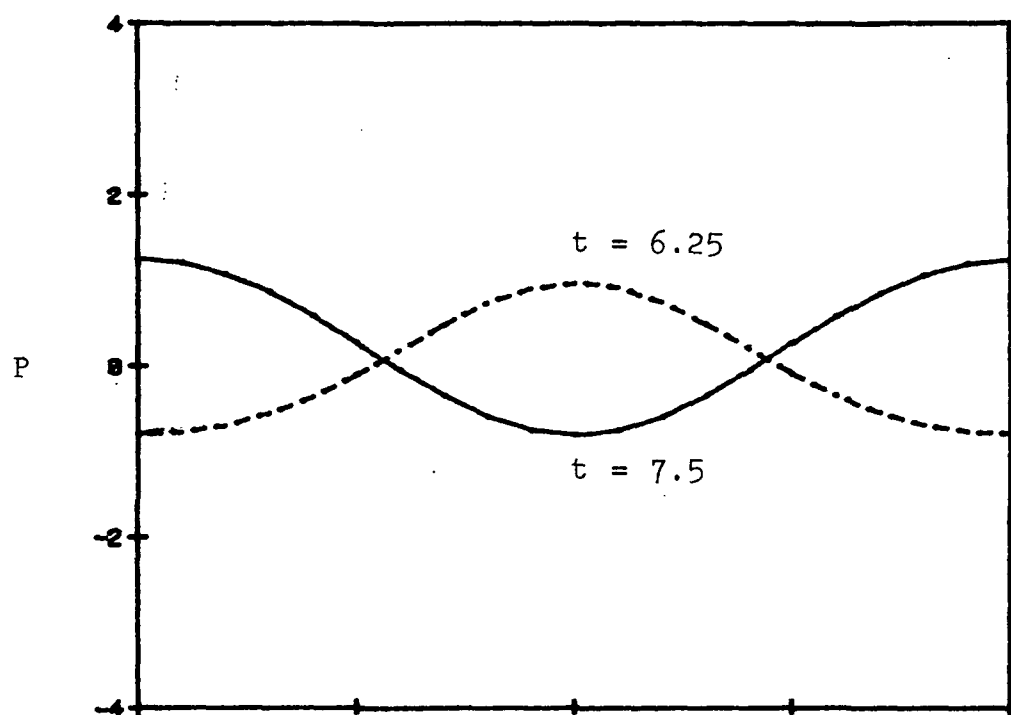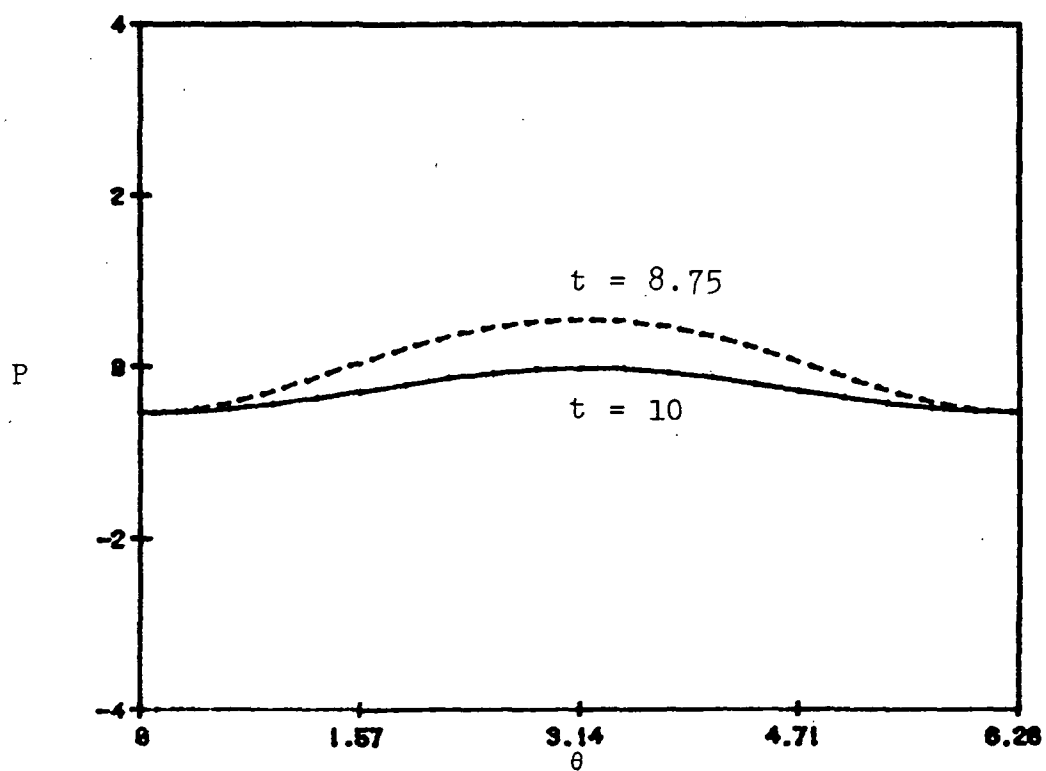
Figure 7. The Wall Pressure Waveforms for Standing Waves
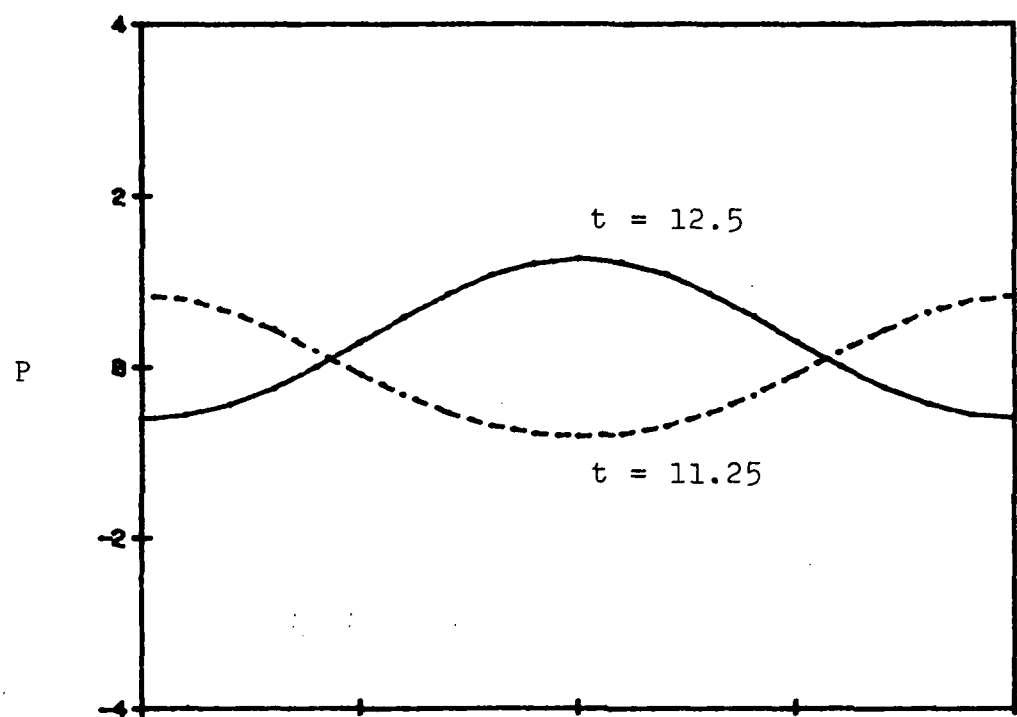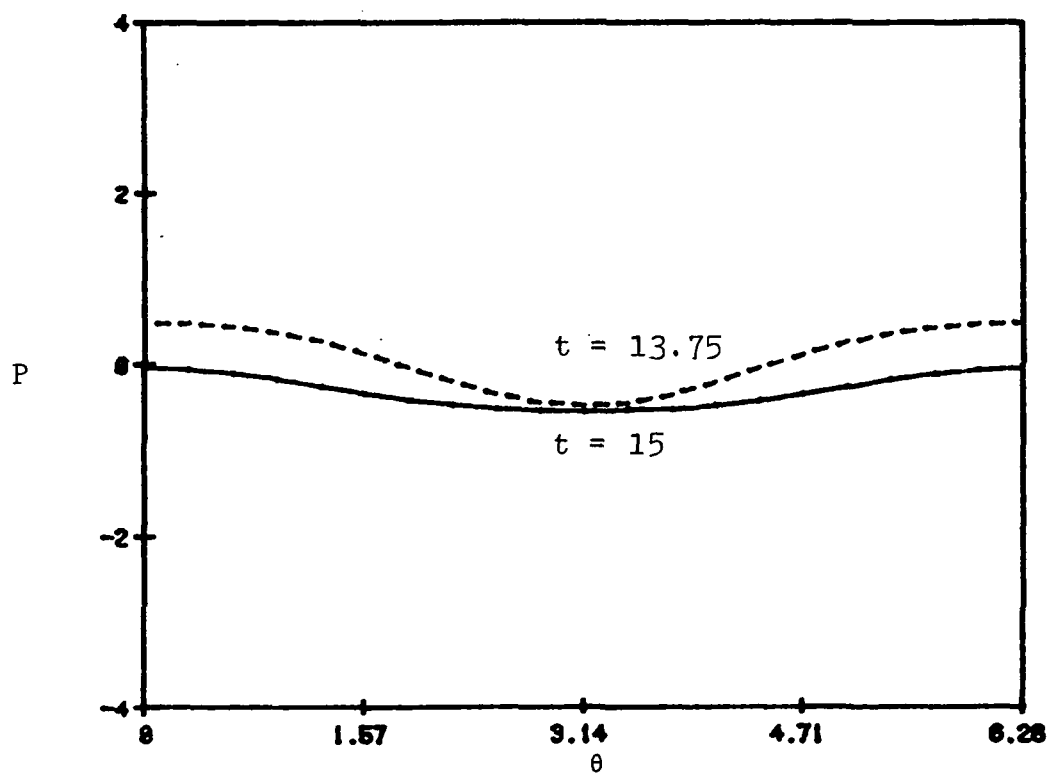
Figure 8. The Wall Pressure Waveforms for Standing Waves
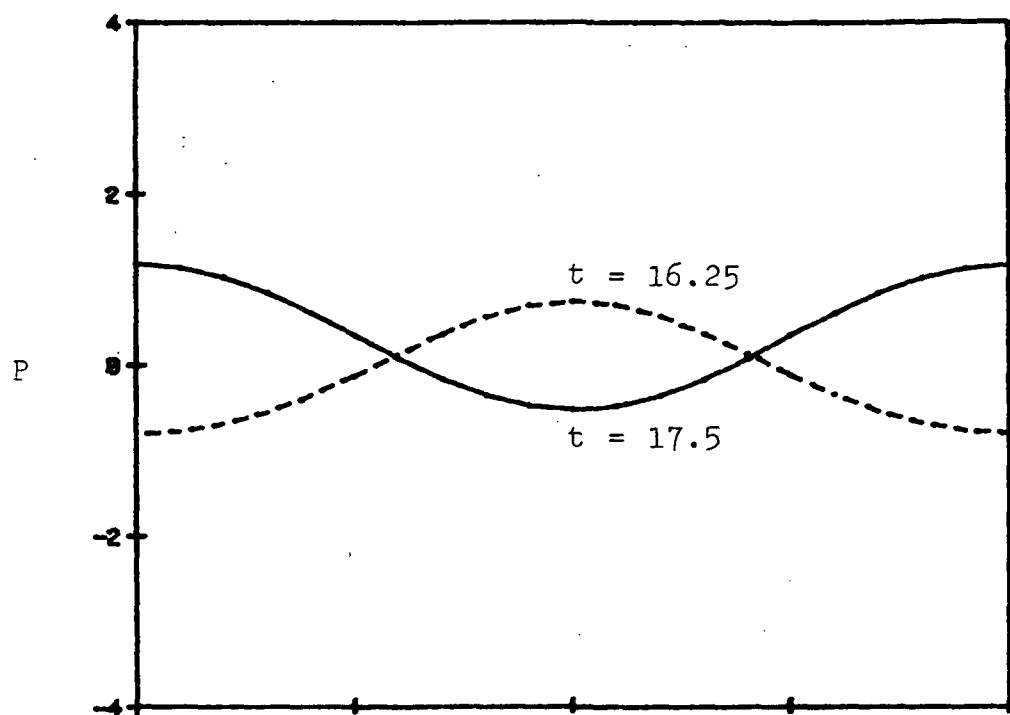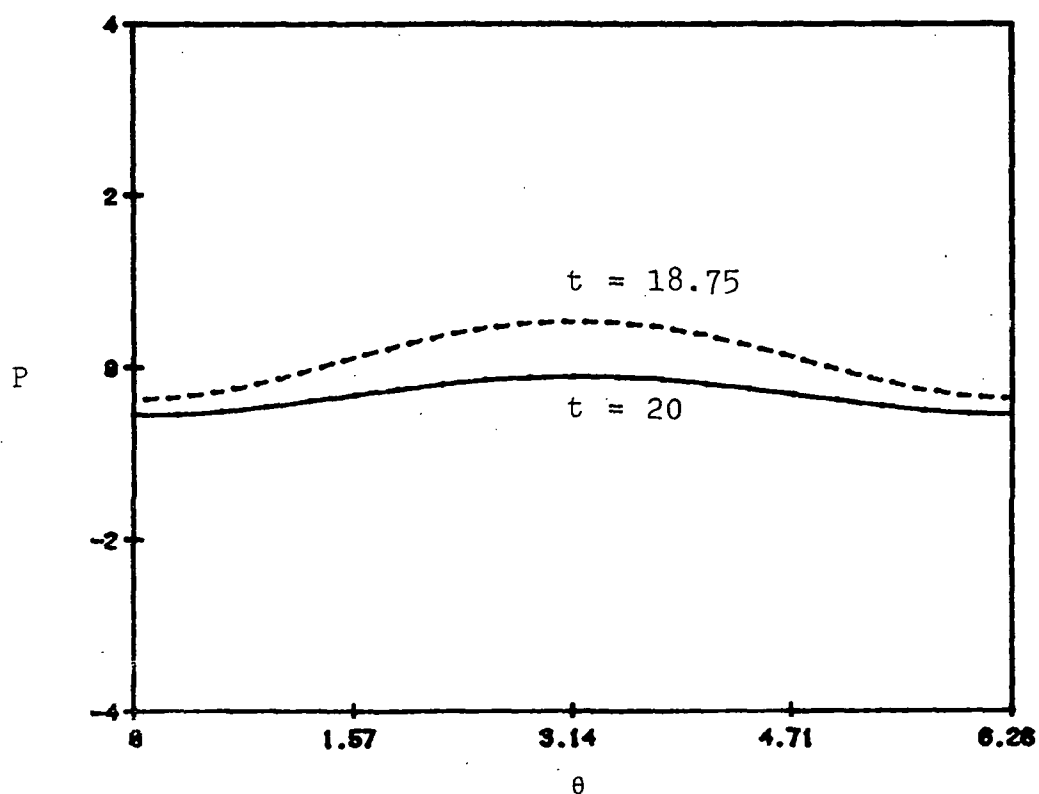
Figure 9. The Wall Pressure Waveforms for Standing Waves
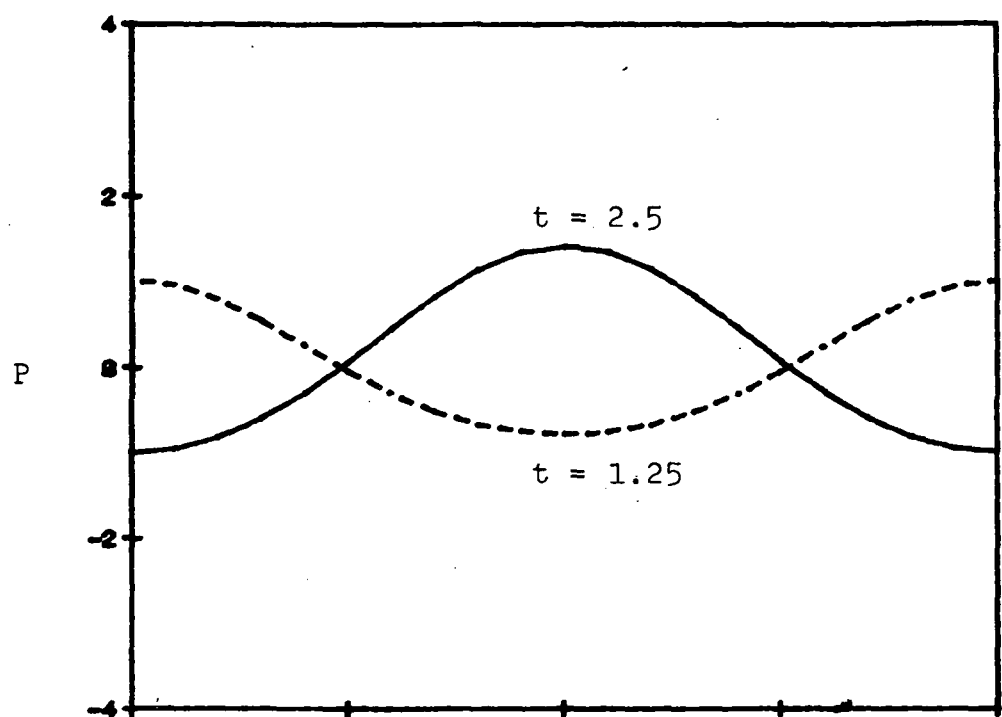
Figure 10. The Wall Pressure Waveforms for Standing Waves
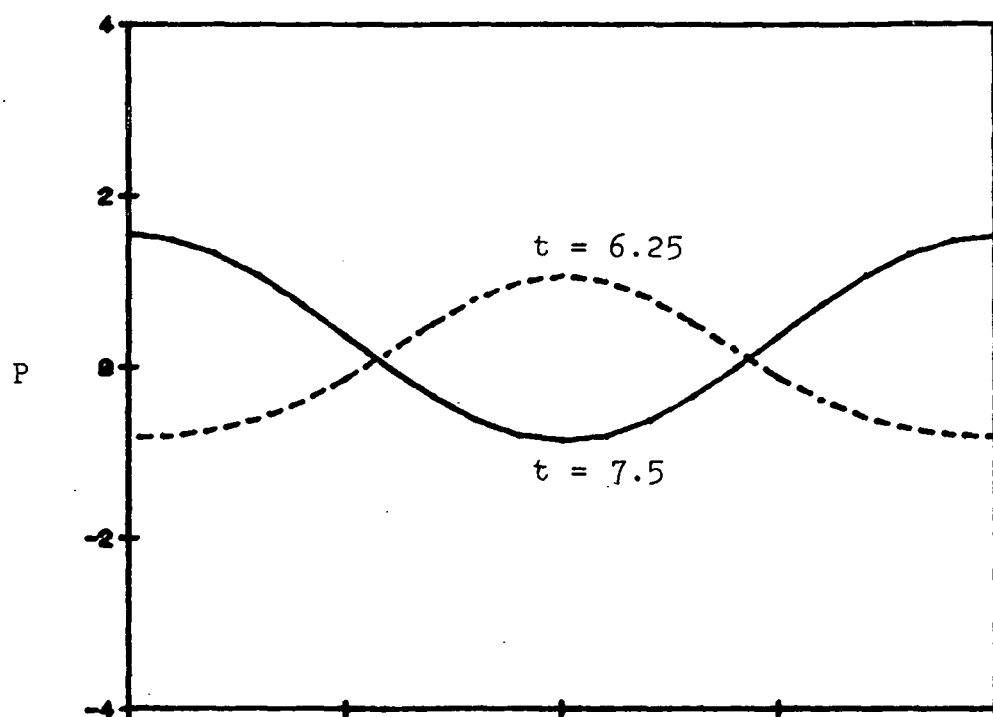
Figure 11. The Wall Pressure Waveforms for Standing Waves
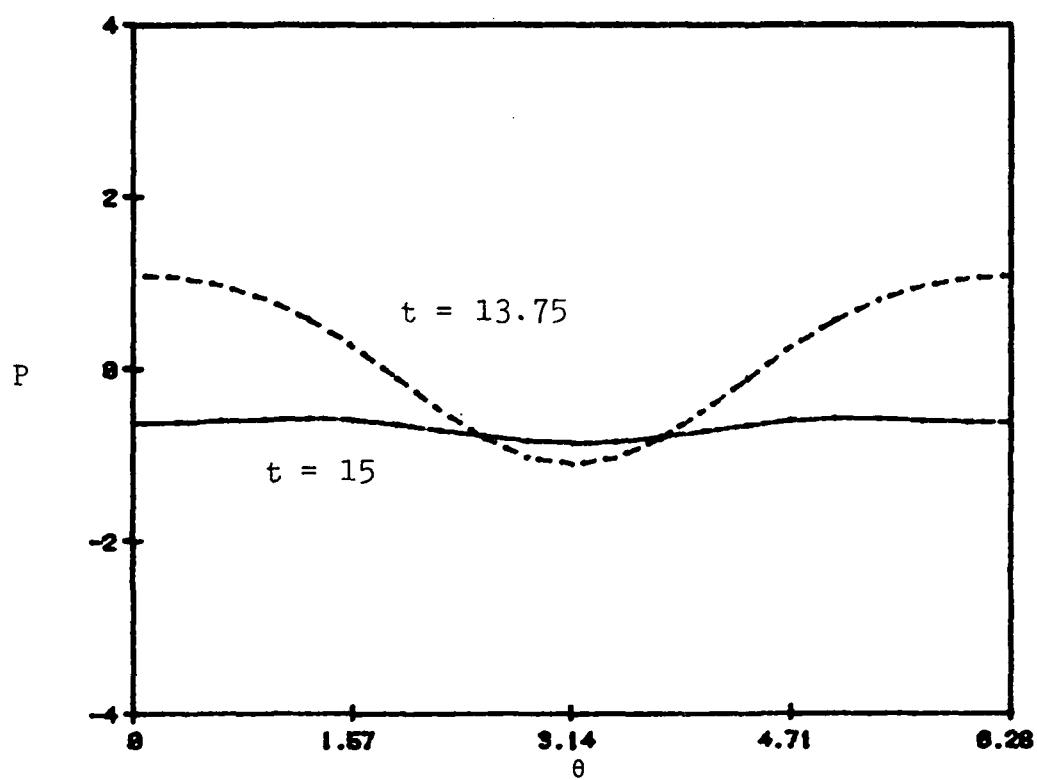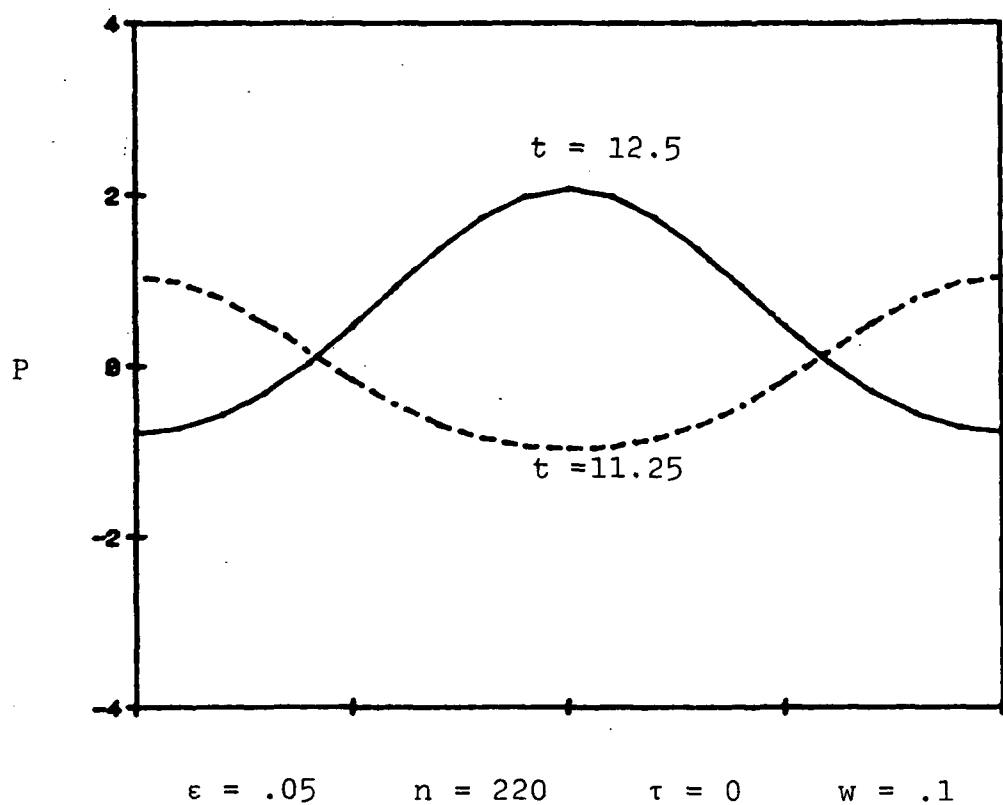
Figure 12. The Wall Pressure Waveforms for Standing Waves

$\epsilon = .05$ $n = 220$ $\tau = 0$ $\underline{w} = .1$
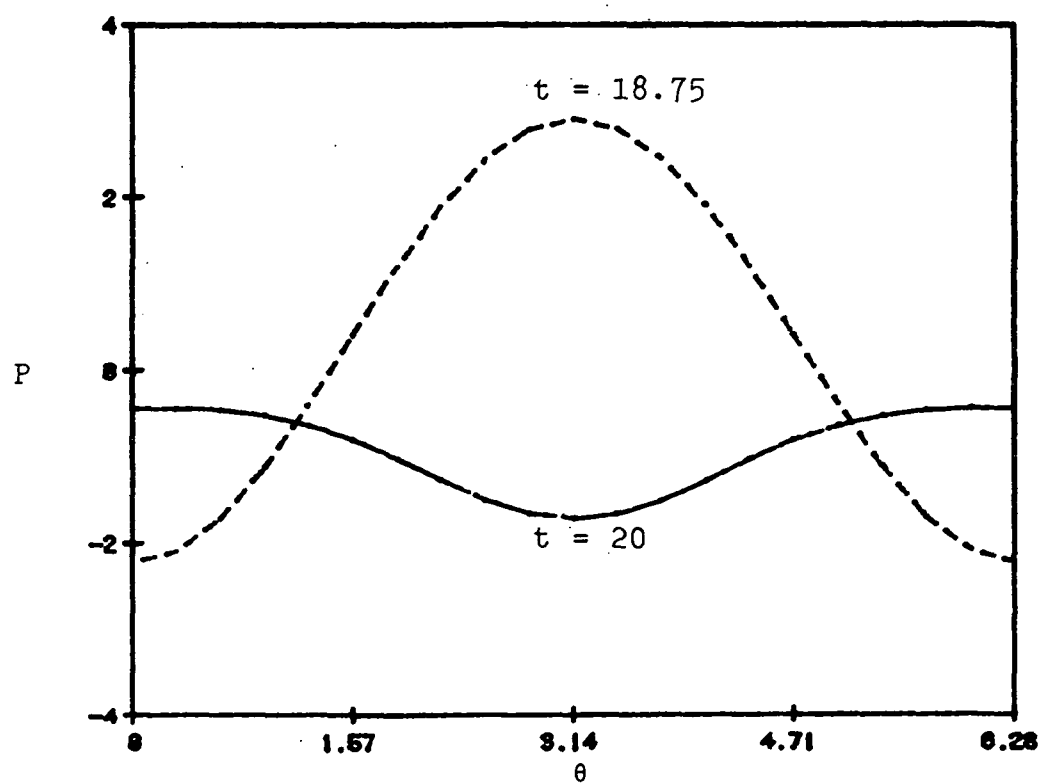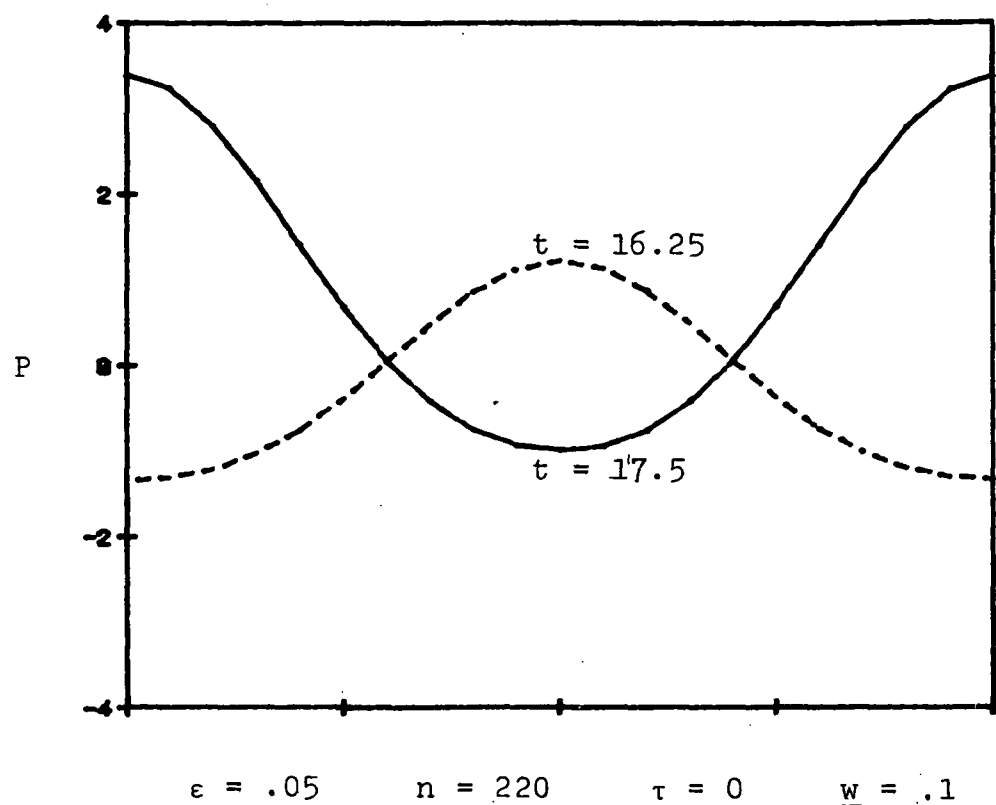
Figure 13.   The Wall Pressure Waveforms for Standing Waves
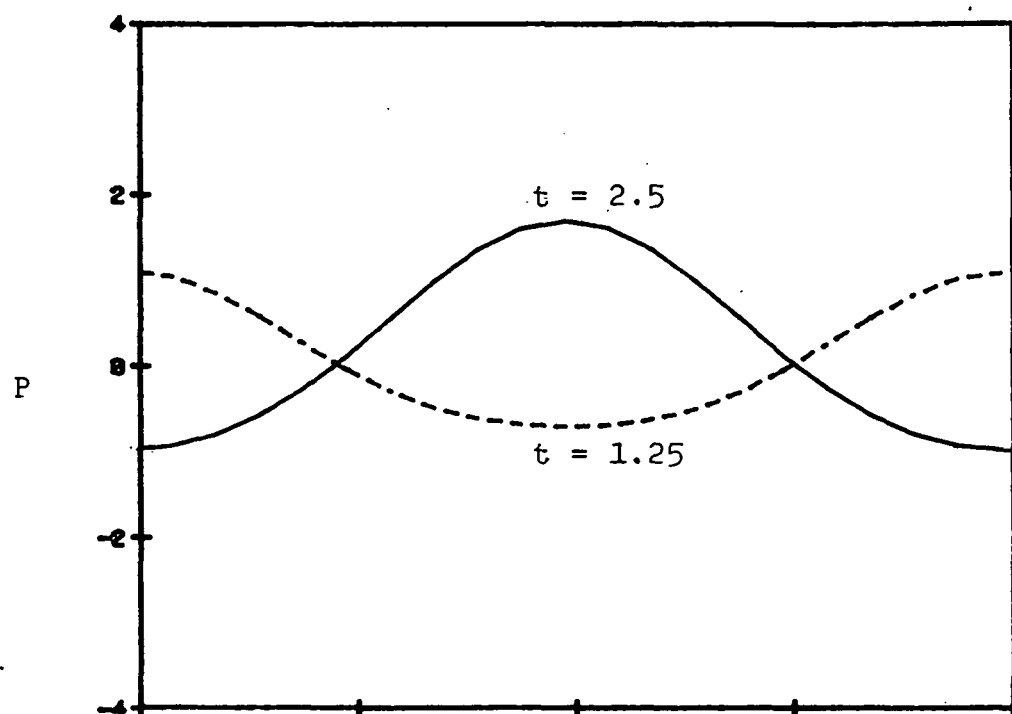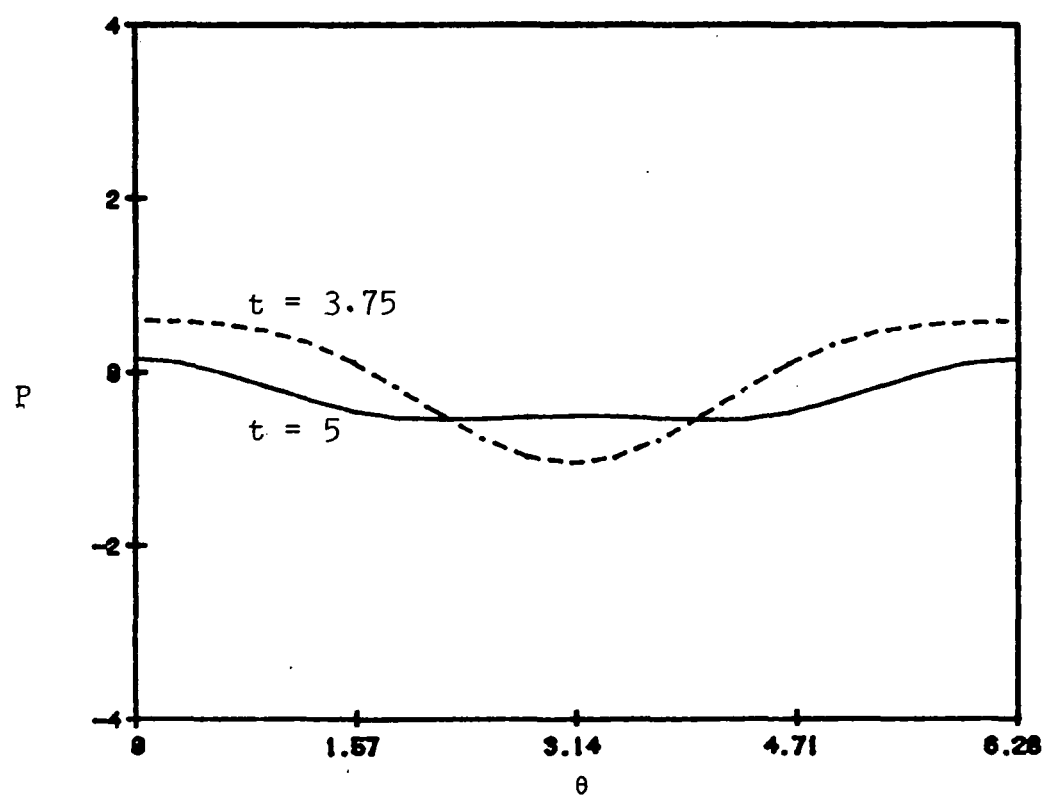
$$\epsilon = .05 \qquad n = 345 \qquad \tau = \pi \qquad \underline{w} = .1$$
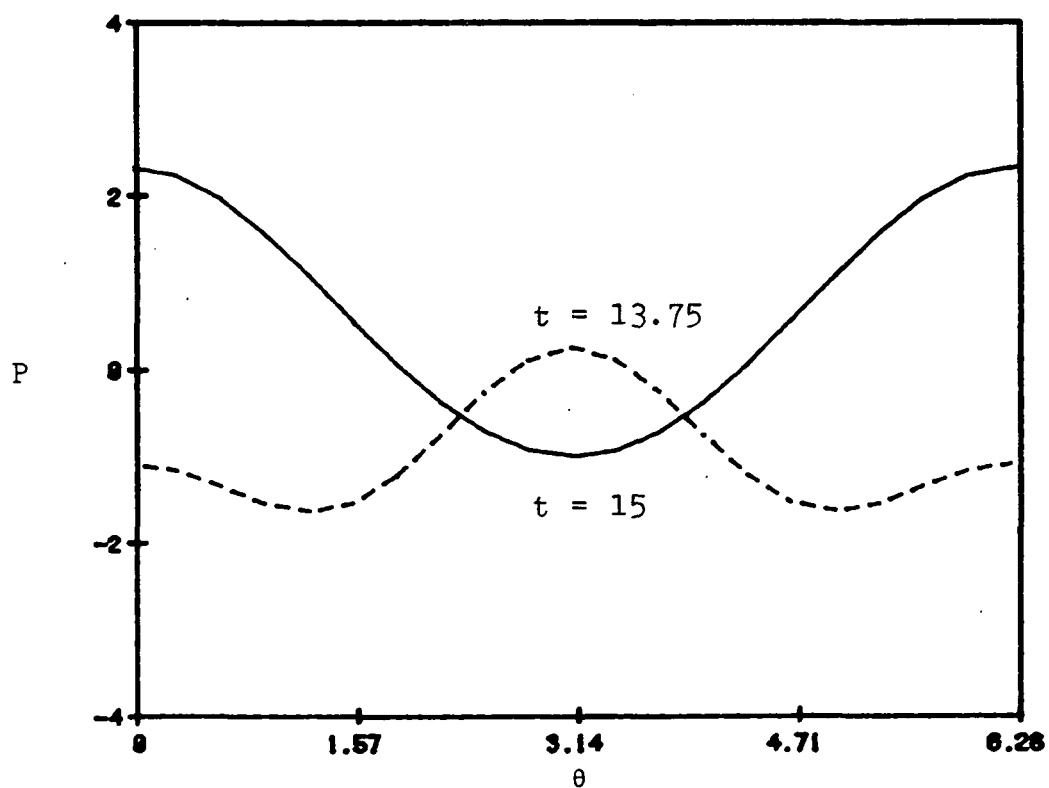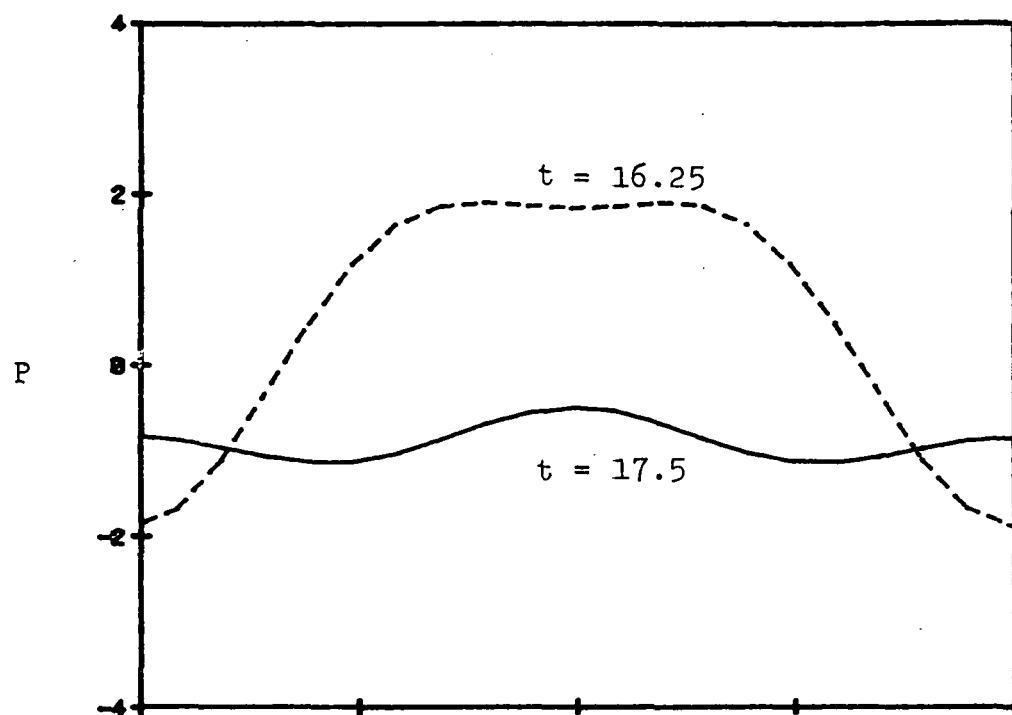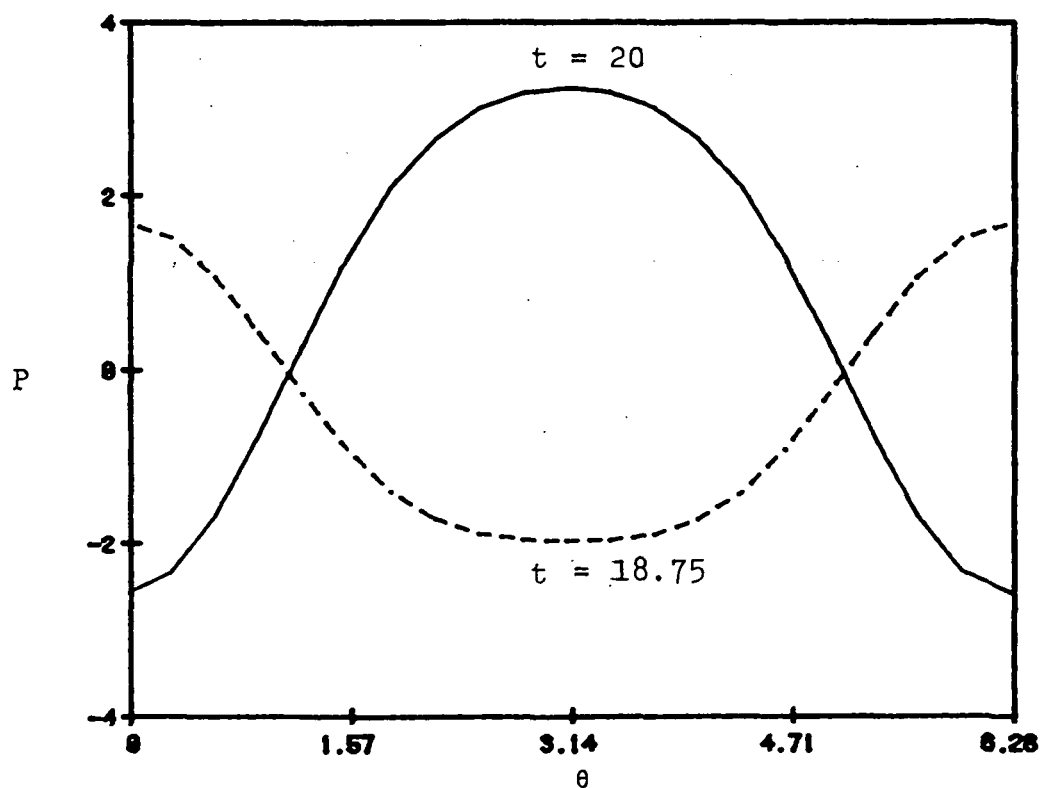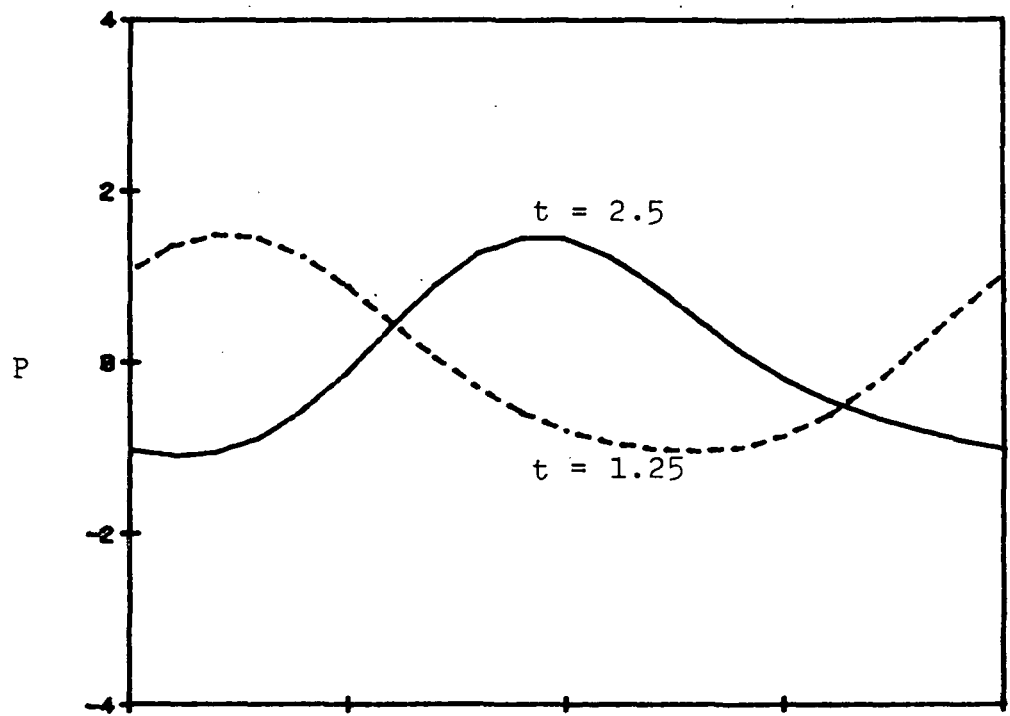
Figure 14. The Wall Pressure Waveforms for Standing Waves
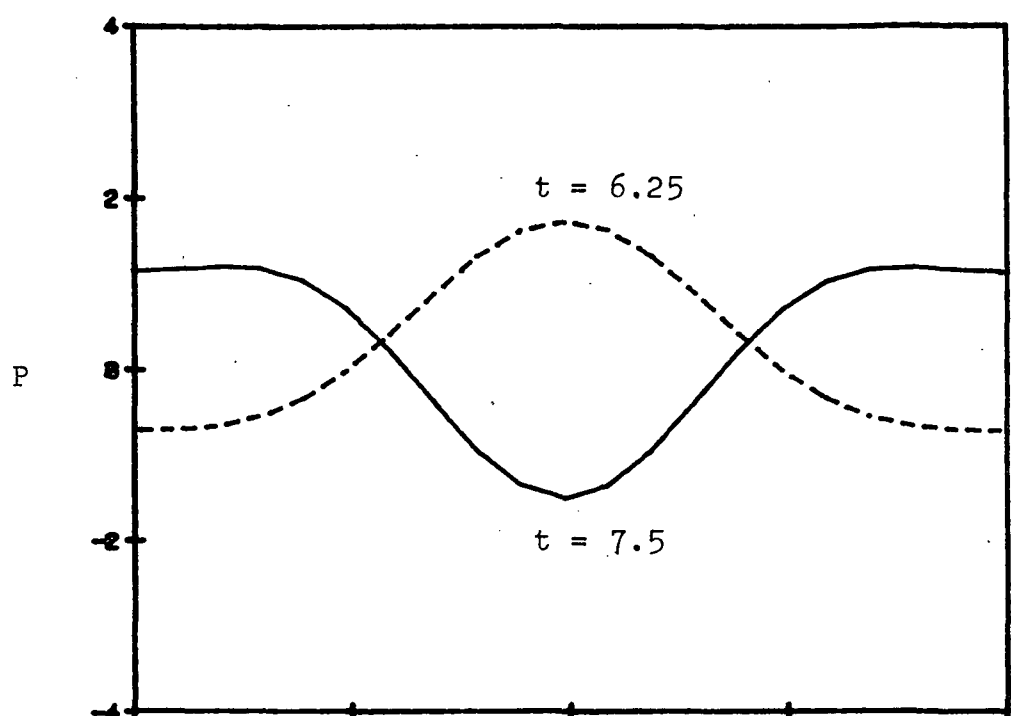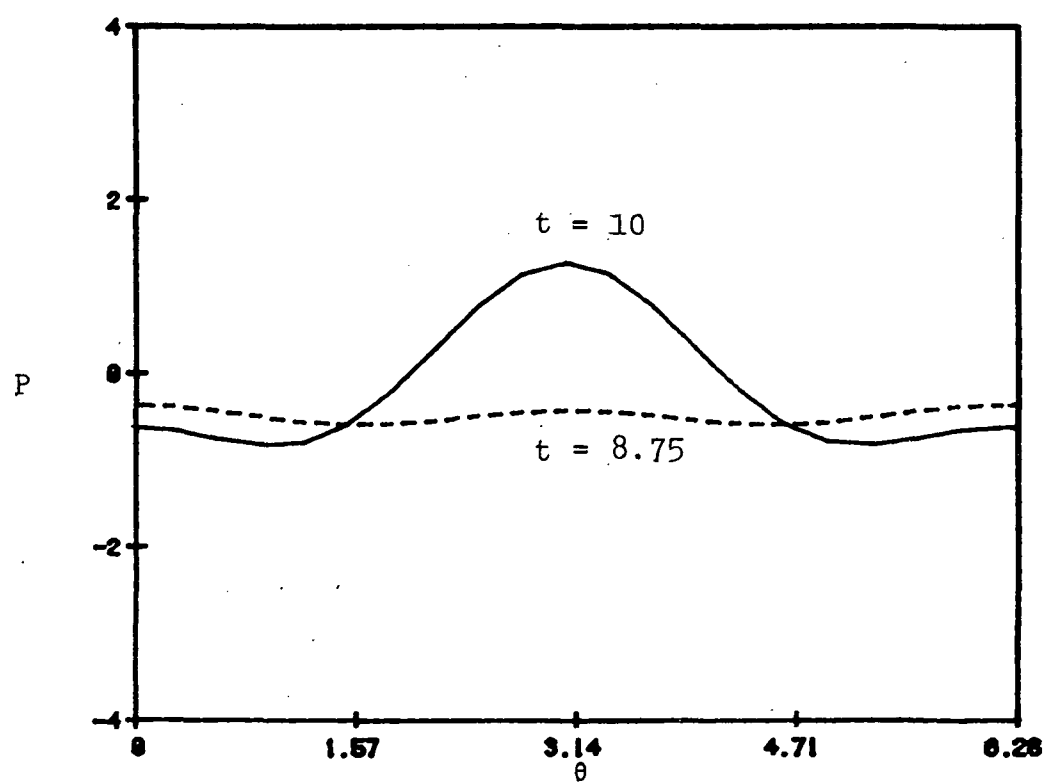
Figure 15.   The Wall Pressure Waveforms for Standing Waves
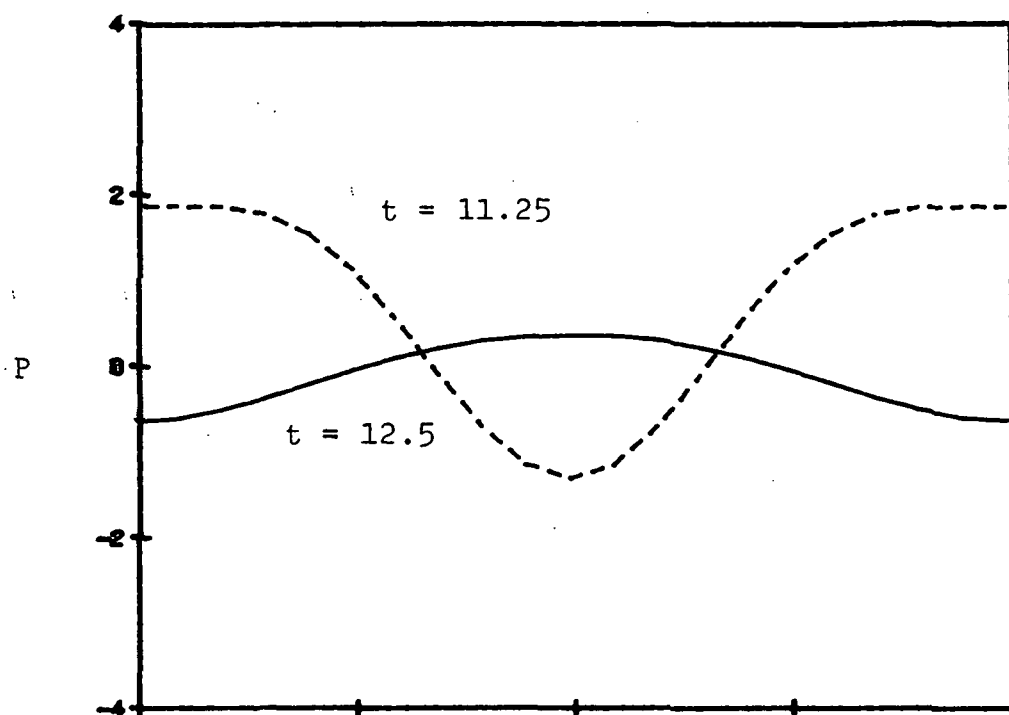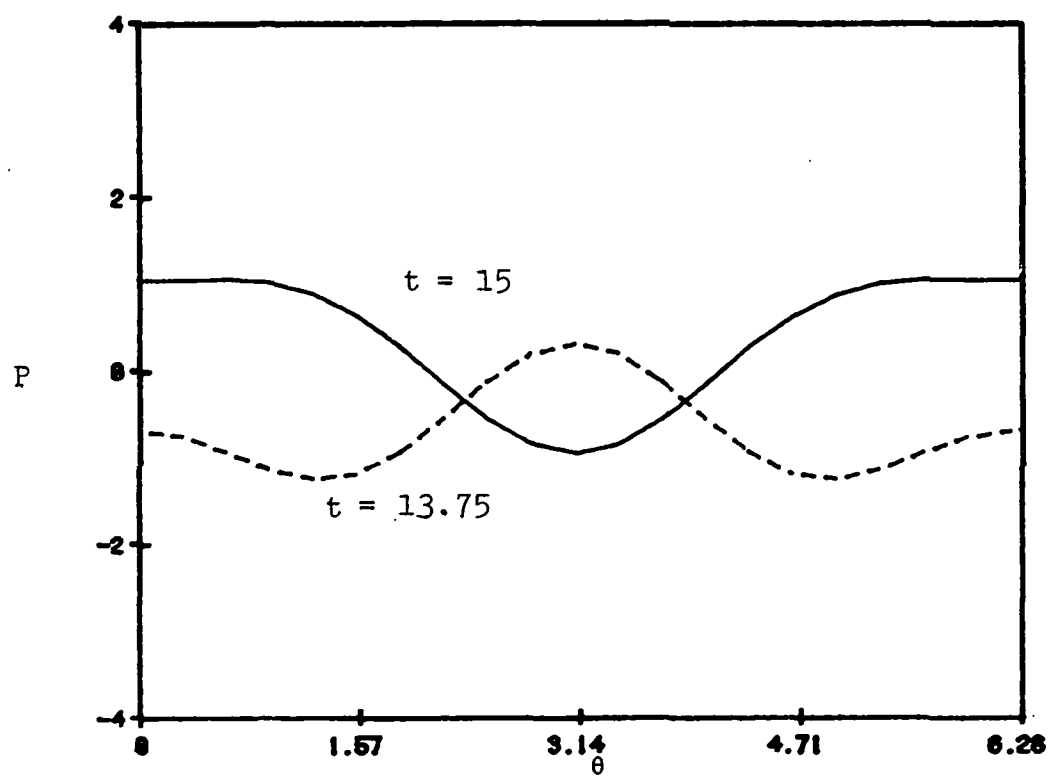
$\epsilon = .05 \qquad n = 345 \qquad \tau = \pi \qquad \underline{w} = .1$

Figure 16. The Wall Pressure Waveforms for Standing Waves
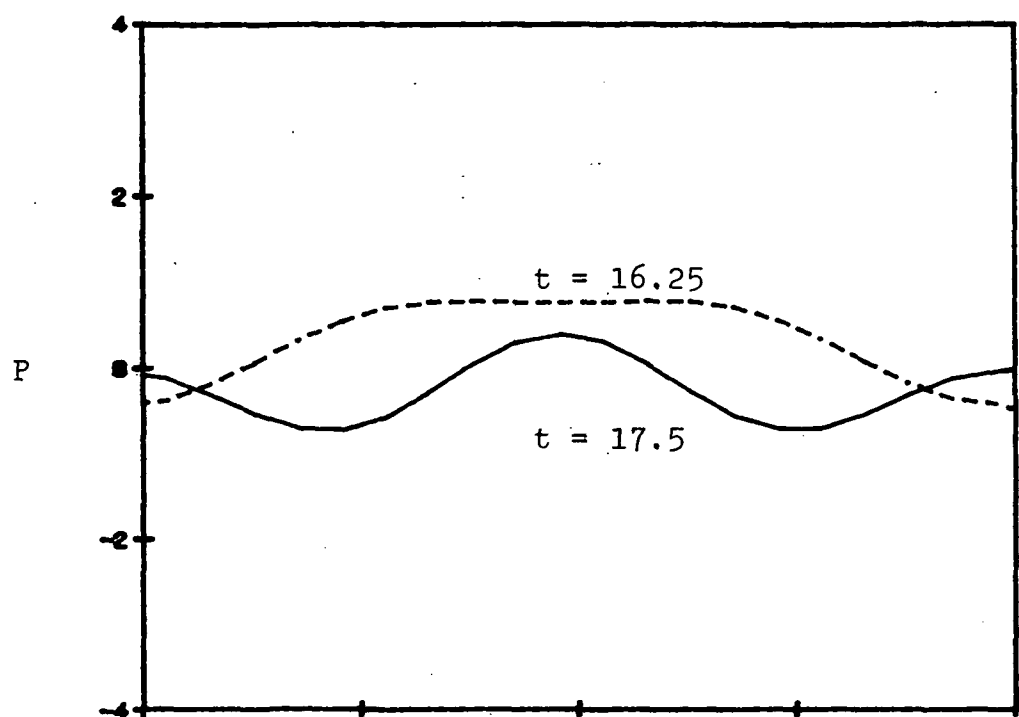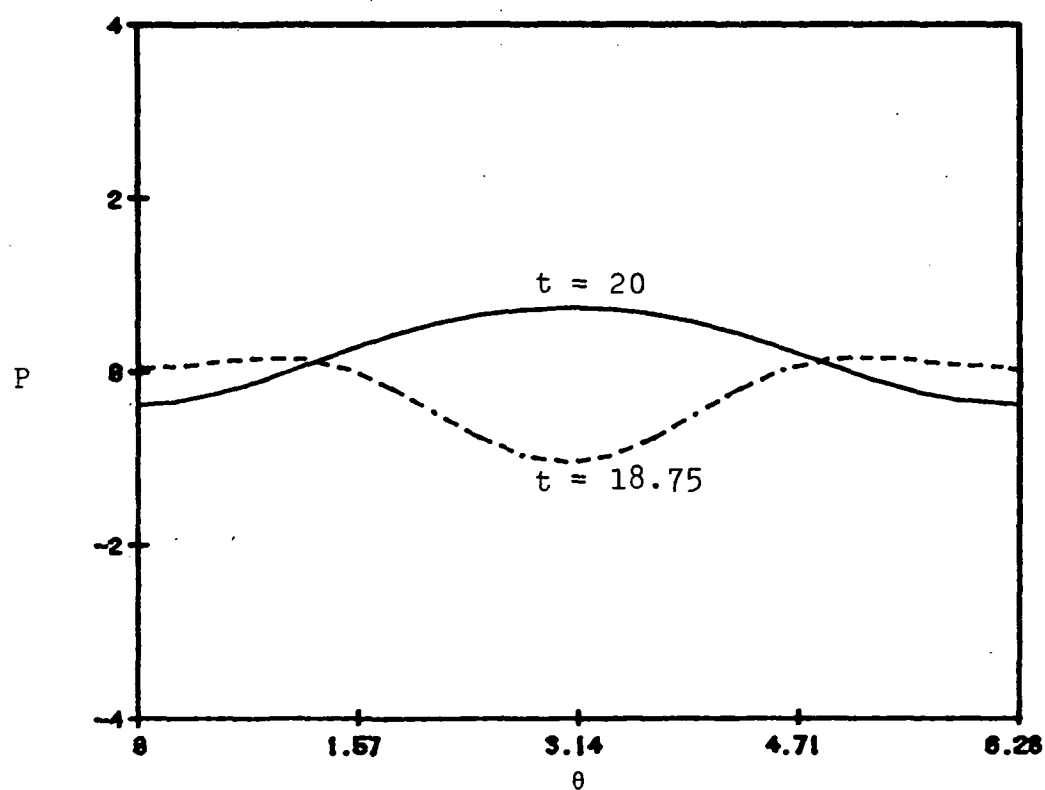
Figure 17. The Wall Pressure Waveforms for Standing Waves
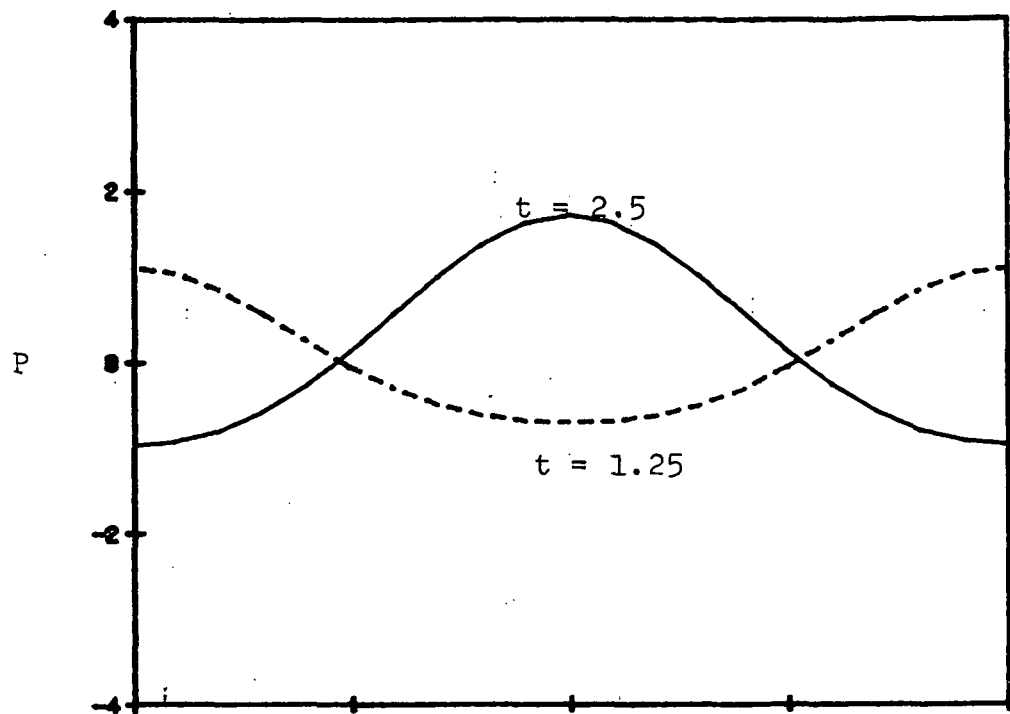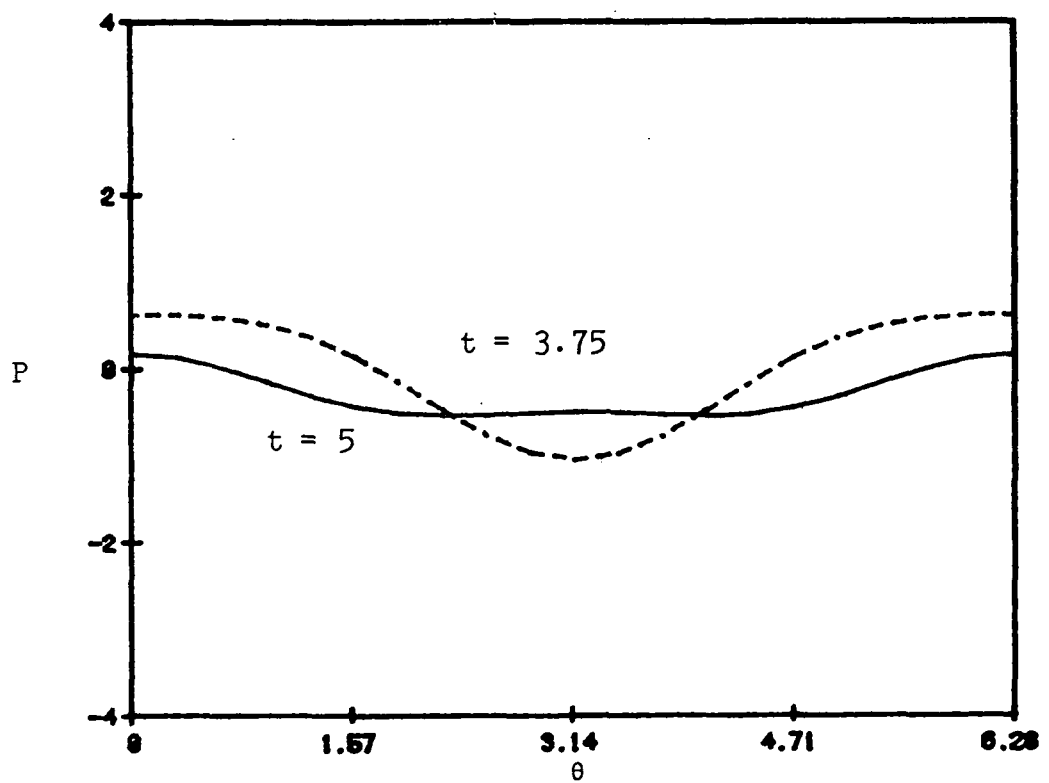
$\varepsilon = .05$ $n = 352$ $\tau = \pi$ $\underline{w} = .1$

Figure 18.   The Wall Pressure Waveforms for Standing Waves
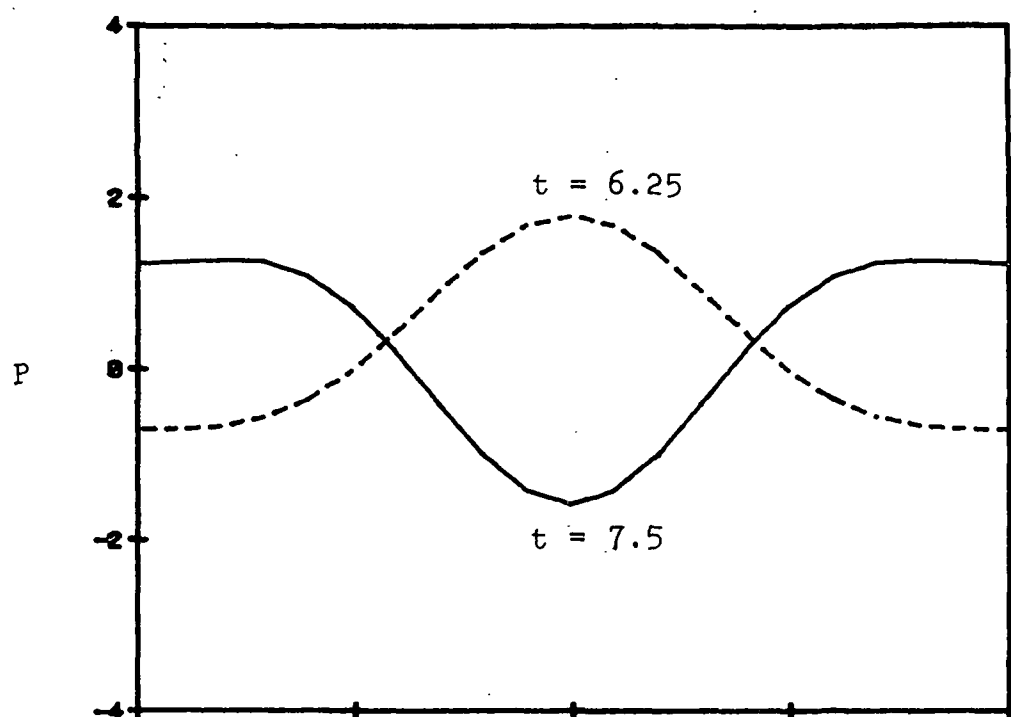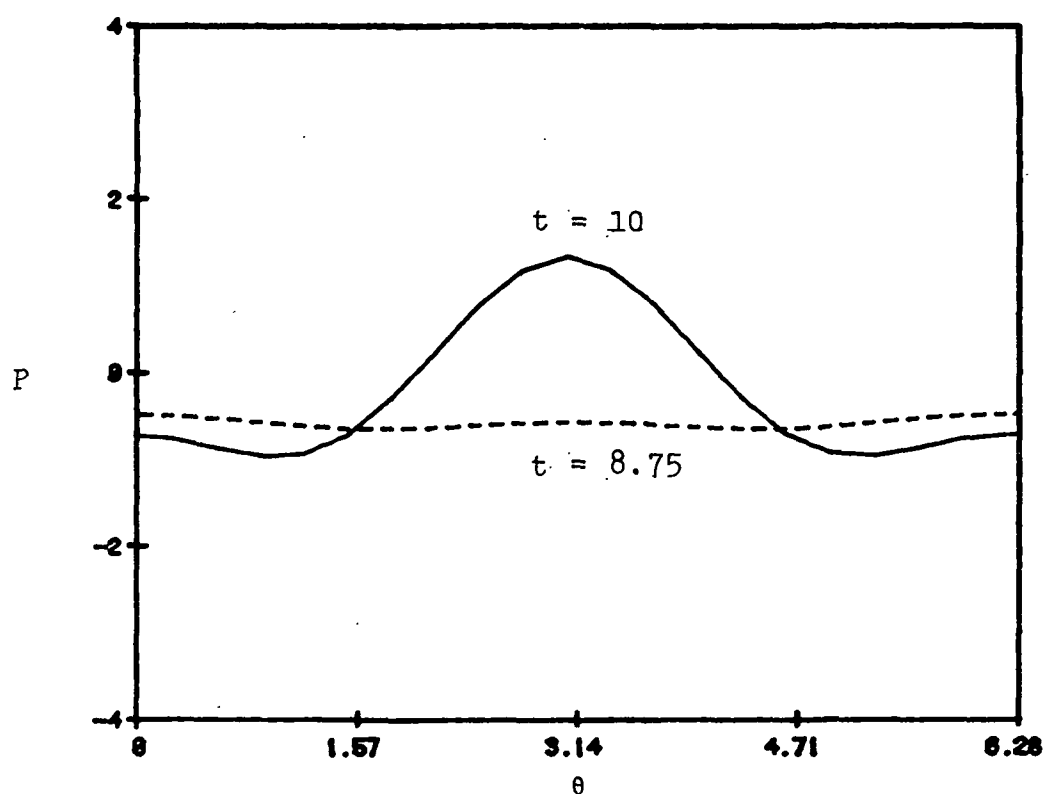
Figure 19. The Wall Pressure Waveforms for Standing Waves
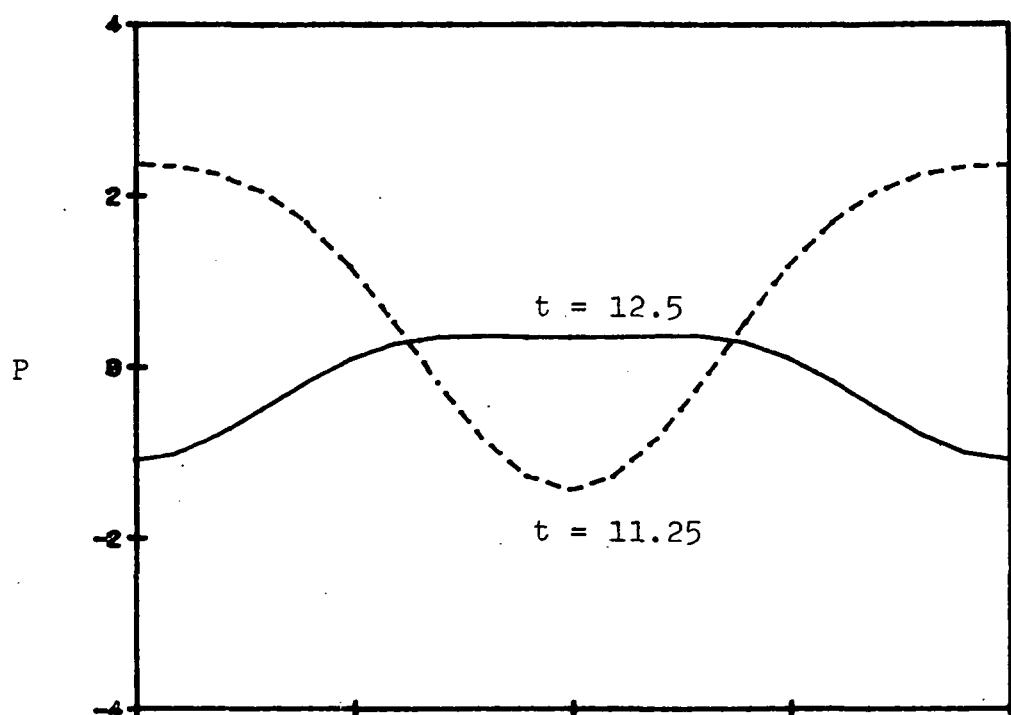
$$\epsilon = .05 \qquad n = 352 \qquad \tau = \pi \qquad \underline{w} = .1$$

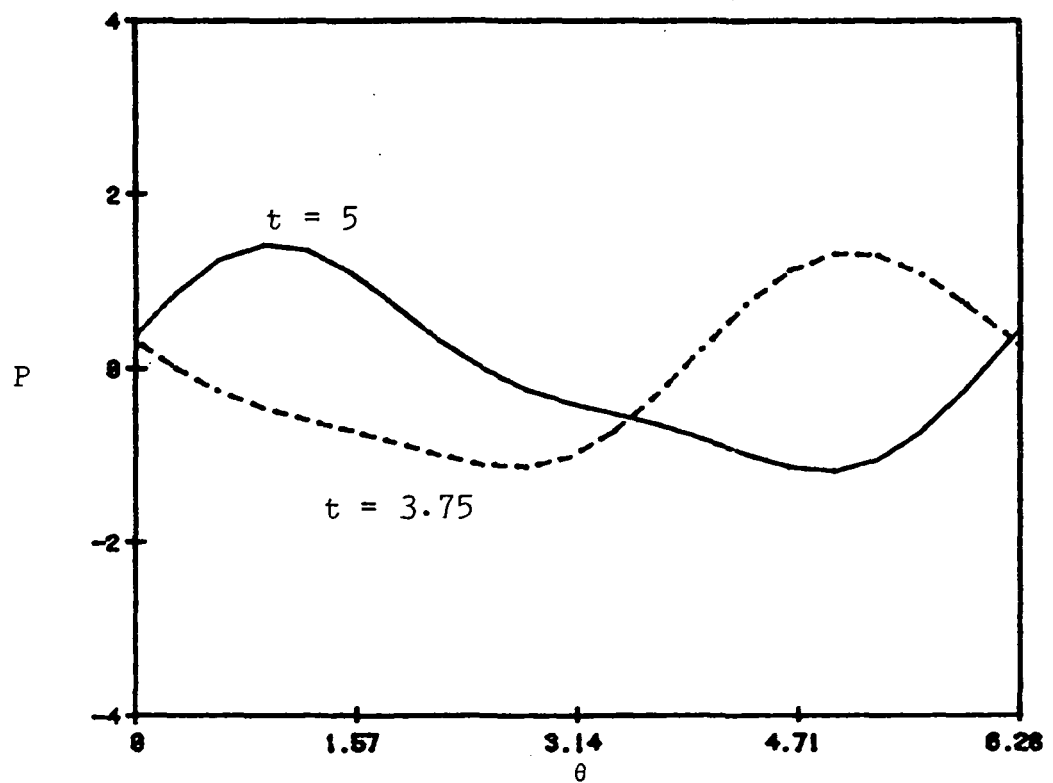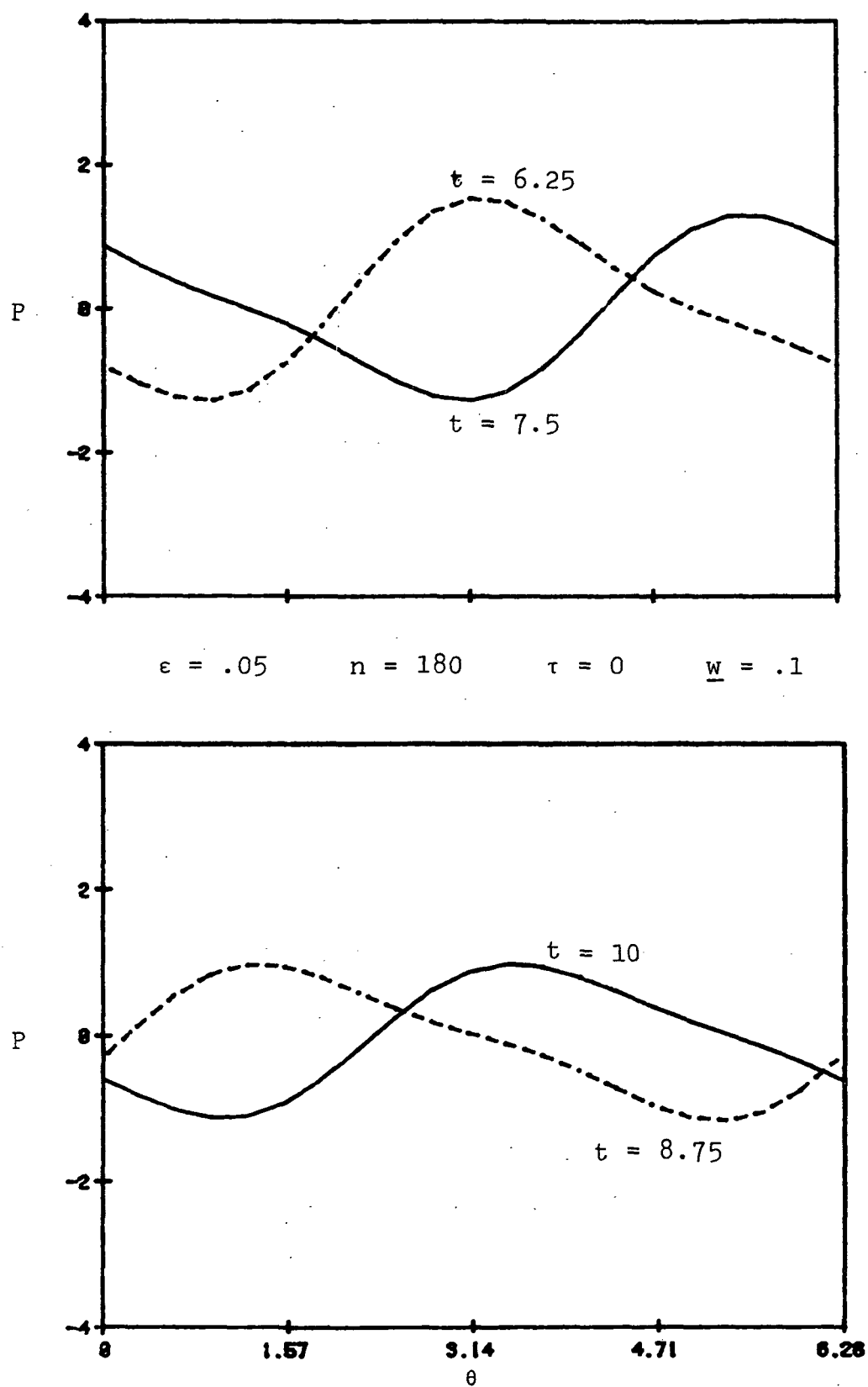Figure 20. The Wall Pressure Waveforms for Standing Waves

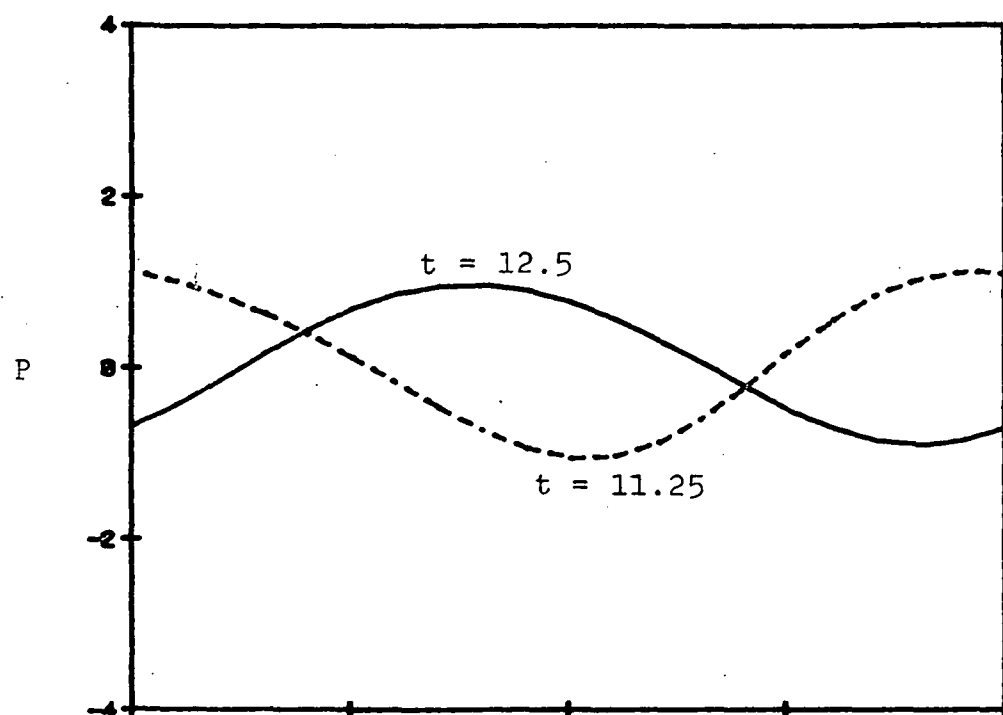Figure 21. The Wall Pressure Waveforms for Standing Waves

Figure 22. The Wall Pressure Waveforms for Traveling Waves

$\epsilon = .05 \qquad n = 180 \qquad \tau = 0 \qquad \underline{w} = .1$

Figure 23. The Wall Pressure Waveforms for Traveling Waves

$\varepsilon = .05 \qquad n = 180 \qquad \tau = 0 \qquad \underline{w} = .1$

Figure 24.   The Wall Pressure Waveforms for Traveling Waves

Figure 25. The Wall Pressure Waveforms for Traveling Waves
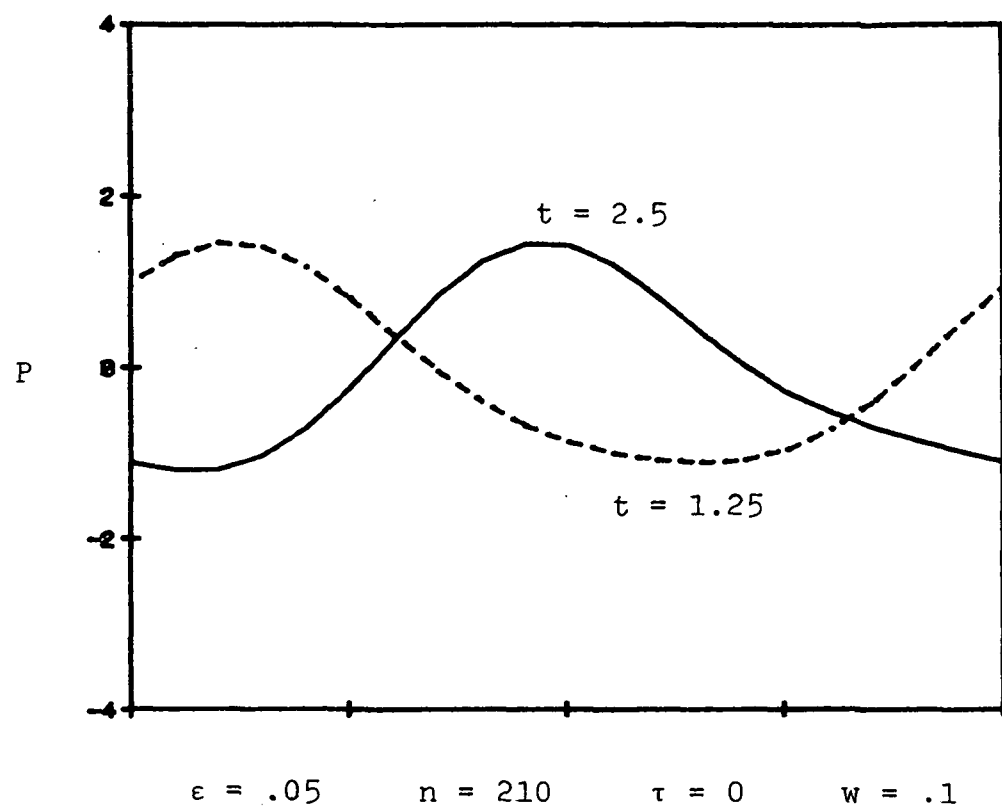
Figure 26.   The Wall pressure Waveforms for Traveling Waves

$\varepsilon = .05 \qquad n = 210 \qquad \tau = 0 \qquad \underline{w} = .1$
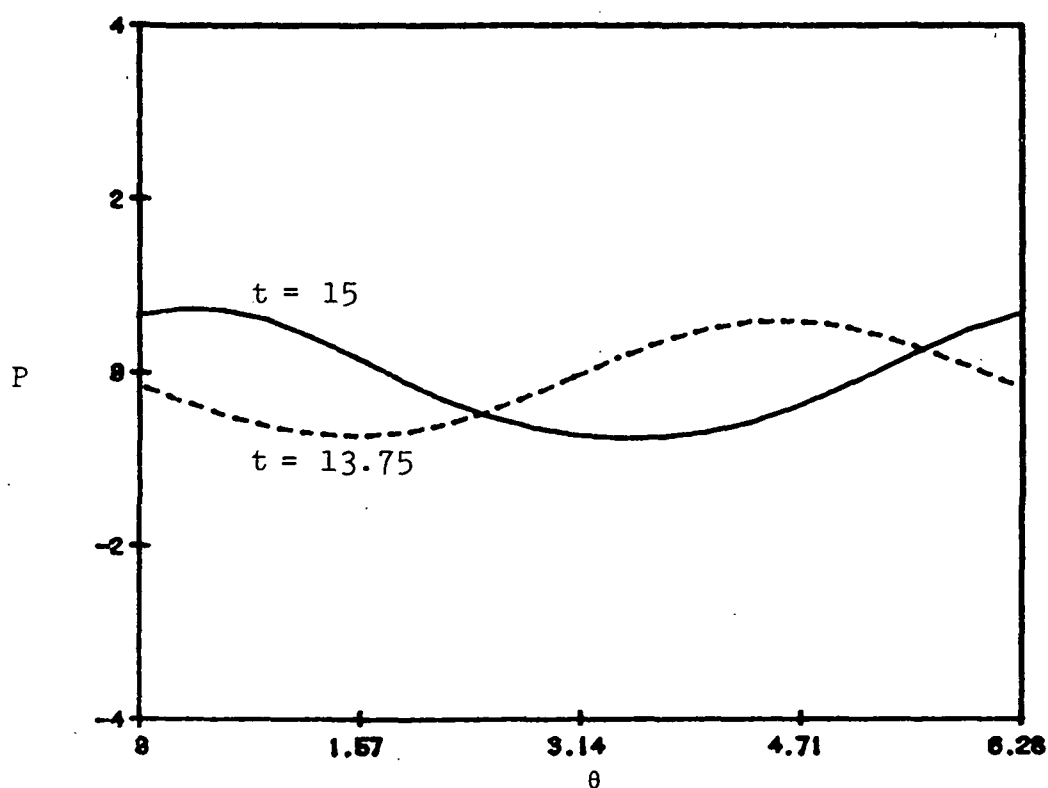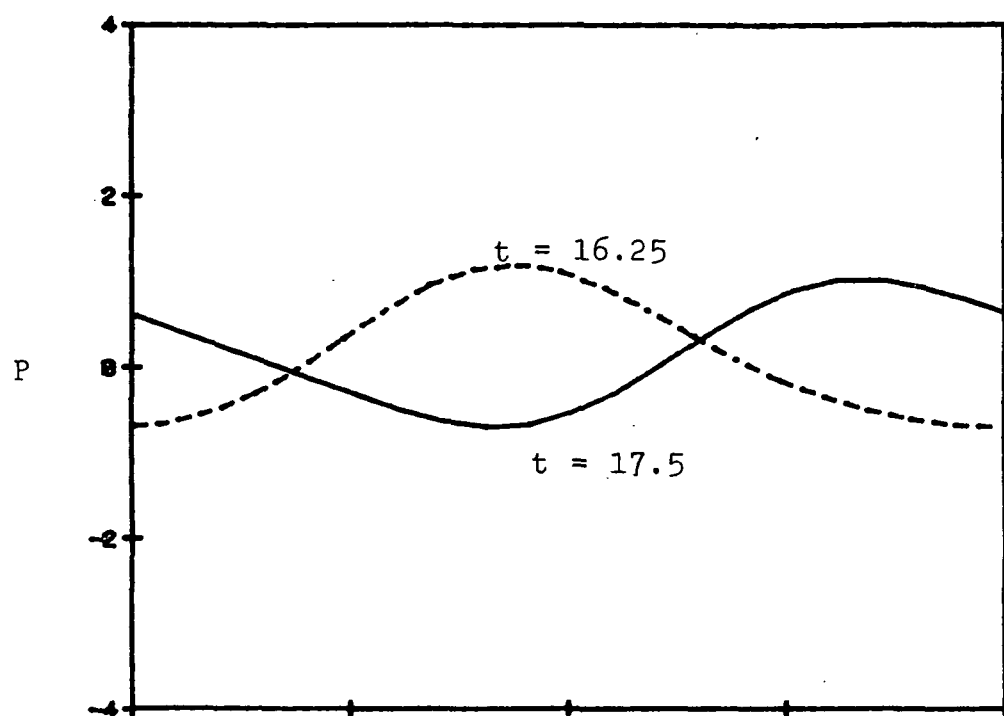
Figure 27. The Wall Pressure Waveforms for Traveling Waves

$\varepsilon = .05$ $n = 210$ $\tau = 0$ $\underline{w} = .1$
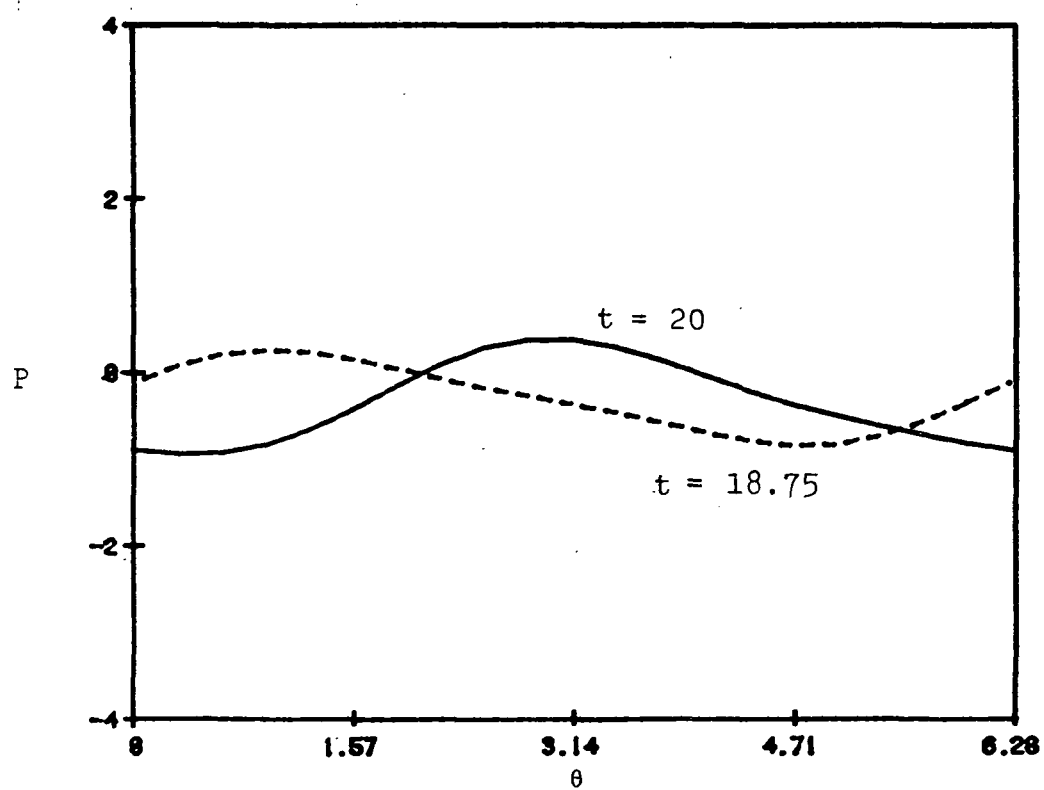
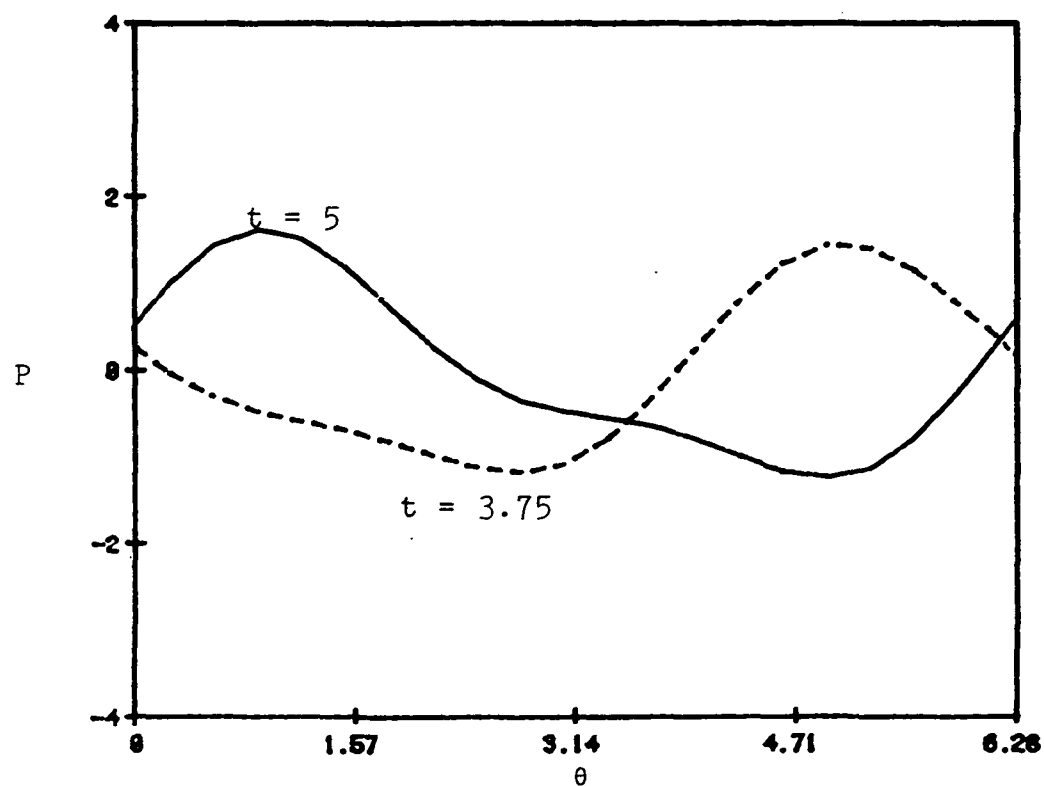Figure 28. The Wall Pressure Waveforms for Traveling Waves
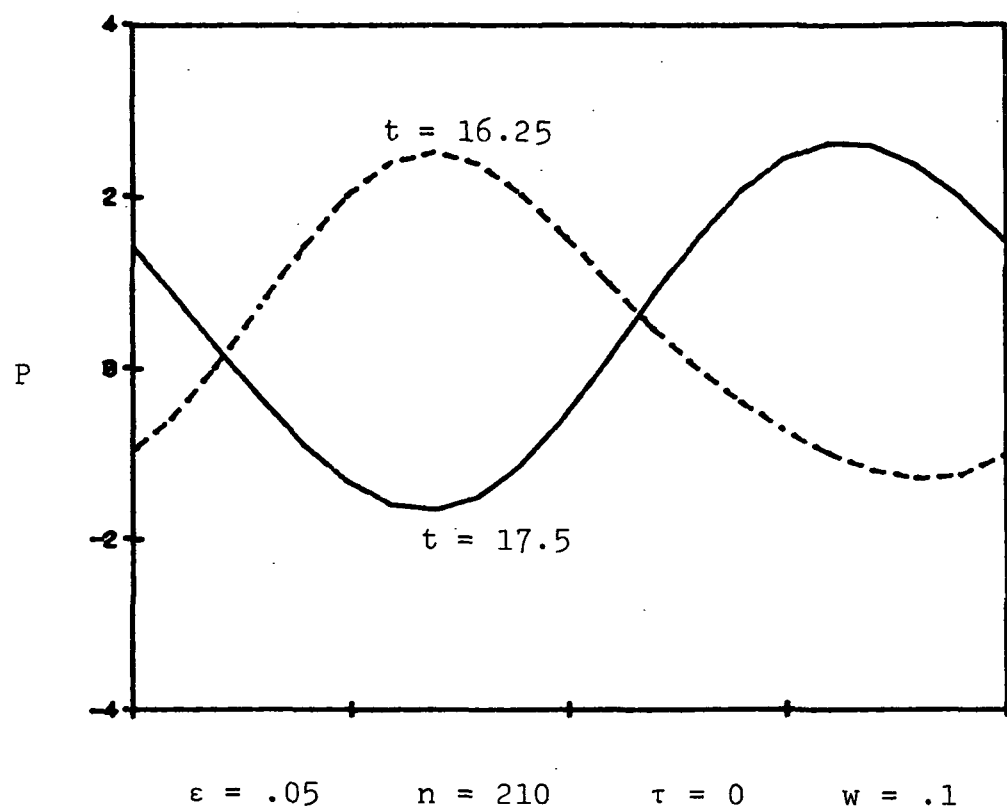
Figure 29. The Wall Pressure Waveforms for Traveling Waves
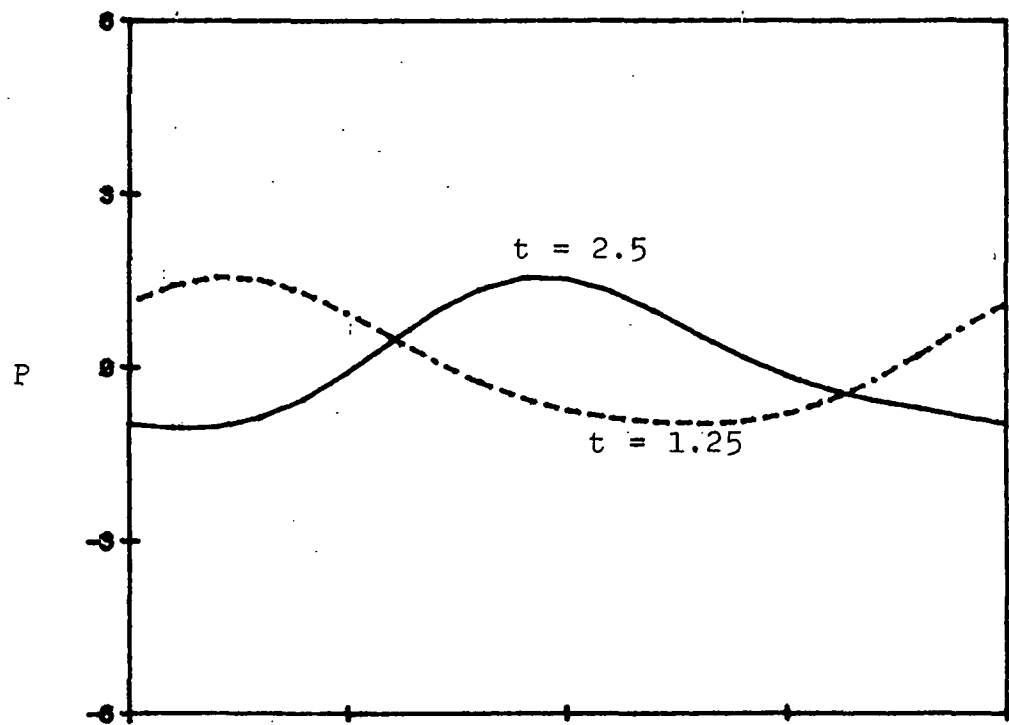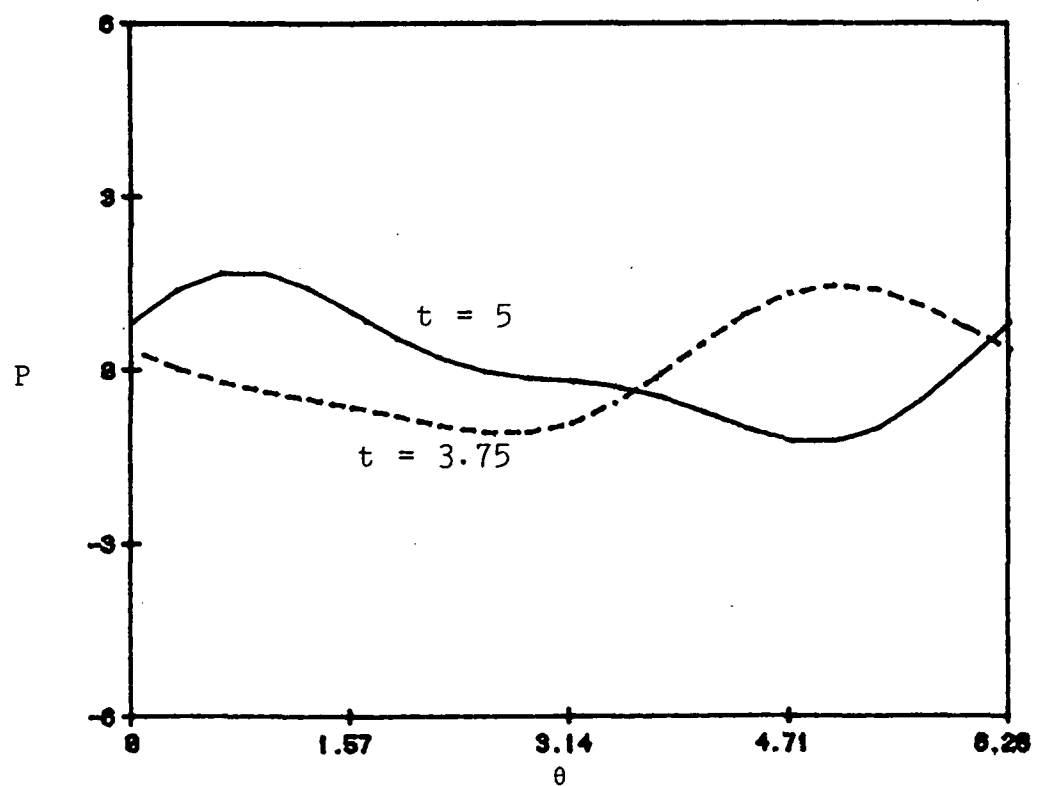
$$\epsilon = .05 \qquad n = 197 \qquad \tau = \pi \qquad \underline{w} = .1$$

Figure 30. The Wall Pressure Waveforms for Traveling Waves
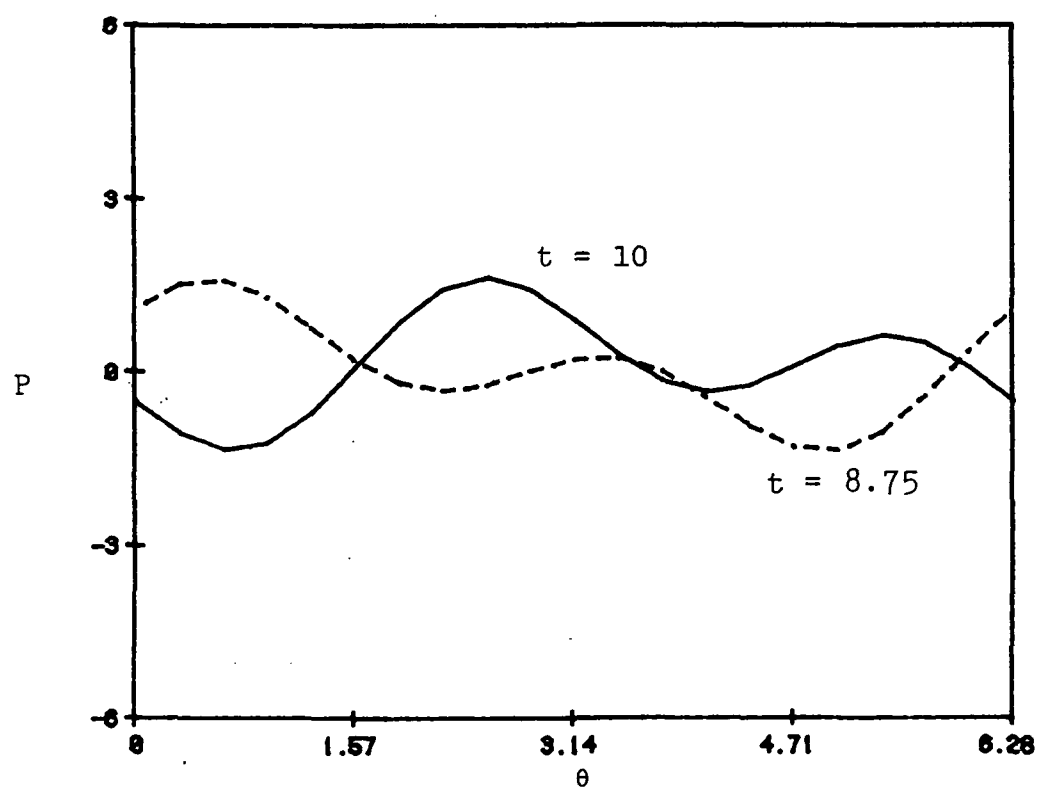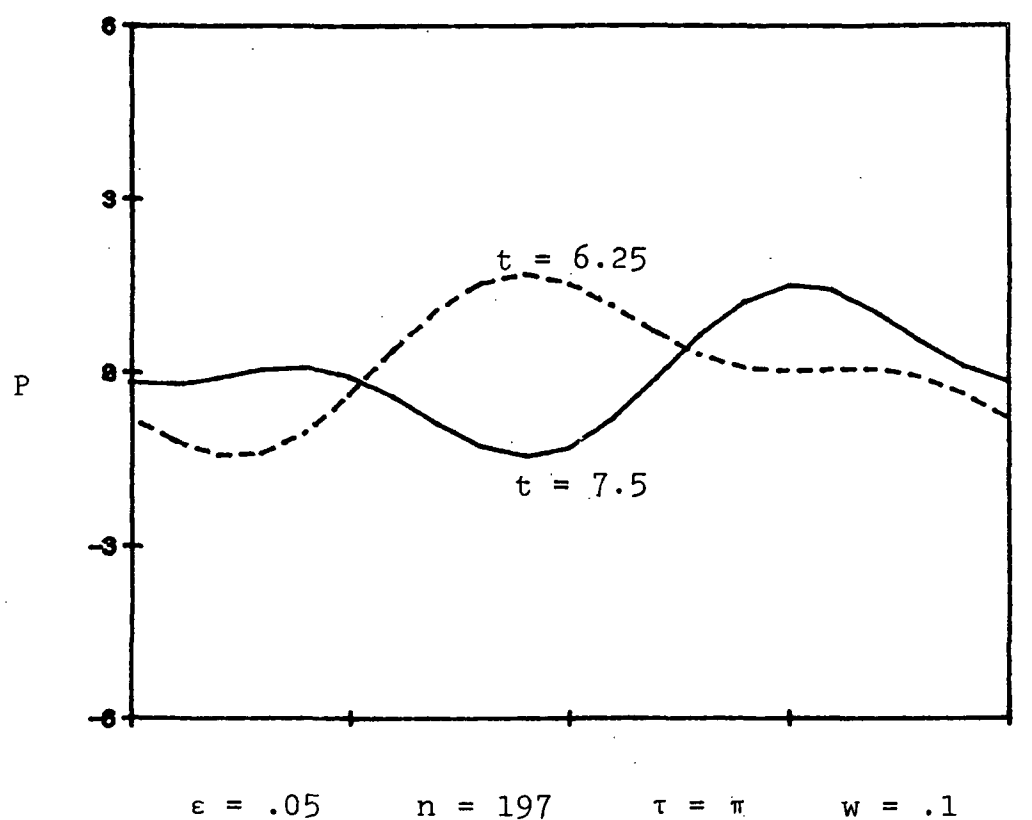
Figure 31. The Wall Pressure Waveforms for Traveling Waves
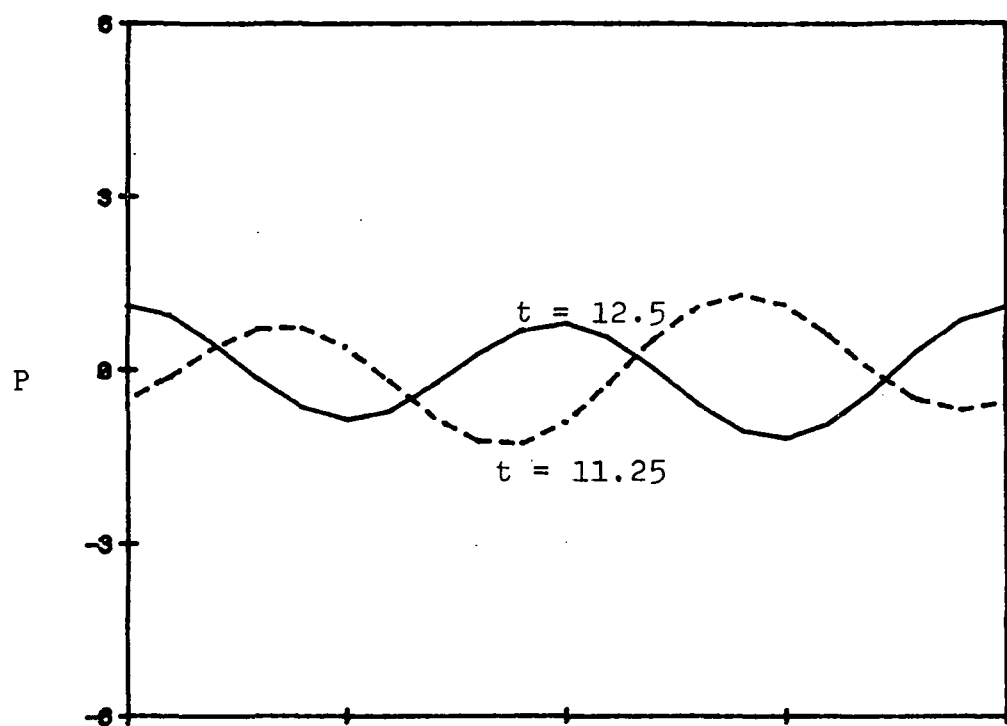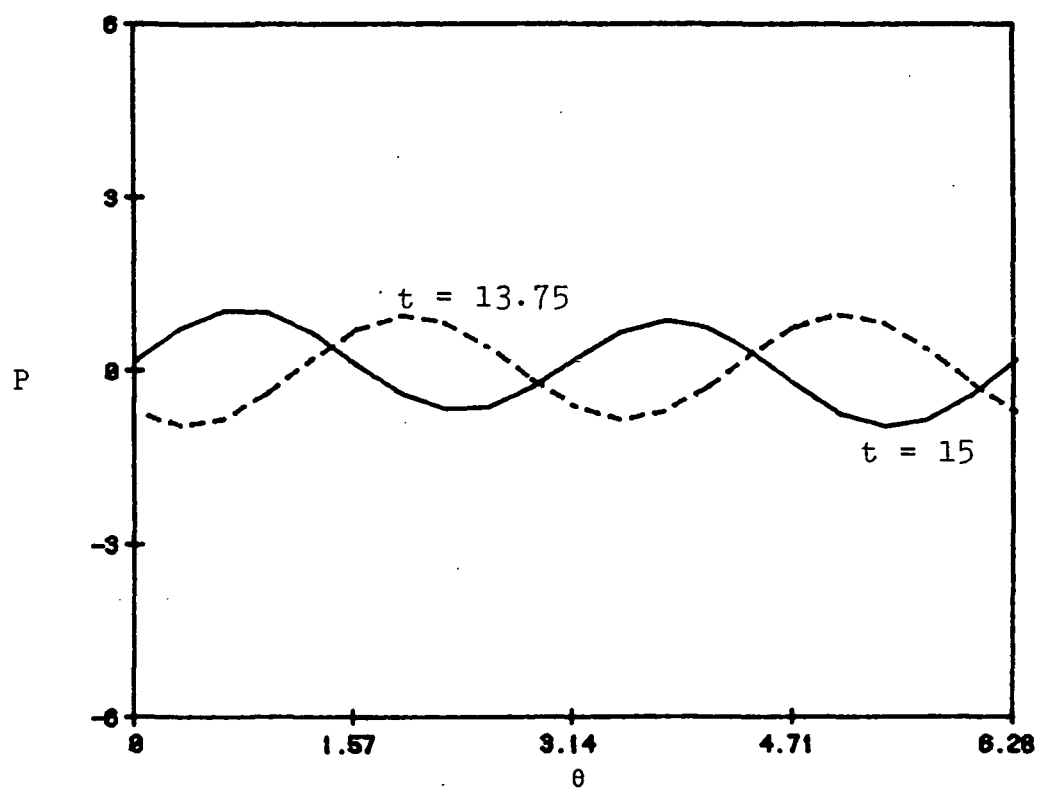
$$\varepsilon = .05 \qquad n = 197 \qquad \tau = \pi \qquad \underline{w} = .1$$

Figure 32. The Wall Pressure Waveforms for Traveling Waves
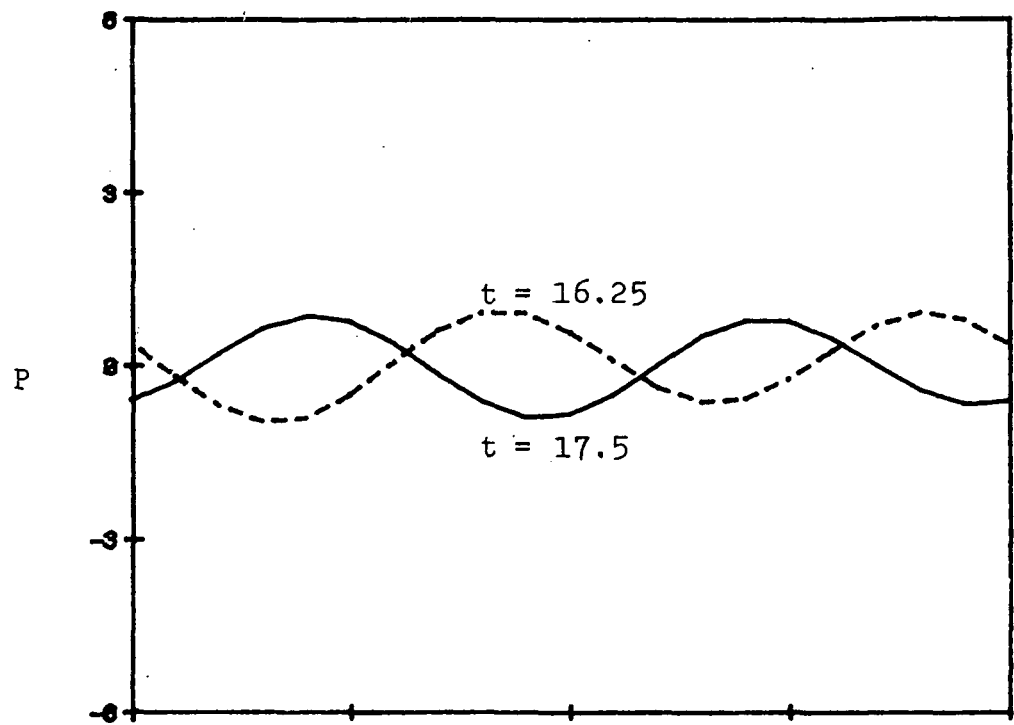
$\epsilon = .05 \qquad n = 197 \qquad \tau = \pi \qquad \underline{w} = .1$
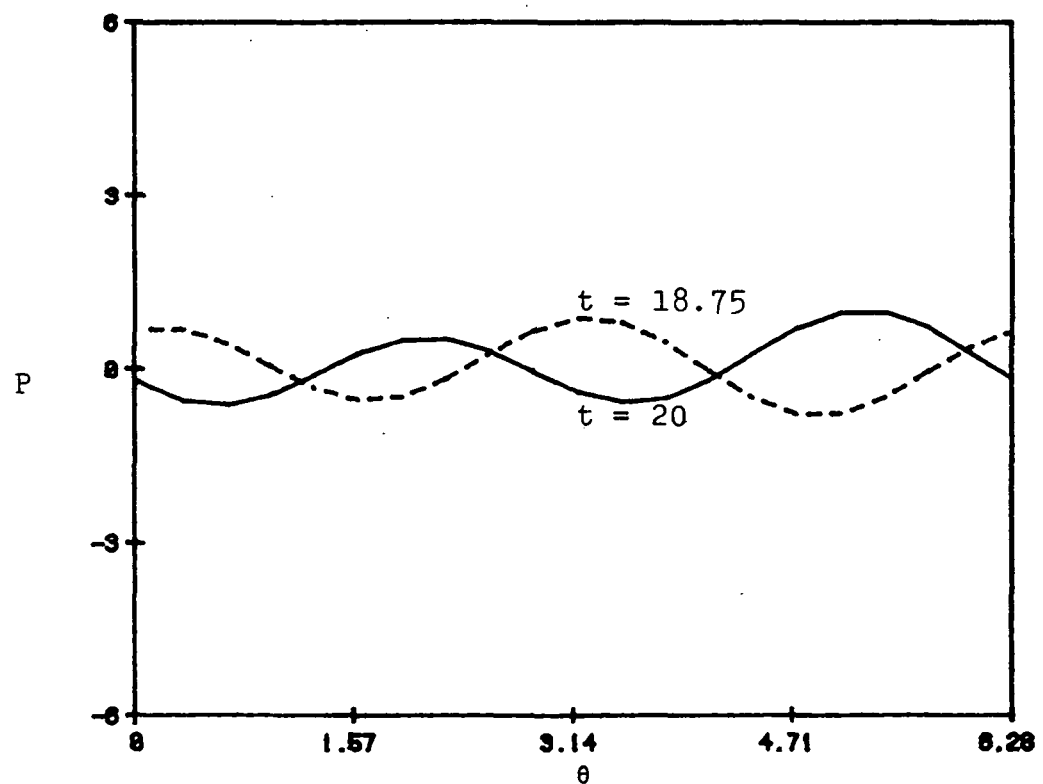
Figure 33. The Wall Pressure Waveforms for Traveling Waves
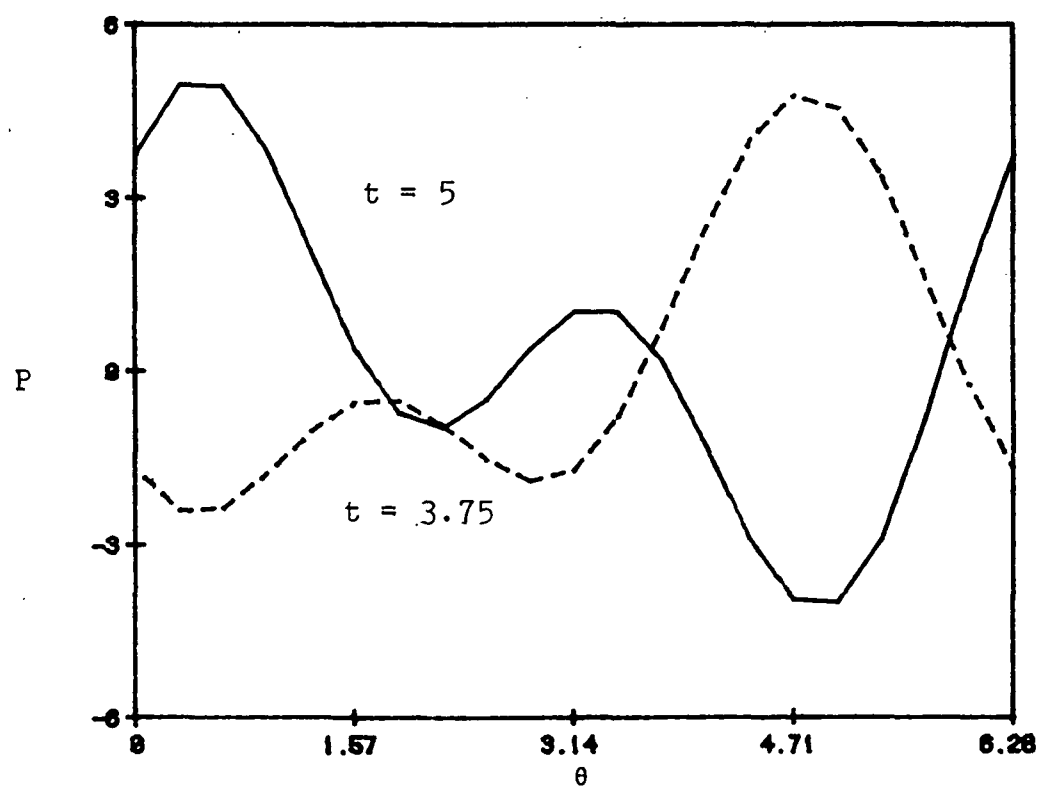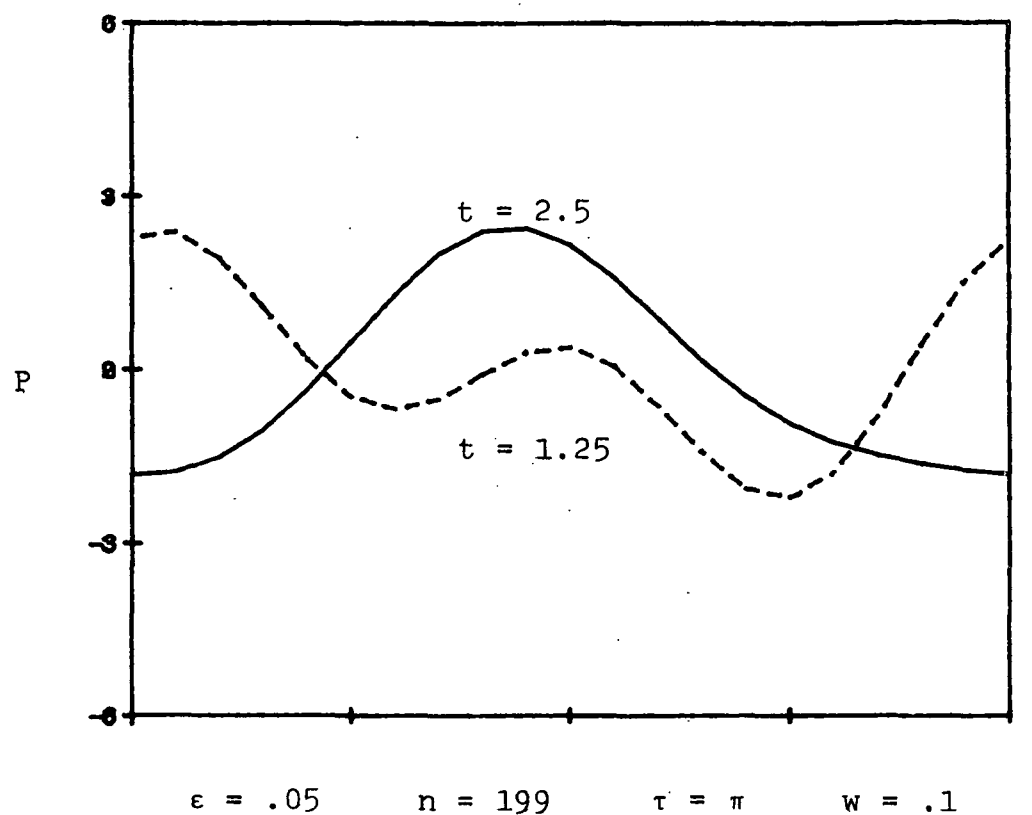
Figure 34. The Wall Pressure Waveforms for Traveling Waves
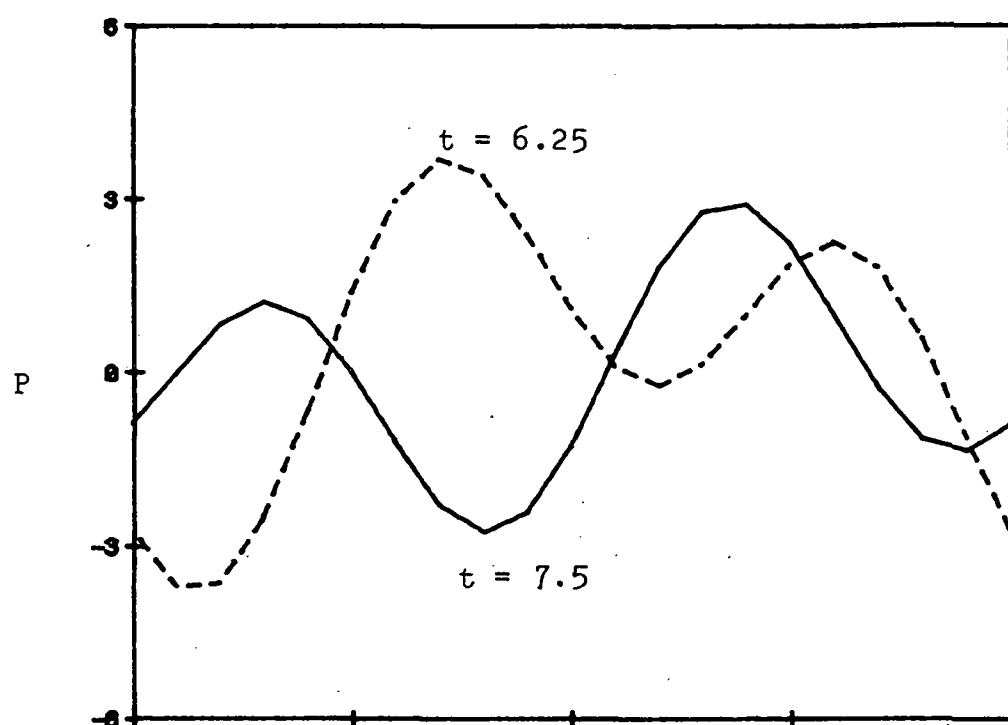
ε = .05   n = 199   τ = π   w̲ = .1
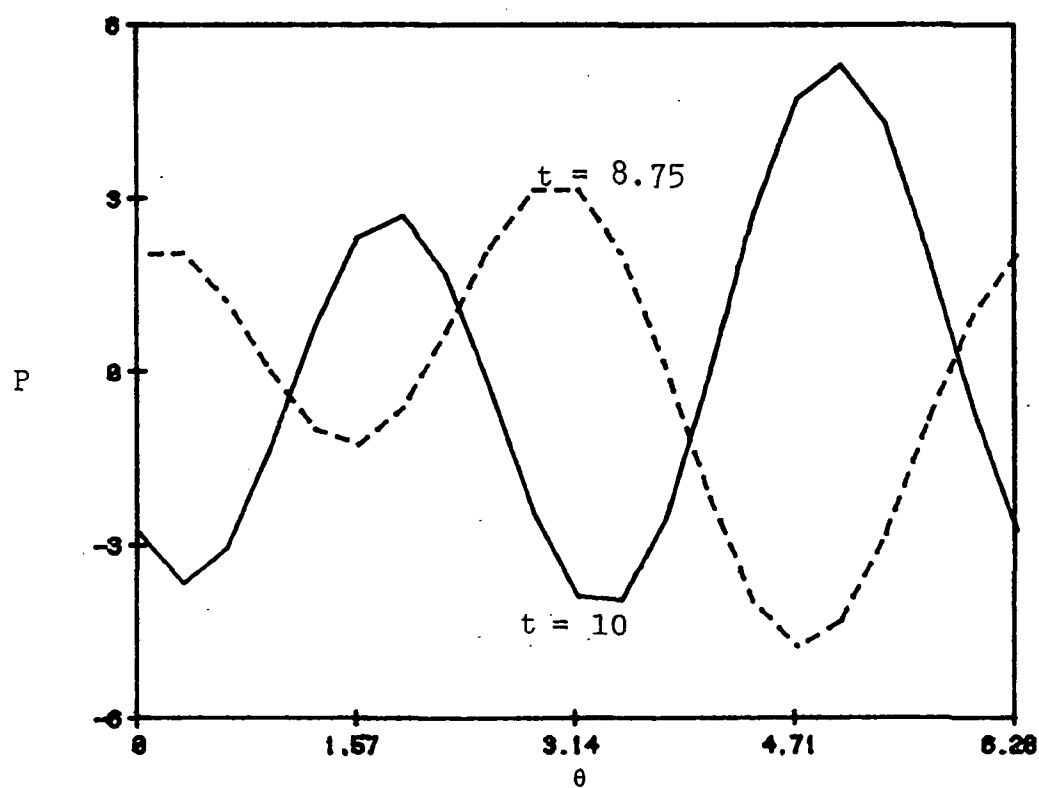
Figure 35. The Wall Pressure Waveforms for Traveling Waves
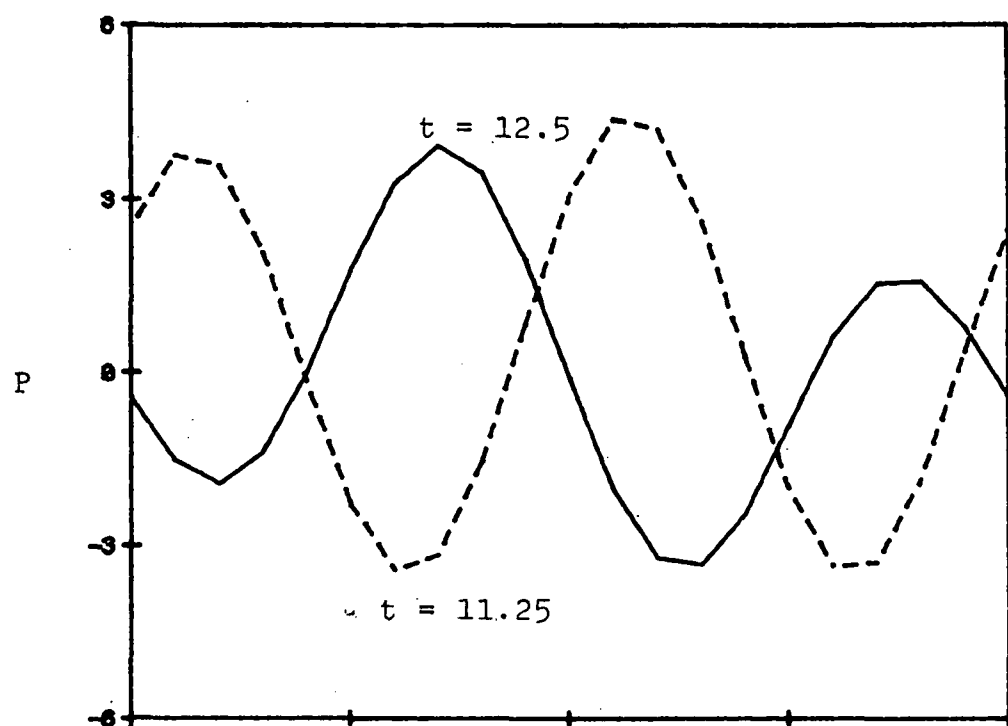
$$\epsilon = .05 \qquad n = 199 \qquad \tau = \pi \qquad \underline{w} = .1$$
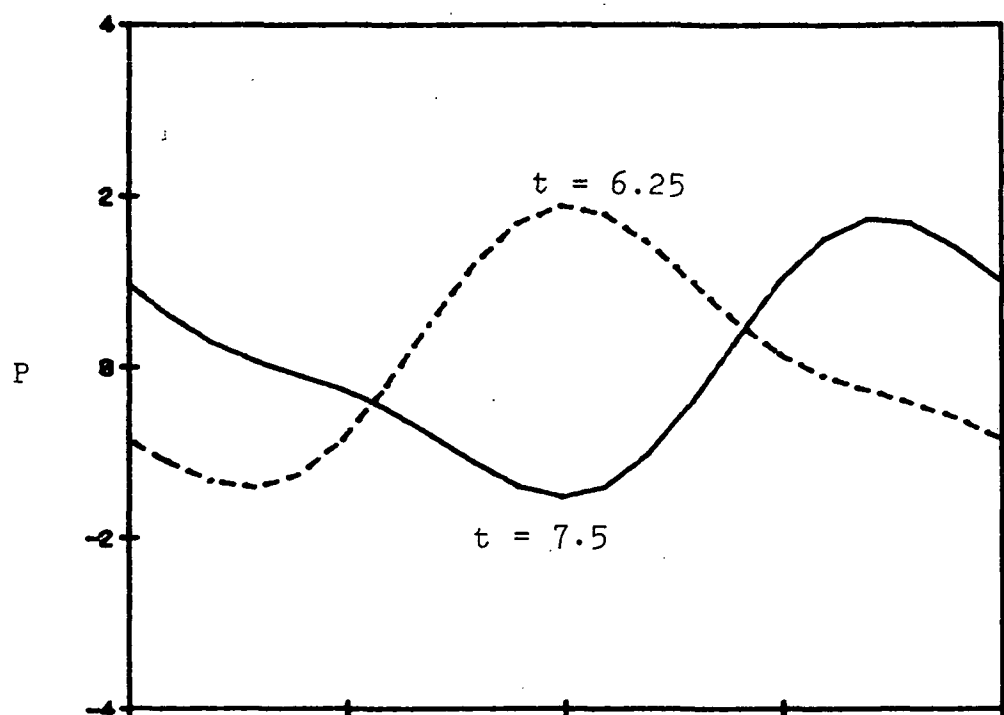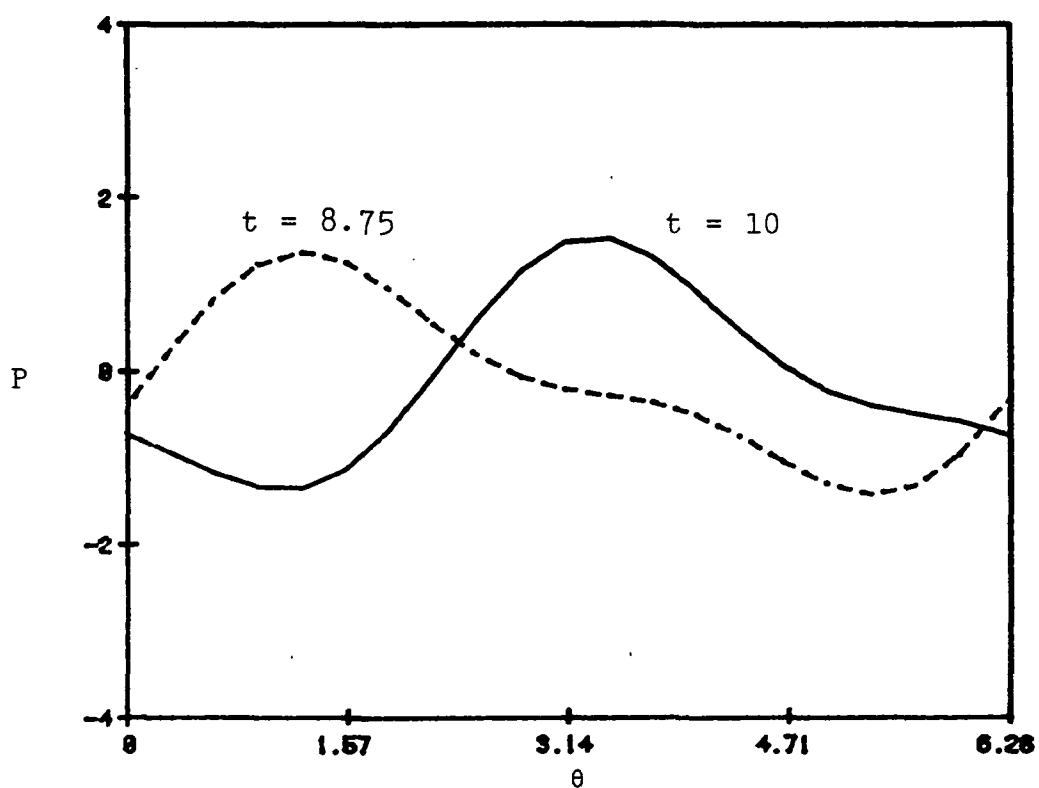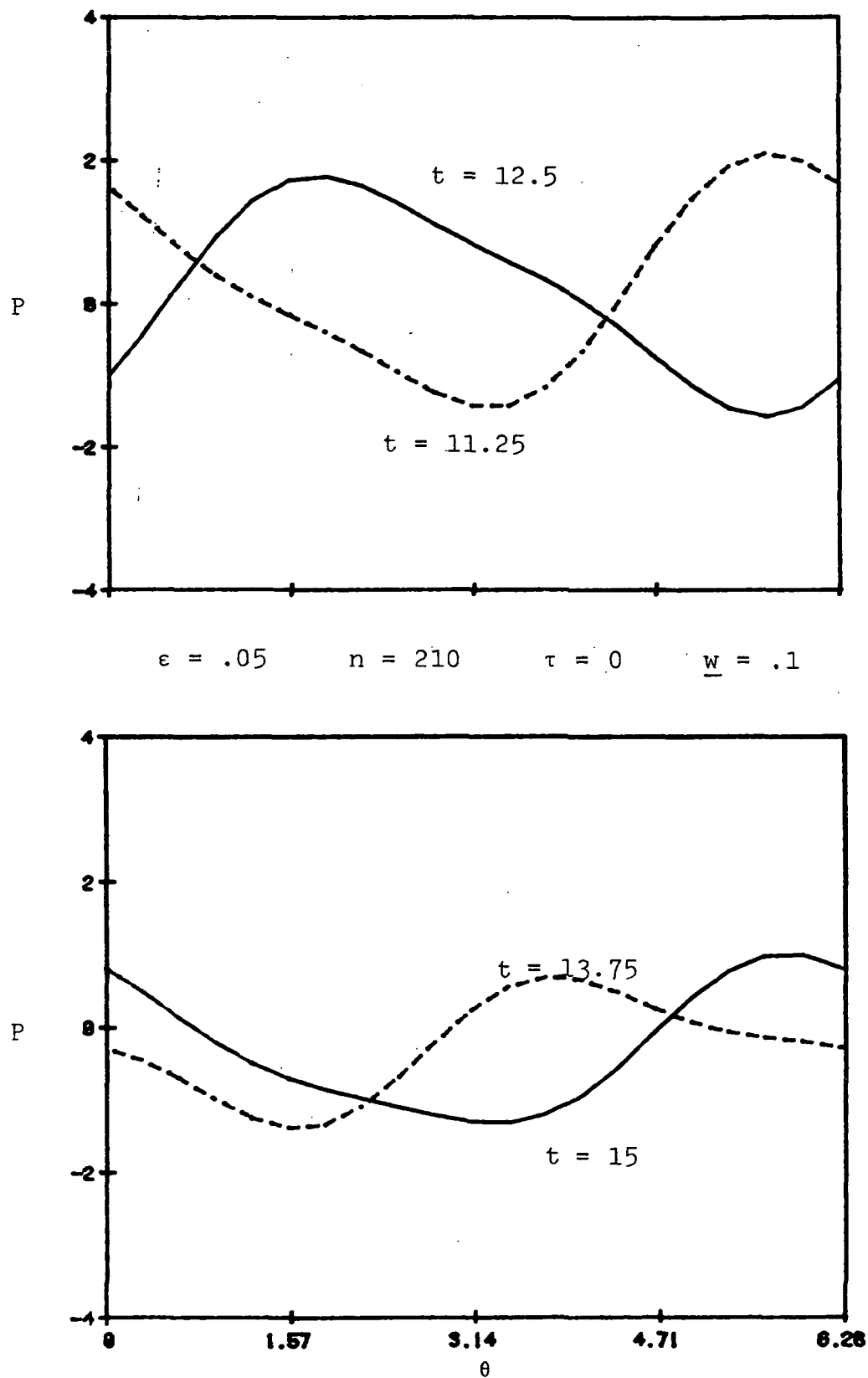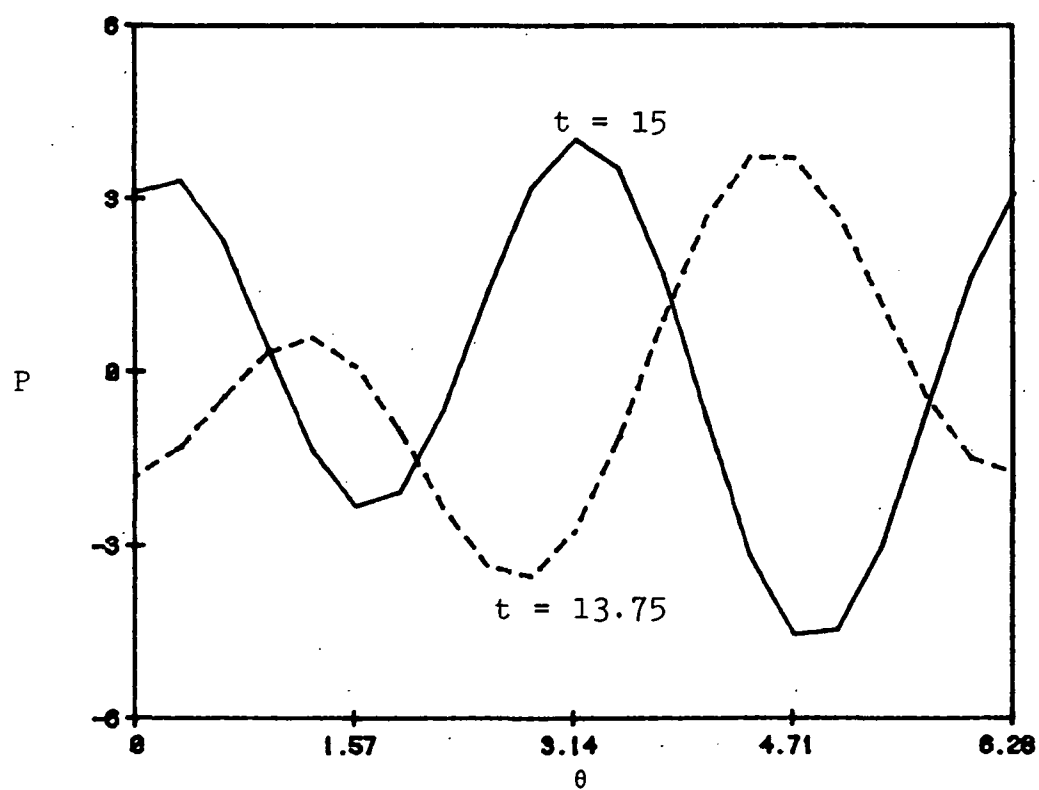
Figure 36. The Wall Pressure Waveforms for Traveling Waves
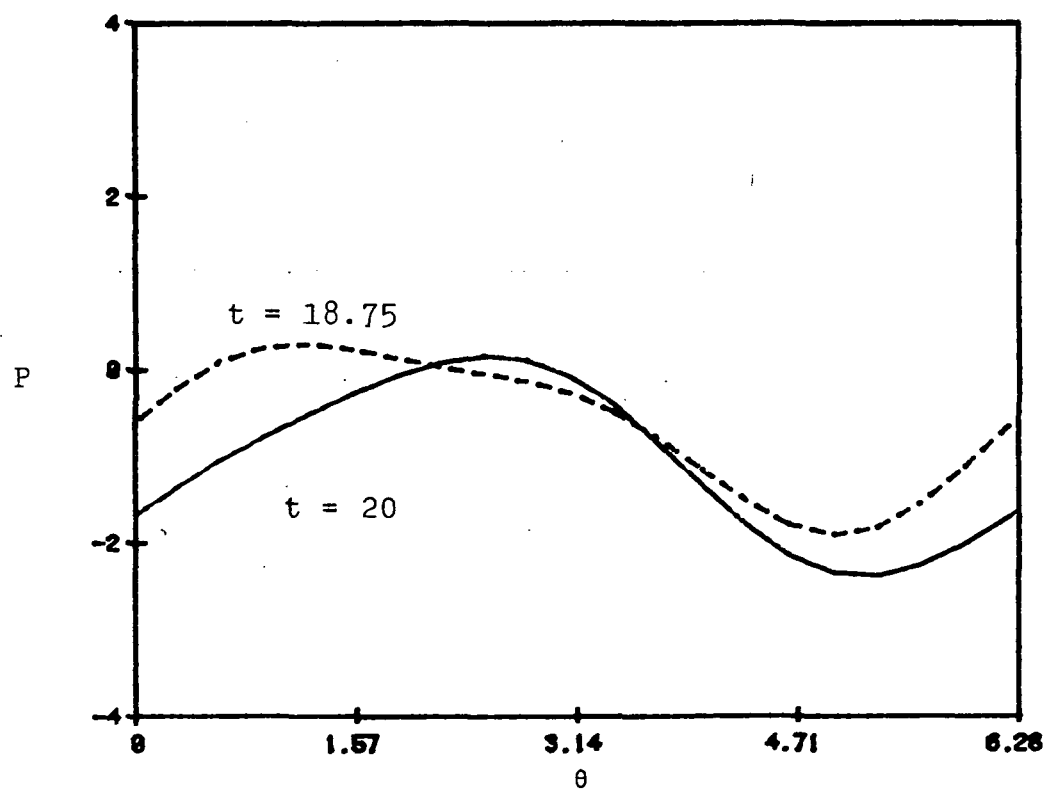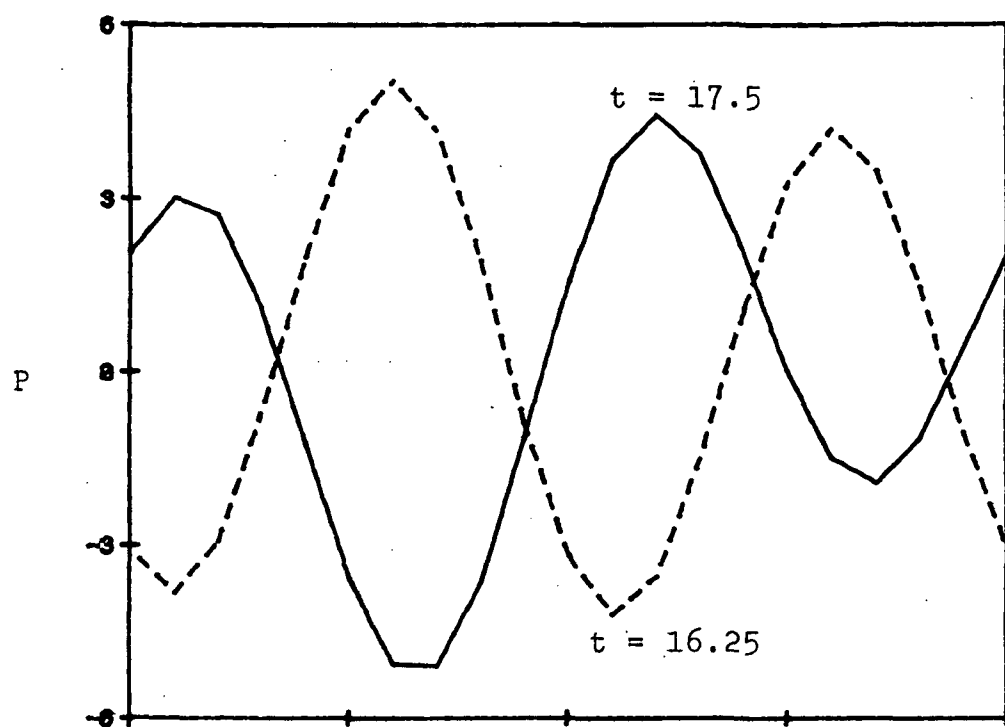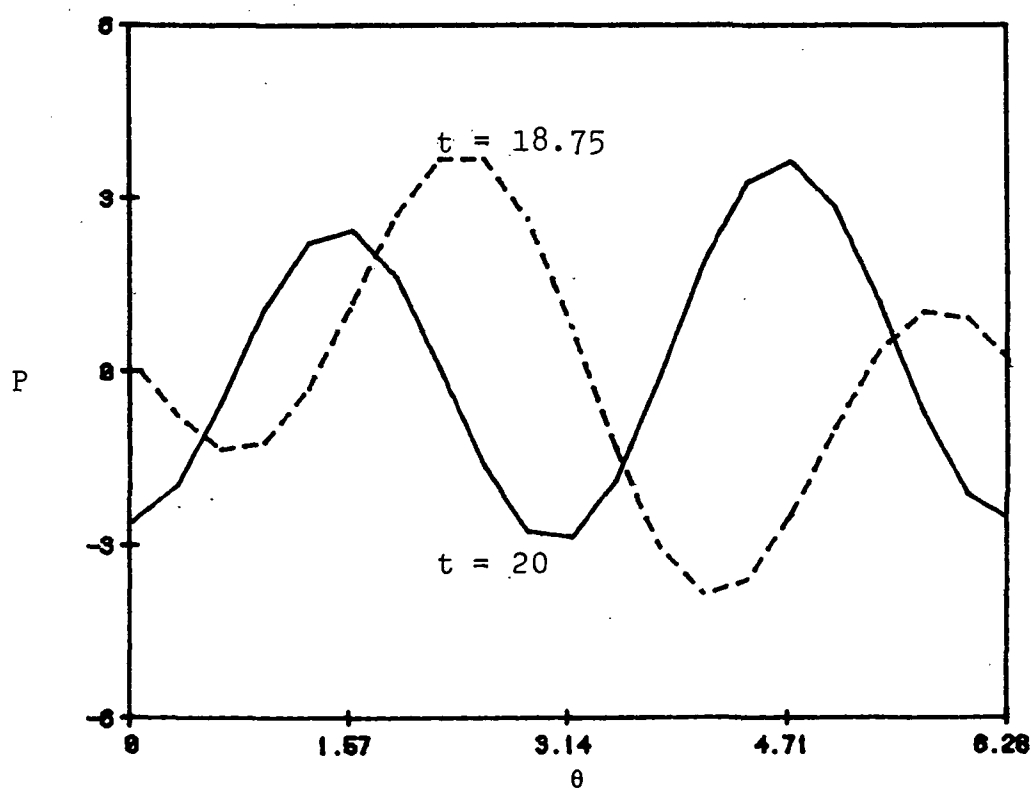
Figure 37. The Wall Pressure Waveforms for Traveling Waves

APPENDIX A

## DERIVATION OF THE COEFFICIENTS

In this section, the coefficients b_{ij}, c_{ij}, and d_{ij} appearing in chapter 3 and 5 are derived and their numerical values are presented in Table 6, 7, and 8 respectively.

In chapter 3, for initial condition (3.7), one assumes

$$\partial_{tt}\phi_2 - \nabla^2\phi_2 = \sum_{m=0}^{\infty} H_m(r)\cos(m\theta)\sin(2S_{11}t).$$

By comparing coefficient yields

$$H_0(r) = \tfrac{1}{4}S_{11}(2S_{11}^2 J_0^2 - (\gamma-1)S_{11}^2 J_1^2 - 4S_{11}J_0 J_1/r + 4J_0^2/r^2)$$

$$H_1(r) = 0$$

$$H_2(r) = \tfrac{1}{4}S_{11}(2S_{11}^2 J_0^2 - (\gamma-1)S_{11}^2 J_1^2 - 4S_{11}J_0 J_1/r)$$

$$H_m(r) = 0 \qquad\qquad \text{for } m = 3, 4, \ldots, \infty.$$

Then expanding ϕ_2 in a Fourier-Bessel series and expanding $H_m(r)$ in a Bessel series leads to

$$b_{ij} = 2S_{ij}^2 \int_0^1 H_i(r)J_i(S_{ij}r)r\,dr / \{(S_{ij}^2 - i^2)J_i^2(S_{ij})\}.$$

This integral must be computed numerically. For the sake of brevity only the first five coefficients in each series are calculated and presented in Table 6.

Table 6

BESSEL SERIES COEFFICIENTS FOR ANALYICAL SOLUTION

n	b_{0n}	b_{2n}
0	$1.11738 - 0.37246\gamma$	
1	$0.50462 + 0.37912\gamma$	$0.27181 - 1.09482\gamma$
2	$-0.09246 - 0.00802\gamma$	$-0.11390 - 0.01110\gamma$
3	$0.05019 + 0.00184\gamma$	$0.05479 + 0.00208\gamma$
4	$-0.03290 - 0.00067\gamma$	$-0.03451 - 0.00071\gamma$
5	$0.02375 + 0.00030\gamma$	$0.02451 + 0.00033\gamma$

In Chapter 5, equation (5.8) can be written as

$$\phi = f_0\phi_0 + f_1\phi_1 + f_2\phi_2 + g_1\phi_3 + g_2\phi_4 \qquad (A-1)$$

where $\qquad \phi_0 = J_0, \quad \phi_1 = J_1\cos\theta, \quad \phi_2 = J_2\cos2\theta$

$$\phi_3 = J_1\sin\theta, \quad \phi_4 = J_2\sin2\theta.$$

By substituting (A-1) into the governing equation (5.6), yields

$$R = D(\phi) \qquad (A-2)$$

where D is the nonlinear differential operator of equation
(5.6). If (A-1) represented the exact solution to (5.6), R
would vanish. Since this is not the case R has a finite
value. The Galerkin procedure consists of making R orthog-
onal to each of the ϕ_i's. This leads to the equations

$$\int_0^1 \int_0^{2\pi} R\phi_i \, r\, dr\, d = 0 \qquad i = 0,1,\ldots,4 \qquad \text{(A-3)}$$

and a set of five second order differential equations are
generated. The angular part of integration can be performed
in closed form while the radial part of integration must be
computed numerically and leads to the integral

$$C_i = \beta_k \int_0^1 F_i(r) J_k(S_{k1} r) r\, dr \qquad \text{(A-4)}$$

where
$$\beta_k = 2S_{k1}^2 / \{ (S_{k1}^2 - k^2) J_k^2(S_{k1}) \}. \qquad \text{(A-5)}$$

The numerical values of C_i are listed in Table 7 for
$\gamma = 1.2$. Also listed in this table are the functional forms
of F_i's. In writing these the notation

$$R_i = S_{11}^2 (\gamma-1) J_i'' + S_{11} J_i'/r - i^2 J_i/r^2, \qquad i=0,1,2 \qquad \text{(A-6)}$$

is used. Similarly the numerical values of

$$d_{ij} = \beta_i \int_0^1 G_{ij} J_i(S_{11} r) r\, dr \qquad \text{(A-7)}$$

and functional forms of G_{ij}'s are listed in Table 8.

Table 7

COEFFICIENTS APPEARING IN EQUATIONS (5.9) $\gamma = 1.2$

i	k	C_i	F_i
1	0	4.137	$R_0 J_0 + 2S_{01}^2 {J_0'}^2$
2	0	1.042	$R_1 J_1/2 + S_{11}^2 {J_1'}^2 + J_1^2/r^2$
3	0	-0.208	$R_2 J_2/2 + S_{21}^2 {J_2'}^2 + 4J_2^2/r^2$
4	1	-1.939	$R_0 J_1 + 2S_{01}S_{11}J_0'J_1'$
5	1	-2.312	$R_1 J_0 + 2S_{01}S_{11}J_0'J_1'$
6	1	1.719	$R_1 J_2/2 + S_{11}S_{21}J_1'J_2' + 2J_1 J_2/r^2$
7	1	1.483	$R_2 J_1/2 + S_{11}S_{21}J_1'J_2' + 2J_1 J_2/r^2$
8	2	-2.785	$R_0 J_2 + 2S_{01}S_{21}J_0'J_2'$
9	2	-3.039	$R_2 J_0 + 2S_{01}S_{21}J_0'J_2'$
10	2	1.132	$R_1 J_1/2 + S_{11}^2 {J_1'}^2 - J_1^2/r^2$
11	0	2.586	$S_{01}^2 {J_0'}^2$
12	0	0.480	$\tfrac{1}{2}(S_{11}^2 {J_1'}^2 + J_1^2/r^2)$
13	0	-0.196	$S_{21}^2 {J_2'}^2/2 + 2J_2^2/r^2$
14	1	-4.849	$2S_{01}S_{11}J_0'J_1'$
15	1	1.503	$S_{11}S_{21}J_1'J_2' + 2J_1 J_2/r^2$
16	2	-0.576	$\tfrac{1}{2}(S_{11}^2 {J_1'}^2 - J_1^2/r^2)$
17	2	-3.481	$2S_{01}S_{21}J_0'J_2'$

Table 8

COEFFICIENTS APPEARING IN EQUATION (5.12)

i	j	d_{ij}	G_{ij}
0	1	1.000	$J_0(S_{01}r)$
0	2	1.293	$\frac{1}{2}S_{01}^2 J_0'^2$
0	3	0.240	$\frac{1}{4}(S_{11}^2 J_1'^2 + J_1^2/r^2)$
0	4	-0.098	$\frac{1}{2}(S_{21}^2 J_2'^2/2 + 2J_2^2/r^2)$
0	5	-0.176	$-\frac{1}{2}J_0^2$
0	6	0.061	$-\frac{1}{4}J_1^2$
0	7	0.049	$-\frac{1}{4}J_2^2$
1	1	1.000	$J_1(S_{11}r)$
1	2	-1.212	$S_{01}S_{11}J_0'J_1'$
1	3	0.927	$\frac{1}{2}(S_{11}S_{21}J_1'J_2' + 2J_1J_2/r^2)$
1	4	0.165	$-J_0J_1$
1	5	-0.199	$-\frac{1}{2}J_1J_2$
2	1	1.000	$J_2(S_{21}r)$
2	2	-1.741	$S_{01}S_{21}J_0'J_2'$
2	3	-0.223	$\frac{1}{4}(S_{11}^2 J_1'^2 - J_1^2/r^2)$
2	4	0.237	$-J_0J_2$
2	5	-0.175	$-\frac{1}{4}J_1^2$

APPENDIX B

PROGRAM FOR STABILITY BOUNDARY CURVES

```
$SET LIST FREE
C
C      KIN-WING WONG                    JUN 30 1978
C
C      CCMBUSTION INSTABILITY
C
C.     METHOD   GALERKIN METHOD
C*     THIS PROGRAM GENERATE THE STABILITY CURVE.
C
C      INPUT INFORMATION
C
C      THE PROGRAM USED THE FORMAT FREE INPUT OUTPUT.  A
C      CCMMA SERVES AS A DELIMITER AND THE INPUT VARIABLES
C      ARE ENTER IN THE FOLLOWING ORDER
C           TI           INITIAL TIME
C           TF           FINAL TIME
C           DT           STEP SIZE FOR TIME
C           WB           BURNING RATE
C           TDELAY       DELAY TIME
C
C           EI           INITIAL EPS
C           EF           FINAL EPS
C           DE           STEP SIZE FOR EPS
C           DA           ASSUME POSITION FOR N
C           FO,FD        ARE THE INITIAL CONDITION MODIFIER AND
C                        HAVING THE VALUE EITHER 1 OR 0
C
C      ANOTHER SETS OF DATA CAN BE ENTER BY ENTERING
C          EI,EF,DE,DA,FO AND FD.
C
       DIMENSION DY(10),FO(5),DF(5),G(10,500),Y(10)
       COMMON EP,     RK,WB,EPANV
       COMMON /SLIST/S0,S1,S2
       COMMON /BLK1/C1,C2,C3,C4,C5,C6,C7,C8,C9,C10,C11,C12
      1,C13,C14,        C15,C16,C17
       LOGICAL PASS,GROW
       DATA MAXITR,EPS/20,.1/
       DATA PI/3.14159/
       READ(5,/) TI,TF,DT,WB,TDELAY
       PRINT*//,TI,TF,DT,WB,TDELAY
       TDELAY=PI*TDELAY
       K=TDELAY/DT
       K1=K+1
       IF (K1.GT.500) GO TO 105
       IF (K.LT.1.AND.NDF.EQ.1) K=1
       NSTEP=(TF-TI)/DT
       N=10
       HHALF=DT*.5
       NPROB=0
9      READ(5,/,END=999) EI,EF,DE,DA,FO,DF
       NPROB=NPROB+1
```

```
      PRINT*//,NPROB
      PRINT *//,FO,DF
      NSTEP=(EF-EI)/DE
      EF=EI
      IF (EP.LT.0) EP=.01
      ANV=DA
      PASS=.FALSE.
      DO 100 ISTEP =0,NSTEP
      DO 80 ITR=1,MAXITR
      EPANV=EP*ANV
      IF (EPANV.EQ.0) EPANV=ANV
      DO 10 I=1,K
      DO 10 J=1,N
 10   G(J,I)=0.
      DO 20 I=1,N
 20   Y(I)=0.
C
C     INITIAL CONDITION
C
      Y(2)=FO(1);Y(4)=FO(2);Y(6)=FO(3);Y(8)=FO(4);Y(10)=FO
     1(5)
      Y(1)=DF(1)*SO;Y(3)=DF(2)*S1;Y(5)=DF(3)*S2
      Y(7)=DF(4)*S1;Y(9)=DF(5)*S2
      CALL DLYFUN (N,Y,G,K,EPS,K1)
      T=TI
C
      DO 40 I=1,NSTEP
      CALL RKDELY(N,T,Y,DY,DT,G,K,EP,&110,HHALF,K1)
      DO 30 J=2,N,2
      IF(ABS(Y(J)).GT.2) GO TO 60
 30   CONTINUE
 40   CONTINUE
      GROW=.FALSE.
      IF (PASS) GO TO 50
      ANVDWN=ANV
      ANV=ANV+DA
      GO TO 80
 50   CONTINUE
      ANVDWN=ANV
      GO TO 70
 60   CONTINUE
      PASS=.TRUE.
      GROW=.TRUE.
      ANVUP=ANV
 70   CONTINUE
      IF (ABS(ANVUP-ANVDWN).LT.EPS) GO TO 90
      ANV=(ANVUP+ANVDWN)*.5
 80   CONTINUE
 90   CONTINUE
      NNU=ANV
      PRINT *//,EP,NNU,ITR
```

```
      IF (ITR.EQ.MAXITR) PRINT //,'*** WARNING *** THE
     1 ANSWERMAY NOT CONVERGE'
      EP=EP+DE
      ANV=ANVUP/2;ANVDWN=0
  100 CCNTINUE
      GC TO 9
  105 PRINT //,'DELAY TIME TOO LARGE ',TDELAY
      GC TO 999
  11C PRINT *//,'ILLEGAL DELAY FUNCTION'
  999 STOP
      END
      SUBROUTINE DIFFUN (T,Y,DY)
C
C     THIS SECTION PROVIDE A SET OF FIVE SECOND ORDER
C       EQUATIONS
C     WHERE
C         FO=Y(2)              G1=Y(8)
C         F1=Y(4)              G2=Y(10)
C         F2=Y(6)
C
      DIMENSION Y(10),DY(10)
      CCMMON EP, FK,WB,EPANV
      COMMON /SLIST/SO,S1,S2
      COMMON /BLK1/ C1,C2,C3,C4,C5,C6,C7,C8,C9,C10,C11,C12
     1,C13,C14,      C15,C16,C17
C
      DY(2)=Y(1)
      DY(1)=-SO*SO*Y(2)-EP*(C1*Y(2)*Y(1)+C2*(Y(4)*Y(3)+Y(8)
     1*Y(7))   +C3*(Y(10)*Y(9)+Y(6)*Y(5)))
      DY(4)=Y(3)
      DY(3)=-S1*S1*Y(4)-EP*(C4*Y(2)*Y(3)+C5*Y(4)*Y(1) +
     1 C6*(Y(8)*Y(9)+Y(4)*Y(5))+C7*(Y(6)*Y(3)+Y(10)*Y(7)))
      DY(6)=Y(5)
      DY(5)=-S2*S2*Y(6)-EP*(C8*Y(2)*Y(5)+C9*Y(6)*Y(1)+   C10*
     1(Y(8)*Y(7)-Y(4)*Y(3)))
      DY(8)=Y(7)
      DY(7)=-S1*S1*Y(8)-EP*(C4*Y(2)*Y(7)+C5*Y(8)*Y(1)+   C6*
     1(Y(4)*Y(9)-Y(8)*Y(5))+C7*(Y(10)*Y(3)-Y(6)*Y(7)))
      DY(10)=Y(9)
      DY(9)=-S2*S2*Y(10)-EP*(C8*Y(2)*Y(9)+C9*Y(10)*Y(1)   C10
     1*(Y(8)*Y(3)+Y(4)*Y(7)))
      IF (RK.EQ. 2) RETURN
C
C     THIS PROVIDE THE COMBUSTION TERMS
C
      DY(1)=DY(1)-WB*(Y(1)+EPANV*(C11*Y(2)*Y(2)+C12*(Y(4)*Y
     1(4)+  Y(8)*Y(8))+     C13*(Y(10)*Y(10)+Y(6)*Y(6))))
      DY(3)=DY(3)-WB*(Y(3)+EPANV*(C14*Y(2)*Y(4)+C15*(Y(4)*Y
     1(6)+     Y(8)*Y(10))))
      DY(5)=DY(5)-WB*(Y(5)+EPANV*(C16*(Y(4)*Y(4)-Y(8)*Y(8))
     1        +C17*Y(2)*Y(6)))
```

```
      DY(7)=DY(7)-WB*(Y(7)+EPANV*(C14*Y(2)*Y(8)+C15*(Y(4)*Y
     1(10)  Y(8)*Y(6))))
      DY(9)=DY(9)-WB*(Y(9)+EPANV*(C17*Y(2)*Y(10)+2*C16*Y(4)
     1*Y(8)))
      RETURN
      END
      SUBROUTINE RKDELY(N,T,Y,DY,H,G,K,EPS, *,HHALF,K1)
C
C     THIS SECTION PERFORM A FOURTH ORDER RUNGE-KUTTA METHOD
C     WITH TIME DELAY FUNCTION
C
      DIMENSION Y(10),DY(10),Y2(10),Y3(10),G(10,500)
      COMMON EP,   RK,WB,EPANV
      COMMON /BLK1/ C1,C2,C3,C4,C5,C6,C7,C8,C9,C10,C11,C12
     1,C13,C14,    C15,C16,C17
      CALL DIFFUN(T,Y,DY)
      DO 10 I=1,N
         Y2(I)=Y(I) + HHALF*(DY(I) + G(I,1))
         G(I,1)=(G(I,1)+G(I,2))/2.
 10   CONTINUE
      T=T+HHALF
      CALL DIFFUN(T,Y2,DY)
      DO 20 I=1,N
         Y3(I)=Y(I) + HHALF*(DY(I) + G(I,1))
 20      Y2(I)= Y2(I) + 2.*Y3(I)
      CALL DIFFUN( T,Y3,DY)
      DO 40 I=1,N
         Y3(I)=Y(I) + H*(DY(I) + G(I,1))
      IF(K.LT.1) GO TO 40
      DO 30 J=1,K
 30   G(I,J)=G(I,J+1)
 40      Y2(I)=Y2(I) + Y3(I)
      T=T+HHALF
      CALL DIFFUN (T   ,Y3,DY)
      DO 50 I=1,N
         Y(I) = (Y2(I) - Y(I) + HHALF*(DY(I) + G(I,1)))/3.
 50   CONTINUE
      ENTRY  DLYFUN (N,Y,G,K,EPS,K1)
C
C     THIS GIVES THE FORM OF DELAY FUNCTION G
C
      IF (K.LT.1) RETURN
      IF (RK.EQ.2) RETURN
      G(1,K1)=     WB*        EPANV*(C11*Y(2)*Y(2)+C12*(Y(4)*Y
     1(4)+  Y(8)*Y(8))+   C13*(Y(10)*Y(10)+Y(6)*Y(6)))
      G(3,K1)=     WB*        EPANV*(C14*Y(2)*Y(4)+C15*(Y(4)*Y
     1(6)+   Y(8)*Y(10)))
      G(5,K1)=WB*EPANV*(C16*(Y(4)*Y(4)-Y(8)*Y(8))+C17*Y(2)*Y
     1(6))
      G(7,K1)=     WB*        EPANV*(C14*Y(2)*Y(8)+C15*(Y(4)*Y
     1(10)  Y(8)*Y(6)))
```

```
G(9,K1)=WB*EPANV*(C17*Y(2)*Y(10)+2*C16*Y(4)*Y(8))
RETURN
END
BLOCK DATA
COMMON /BLK1/C1,C2,C3,C4,C5,C6,C7,C8,C9,C10,C11,C12
1,C13,C14,     C15,C16,C17
COMMON /SLIST/S0,S1,S2
DATA S0,S1,S2/3.83171,1.84118,3.05424/
DATA C1,C2,C3,C4/4.1373,1.0423,-.2084,-1.9394/
DATA C5,C6,C7,C8,C9 /-2.3123,1.7187,1.4828,-2.785,
1-3.0388/
DATA C10,C11,C12,C13/1.1318,2.586,.480,-.196/
DATA C14,C15,C16,C17/-2.4243,1.8534445,-.447,-3.481/
END
```

APPENDIX C

PROGRAM FOR MODAL AMPLITUDE AND PRESSURE

```
$SET LISTUTOBIND
$BIND =   FROM *FORTLIB/= FREE
FILE  1(KIND=DISK,MAXRECSIZE=15,BLOCKSIZE=420,AREAS=4
     1,AREASIZE=1400,FILETYPE=7)
C
C     KIN-WING WONG                   JUN 30 1978
C
C     CCMBUSTION INSTABILITY
C
C     METHOD:  THIS PROGRAM USED THE GALERKIN METHOD TO
C        GENERATE FIVE SECOND ORDER DIFFERENTIAL EQUATIONS.
C        A FOURTH ORDER RUNGE-KUTTA METHOD IS USED TO SOLVE
C        THE RESULTING EQUATIONS.
C
C     THE PROGRAM GIVES THE MODAL AMPLITUDE AND THE PERTUBED
C        PRESSURE IN GRAPHICAL FORM.
C
C     THERE ARE TWO TYPES OF INPUT DATAS.  THE FIRST SET OF
C        INPUT DATA USED FORMAT FREE INPUT.  A COMMA SERVES
C        AS A DELIMITER AND THE DATA ENTER AS FOLLOW:
C             TI    INITIAL TIME
C             TF    FINAL TIME
C             DT    STEP SIZE FOR TIME
C             NP    PRINT FREQUENCY
C             NOF   1 FOR THE DELAY TIME APPROCHING 0
C                   0 OTHERWISE
C             IGAS  1 FOR GAS-DYNAMIC TERMS
C                   0 OTHERWISE
C             FO,   INITIAL CONDITION MODIFIER
C             DF    EITHER 1 OR 0
C             R     RADIUS OF THE CYLINDER
C
C     THE SECOND SET OF DATA USED THE NAMELIST (LIST)
C        INPUT OUTPUT OPTION.  THE DATA CAN BE ENTERED IN
C        ANY ORDER.  HOWEVER THE FOLLOWING DATA MUST BE
C        PROVIDED INITIALLY.
C          TDELAY    DELAY TIME IN MULTIPLE OF PI
C             EP     ORDER PARMETER
C             WB     STEADY BURNING RATE
C             ANV    INTERACTION PARMETER
C             PLOT T FOR PRESSURE PLOT
C                  F OTHERWISE
C
C     IF PLOT IS TRUE, ONE MORE DATA (NUMPT) IS NEEDED TO
C        PROVIDE THE NUMBER OF POINT WITHIN 0 AND 2*PI.
C
      DIMENSION   XX(100),YY(100),DY(10),P(5),FO(5),DF(5),G
     1(10,500),Y(10)
      CCMMON EP,IGAS,     RK,WB,EPANV
      CCMMON /SLIST/SC,S1,S2
      CCMMON /BLK1/ C1,C2,C3,C4,C5,C6,C7,C8,C9,C10,C11,C12
```

```
      1,C13,C14,      C15,C16,C17
      COMMON /BLK2/C02,C03,C04,C05,C06,C07,C12P,C13P,C14P
      1,C15P,              C22,C23,C24,C25,GAMA
      COMMON /BLK3/ BJO,BJ1,BJ2,COSQ,COS2Q,SINQ,SIN2Q
      DATA PI/3.14159/
      LCGICAL PLOT
      NAMELIST /LIST/ TDELAY,EP,WB,ANV,PLOT
      READ(5,/) TI,TF,DT,NP,NDF,IGAS,FO,DF,R
      PRINT *//,TI,TF,DT,NP,NDF
      IF (IGAS.EQ.0) PRINT //,'GAS DYNAMIC TERM IS OFF'
      PRINT *//,FO,DF,R
      EFS=1.E-6
      CALL BESJ(SO*R,0,BJO,EPS,IER)
      CALL BESJ(S1*R,1,BJ1,EPS,IER)
      CALL BESJ(S2*R,2,BJ2,EPS,IER)
999   READ(5,LIST,END=99)
      REWIND 1
      TDLY=PI*TDELAY
      EFANV=EP*ANV
      IF (EPANV.EQ.0) EPANV=ANV
      WRITE(6,LIST)
      N=10
      HHALF=DT*.5
      K=TDLY/DT
      K1=K+1
      IF (K1 .GT. 500) GO TO 500
      IF (K.LT.1.AND.NDF.EQ.1) K=1
      DC 30 I=1,K
      CC 30 J=1,N
30    G(J,I)=0.
      DO 10 I=1,N
10    Y(I)=0.
C     INITIAL CONDITION
C
      T=TI
      Y(2)=F0(1);Y(4)=F0(2);Y(6)=F0(3);Y(8)=F0(4);Y(10)=F0
      1(5)
      Y(1)=DF(1)*SO;Y(3)=DF(2)*S1;Y(5)=DF(3)*S2
      Y(7)=DF(4)*S1;Y(9)=DF(5)*S2
      NSTEP=(TF-TI)/DT
      IF (.NOT.PLOT) GO TO 40
      CALL PRESUE(Y,P)
      WRITE(1) T,P
40    CCNTINUE
      PRINT //,"FUNCTION"
      WRITE(6,100) T,(Y(I),I=2,N,2)
45    CONTINUE
      CALL DLYFUN (N,Y,G,K,EPS,K1)
      DC 20 I=1,NSTEP
      CALL RKDELY(N,T,Y,DY,DT,G,K,EP, &400,HHALF,K1)
      DC 55 J=2,N,2
```

```
      IF(ABS(Y(J)).LT.2) GO TO 55
      RK=2
55    CONTINUE
      IF (MOD(I,NP).NE.0) GO TO 20
      IF (.NOT.PLOT) GO TO 60
      CALL PRESUE(Y,P)
      WRITE(1) T,P
60    WRITE(6,100)  T,(Y(J),J=2,N,2)
65    CONTINUE
20    CONTINUE
      IF (RK.GT.0) PRINT //,'UNSTABLE'
      IF (.NOT.PLOT) GO TO 70
      ENDFILE 1
      REWIND 1
      PRINT //,'PRESSURE'
      READ(5,/) NUMPT
      DG=PI*2./NUMPT
      NUM=NUMPT+1
      TEMP=0;XX(1)=0;
      DC 75 I=2,NUM
      TEMP=TEMP+DQ
75    XX(I)=TEMP
98    READ(1,END=70) T,P
      PRINT //,"TIME= ",T
      SUMY=C.
      DO 80 I=1, NUM
      QG=XX(I)
      YY(I)= -GAMA*(P(1)+P(2)*COS(QQ)+P(3)*COS(2*QQ)+P(4)
     1*SIN(QQ)+      P(5)*SIN(2*QQ))
      SUMY=SUMY+YY(I)
80    CONTINUE
      IF (SUMY.NE.0.) CALL PLOT2D(XX,YY,NUM,100,100)
      GO TO 98
70    CONTINUE
      RK=0
      GO TO 999
400   PRINT *//,'ILLEGAL DELAY FUNCTION'
      GC TO 99
50C   PRINT *//,'DELAY TIME TOO LARGE'
99    STOP
100   FCRMAT (X,8E12.5)
11C   FORMAT(13X,7E12.5)
      END
      SUBROUTINE DIFFUN (T,Y,DY)
      CIMENSION Y(10),DY(10)
      CCMMON EP,IGAS, RK,W3,EPANV
      COMMON /SLIST/S0,S1,S2
      COMMON /BLK.1/ C1,C2,C3,C4,C5,C6,C7,C8,C9,C10,C11,C12
     1,C13,C14,     C15,C16,C17
C
      DY(2)=Y(1)
```

```
      DY(1)=-SO*SO*Y(2)-EP*IGAS*(C1*Y(2)*Y(1)+C2*(Y(4)*Y(3)
     1+Y(8)*Y(7))    *C3*(Y(10)*Y(9)+Y(6)*Y(5)))
      DY(4)=Y(3)
      DY(3)=-S1*S1*Y(4)-EP*IGAS*(C4*Y(2)*Y(3)+C5*Y(4)*Y(1) +
     1    C6*(Y(8)*Y(9)*Y(4)*Y(5))+C7*(Y(6)*Y(3)+Y(10)*Y
     2(7)))
      DY(6)=Y(5)
      DY(5)=-S2*S2*Y(6)-EP*IGAS*(C8*Y(2)*Y(5)+C9*Y(6)*Y(1)+
     1 C10*(Y(8)*Y(7)-Y(4)*Y(3)))
      DY(8)=Y(7)
      DY(7)=-S1*S1*Y(8)-EP*IGAS*(C4*Y(2)*Y(7)+C5*Y(8)*Y(1)+
     1 C6*(Y(4)*Y(9)-Y(8)*Y(5))+C7*(Y(10)*Y(3)-Y(6)*Y(7)))
      DY(10)=Y(9)
      DY(9)=-S2*S2*Y(10)-EP*IGAS*(C8*Y(2)*Y(9)+C9*Y(10)*Y(1)
     1 C10*(Y(8)*Y(3)+Y(4)*Y(7)))
      IF (RK.EQ. 2) RETURN
      DY(1)=DY(1)-WB*(Y(1)+EPANV*(C11*Y(2)*Y(2)+C12*(Y(4)*Y
     1(4)+   Y(8)*Y(8))+     C13*(Y(10)*Y(10)+Y(6)*Y(6))))
      DY(3)=DY(3)-WB*(Y(3)+EPANV*(C14*Y(2)*Y(4)+C15*(Y(4)*Y
     1(6)+   Y(8)*Y(10))))
      DY(5)=DY(5)-WB*(Y(5)+EPANV*(C16*(Y(4)*Y(4)-Y(8)*Y(8))
     1       +C17*Y(2)*Y(6)))
      DY(7)=DY(7)-WB*(Y(7)+EPANV*(C14*Y(2)*Y(8)+C15*(Y(4)*Y
     1(10)   Y(8)*Y(6))))
      DY(9)=DY(9)-WB*(Y(9)+EPANV*(C17*Y(2)*Y(10)+2*C16*Y(4)
     1*Y(8)))
      RETURN
      END
      SUBROUTINE RKDELY(N,T,Y,DY,H,G,K,EPS, *,HHALF,K1)
      DIMENSION Y(10),DY(10),Y2(10),Y3(10),G(10,500)
      COMMON EP,IGAS,    RK,WB,EPANV
      COMMON /BLK1/ C1,C2,C3,C4,C5,C6,C7,C8,C9,C10,C11,C12
     1,C13,C14,    C15,C16,C17
      CALL DIFFUN(T,Y,DY)
      DO 1 I=1,N
         Y2(I)=Y(I) + HHALF*(DY(I) + G(I,1))
      G(I,1)=(G(I,1)+G(I,2))/2
    1    CONTINUE
      T=T+HHALF
      CALL DIFFUN(T,Y2,DY)
      DO 2 I=1,N
         Y3(I)=Y(I) + HHALF*(DY(I) + G(I,1))
    2    Y2(I)= Y2(I) + 2*Y3(I)
      CALL DIFFUN( T,Y3,DY)
      DO 3 I=1,N
         Y3(I)=Y(I) + H*(DY(I) + G(I,1))
      IF(K.LT.1) GO TO 3
      DO 10 J=1,K
   10    G(I,J)=G(I,J+1)
    3    Y2(I)=Y2(I) + Y3(I)
      T=T+HHALF
```

```
      CALL DIFFUN (T  ,Y3,DY)
      DC 4 I=1,N
         Y(I) = (Y2(I) - Y(I) + HHALF*(DY(I) + G(I,1)))/3.
    4 CONTINUE
      ENTRY  DLYFUN (N,Y,G,K,EPS,K1)
      IF (K.LT.1) RETURN
      IF (RK.EQ.2) RETURN
      G(1,K1)=      WB*          EPANV*(C11*Y(2)*Y(2)+C12*(Y(4)*Y
     1(4)+  Y(8)*Y(8)))+      C13*(Y(10)*Y(10)+Y(6)*Y(6)))
      G(3,K1)=      WB*          EPANV*(C14*Y(2)*Y(4)+C15*(Y(4)*Y
     1(6)+   Y(8)*Y(10)))
      G(5,K1)=WB*EPANV*(C16*(Y(4)*Y(4)-Y(8)*Y(8))+C17*Y(2)*Y
     1(6))
      G(7,K1)=      WB*          EPANV*(C14*Y(2)*Y(8)+C15*(Y(4)*Y
     1(10)   Y(8)*Y(6)))
      G(9,K1)=WB*EPANV*(C17*Y(2)*Y(10)+2*C16*Y(4)*Y(8))
      RETURN
      END
      SUBROUTINE PRESUE(Y,P)
C
C
C     THIS SECTION PERFORM THE PRESSURE CALCULATION
C
      DIMENSION Y(10),P(5)
      CCMMON EP,IGAS,     RK,WB,EPANV
      CCMMON /BLK2/C02,C03,C04,C05,C06,C07,C12P,C13P,C14P
     1,C15P,               C22,C23,C24,C25,GAMA
      CCMMON /BLK3/BJ0,BJ1,BJ2,COSQ,COS2Q,SINQ,SIN2Q
      DF0=Y(1);DF1=Y(3);DF2=Y(5);DG1=Y(7);DG2=Y(9)
       FO=Y(2); F1=Y(4); F2=Y(6); G1=Y(8); G2=Y(10)
      P(1)=BJ0*(DF0+EP*(C02*FO*FO+C03*(F1*F1+G1*G1)+C04*(F2
     1*F2+G2*G2)      +C05*DF0*DF0+C06*(DF1*DF1+DG1*DG1)+C07*
     2(DF2*DF2+     DG2*DG2)))
      P(2)=BJ1*(DF1+EP*(C12P*FO*F1+C13P*(F1*F2+G1*G2)+C14P
     1*DF0*DF1+      C15P*(DF1*DF2+DG1*DG2)))
      P(3)=BJ2*(DF2+EP*(C22*FO*F2+C23*(F1*F1-G1*G1)+C24*DFO
     1*DF2+       C25*(DF1*DF1-DG1*DG1)))
      P(4)=BJ1*(DG1+EP*(C12P*FO*G1+C13P*(F1*G2-G1*F2)+C14P
     1*CFO*DG1+      C15P*(DF1*DG2-DF2*DG1)))
      P(5)=BJ2*(DG2+EP*(C22*FO*G2+2.*C23*F1*G1+C24*DFO*DG2+
     1       2.*C25*DF1*DG1))
      RETURN
      END
      BLOCK DATA
      COMMON /BLK1/ C1,C2,C3,C4,C5,C6,C7,C8,C9,C10,C11,C12
     1,C13,C14,     C15,C16,C17
      COMMON /SLIST/SO,S1,S2
      CCMMON /BLK2/C02,C03,C04,C05,C06,C07,C12P,C13P,C14P
     1,C15P,               C22,C23,C24,C25,GAMA
      DATA SO,S1,S2/3.83171,1.84118,3.05424/
      DATA C1,C2,C3,C4/4.1373,1.0423,-.2084,-1.9394/
      DATA C5,C6,C7,C8,C9 /-2.3123,1.7187,1.4828,-2.785,
```

```
1-3.0388/
  DATA C10,C11,C12,C13/1.1318,2.586,.480,-.196/
  DATA C14,C15,C16,C17/-2.4243,1.8534445,-.447,-3.481/
  DATA C02,C03,C04,C05,C06,C07/1.2930,0.2400,-.0982,
1-.1762     ,.0607,.0494/C12P,C13P,C14P,C15P/-1.2121
2,.9267,.1651,-.1987/C22,C23,C24,C25/-1.7406,-.2235
3,.2371,-.1754/
  DATA GAMA/1.2/
  END
```